universität wien

MASTERARBEIT / MASTER'S THESIS

Titel der Masterarbeit / Title of the Master's Thesis

„Spatial separation of intracellular signaling domains in CD19 CARs in a Jurkat-based reporter system"

verfasst von / submitted by

Gabriel Kaufmann, BSc

angestrebter akademischer Grad / in partial fulfilment of the requirements for the degree of

Master of Science (MSc)

Wien, 2021 / Vienna, 2021

Studienkennzahl lt. Studienblatt / degree programme code as it appears on the student record sheet:	UA 066 877
Studienrichtung lt. Studienblatt / degree programme as it appears on the student record sheet:	Master's degree programme Genetics and Developmental Biology
Betreut von / Supervisor:	Assoc. Prof. Priv. Doz. Dr. Peter Steinberger

Table of contents

1 Acknowledgments

First of all, I want to sincerely thank Peter Steinberger for giving me the opportunity to work on my master's thesis in his remarkable lab. Your expertise, patience, and friendly manner guided me through my studies and your approach is a textbook example of excellent teaching.

Further, I want to thank my lab colleagues Claire, Judith, Teresa, Kathi and Maxi for the great work environment they created and fun times we shared on an everyday basis. You were always there for me when I needed help or advice. I'm beyond grateful for my supervisor Claire. Whenever I'd need your help or would ask you any question, you never rolled your eyes! On the contrary, you always stayed calm and friendly no matter my mistakes. You helped me in carrying out my experiments in your charming way and without hesitation, especially in the beginning of my time here. I couldn't have asked for a better supervisor.

Moreover, special thanks go to my family and friends who supported me throughout my master's studies, either by encouraging me in difficult times or by distracting me when things got tough. Lastly, I am deeply grateful for my parents' backup. Thank you for encouraging me with your stoical calmness in any way possible. You gave me the necessary support to finish my studies.

2 English Abstract

Adoptive T cell therapy is a highly personalized and promising immunotherapy for treating cancer. Specifically for B cell malignancies chimeric antigen receptors (CARs) are used, which are artificial receptors engineered to target surface molecules on cancer cells redirecting antigen specificity. CARs basically comprise an extracellular antigen-binding domain and a transmembrane domain linked to one or more cytoplasmic signaling domains. Due to the modular system of CARs, fine-tuning of CARs and various combinations of intracellular signaling domains are possible. Adding a costimulatory signaling domain to a 1st generation CAR, which only provides the signal 1 of a T cell response, showed effective in vivo tumor killing and T cell persistence, especially in CD19 CARs. Here we assess T cell activation and tonic signaling after spatially separating the intracellular domains of a 2nd generation CAR (comprising a CD28 or 4-1BB motif) in a Jurkat-based reporter system. Triple parameter reporter (TPR) cells transduced with CD19 CARs allow simultaneous analysis of NF-κB-eCFP, NFAT-eGFP and AP-1-mCherry activation via flow cytometry. Separating CD28 and CD3z domains did not lead to enhanced T cell activation upon CAR stimulation. Spatial separation of 4-1BB and CD3z did not reduce tonic signaling in reporter cells when CARs where highly expressed. All in all, our data indicate that further studies are necessary to achieve optimal CAR expression, activation and safety in 2nd generation CARs.

3 German Abstract

Die adoptive T-Zelltherapie ist eine hoch personalisierte und vielversprechende Immuntherapie zur Behandlung von Krebs. Speziell für B-Zell-Malignome werden chimäre Antigenrezeptoren (CARs) verwendet, bei denen es sich um künstliche Rezeptoren handelt, die so konstruiert sind, dass sie auf Oberflächenmoleküle auf Krebszellen abzielen und die Antigenspezifität umleiten. CARs umfassen im Wesentlichen eine extrazelluläre Antigen-bindende Domäne und eine Transmembrandomäne, die mit einer oder mehreren zytoplasmatischen Signaldomänen verknüpft ist. Aufgrund des modularen Systems der CARs ist eine Feinabstimmung von CARs und verschiedene Kombinationen von intrazellulären Signaldomänen möglich. Das Hinzufügen einer kostimulatorischen Signaldomäne zu einem CAR der 1. Generation, welches nur das Signal 1 einer T-Zell Antwort liefert, zeigte eine effektive in vivo Tumorabtötung und T-Zell-Persistenz, insbesondere in CD19 CARs. Hier untersuchen wir die T-Zell Aktivierung und tonische Signalgebung nach räumlicher Trennung der intrazellulären Domänen eines CARs der 2. Generation (bestehend aus einem CD28 oder 4-1BB Motiv) in einem Jurkat-basierten Reportersystem. Triple Parameter Reporter (TPR) Zellen, die mit CD19 transduziert wurden, ermöglichen die gleichzeitige Analyse von NF-κB-eCFP, NFAT-eGFP und AP-1-mCherry Aktivierung mittels Durchflusszytometrie. Die Trennung der CD28- und CD3z-Domänen führte nicht zu einer verstärkten T-Zell Aktivierung nach Stimulation des CARs. Die räumliche Trennung von 4-1BB und CD3z reduzierte die tonische Signalgebung in Reporterzellen nicht, wenn CARs hoch exprimiert wurden. Summa summarum zeigen unsere Daten, dass weitere Studien notwendig sind, um eine optimale Expression, Aktivierung und Sicherheit von CARs der 2. Generation zu erreichen.

4 Introduction

4.1 T lymphocytes

4.1.1 Functions and development

T lymphocytes, also named T cells, and B lymphocytes are the cells of the adaptive immune system. Their main role lies in recognizing specific foreign antigens and subsequently eradicating target cells (Anaya et al., o. J., S. 77 ff; Bonilla & Oettgen, 2010; Germain, 2002). The T cell receptor complex (TCR) is a multiprotein complex unique for T cells. In most T cells they comprise an α- and β-chain with highly variable binding sites and invariant proteins initiating signaling (Anaya et al., o. J., S. 77 ff; Wucherpfennig et al., 2010). Through somatic recombination of gene segments in the TCR loci a diverse set of TCRs can be attained (Germain, 2002; Wucherpfennig et al., 2010). TCRs can recognize antigens when processed and presented on the cell surface of target cells by the human leukocyte antigen system (HLA-system), also termed major histocompatibility complex (MHC) (Anaya et al., o. J., S. 77 ff; Bonilla & Oettgen, 2010).

T cells are distinguished into two major types depending on which coreceptor, $CD4^+$ or $CD8^+$, is expressed (Germain, 2002). $CD4^+$ T cells are also called T helper cells (T_H) and can be divided into several different subsets, mainly Tfh (T follicular helper cells), T_H1, T_H2 and T_H17 (Bonilla & Oettgen, 2010). The main task of T_H1 cells lies in secreting cytokines, characteristically IFN-γ and IL-2, leading to cell-mediated immune responses by activating $CD8^+$ T cells, natural killer cells (NK cells) and mononuclear phagocytes killing target cells (Mosmann et al., 1986; Bonilla & Oettgen, 2010). T_H2 cells are mainly enhancing antibody production after a cascade of events eventually recruiting mast cells, basophils and eosinophilopoiesis for expulsion of helminths while mainly secreting IL-4, IL-5, IL-10, and IL-13 (Bonilla & Oettgen, 2010). $CD4^+$ T cells engage with peptides expressed on MHC class II molecules, which are present on professional antigen-presenting cells (APCs) such as dendritic cells (DCs). $CD8^+$ T cells, also termed cytotoxic T lymphocytes (CTL) or killer T cells, kill target host cells via contact-dependent engagement with MHC class I molecules presenting antigenic peptides derived from cytosolic proteins (Germain, 2002). MHC class I molecules can be expressed by all nucleated cells (Anaya et al., o. J., S. 77 ff). CTLs release

granzymes and perforins into target cells leading to activation of apoptosis and killing of the target cell (Lieberman, 2003).

T cells develop in the thymus, after hematopoietic stem cells (HSCs) differentiate into multipotent progenitors and migrate out of the bone marrow into the thymus where they are gradually programmed to become functional T cells (Zúñiga-Pflücker, 2004). These early committed T cells lack expression of TCR and differentiate through various signals into double negative (DN) thymocytes in the thymic cortex, meaning they neither express CD4 nor CD8 (Germain, 2002). As cells progress in the DN state, they first express a pre-TCR-α chain which later is paired with the TCR β-chain after somatic DNA rearrangements. This pre-TCR-αβ pair is associated with proteins important for signal transduction and undergo several cell divisions leading to a newly rearranged TCR-α chain yielding a complete TCR. Furthermore, thymocytes begin to express coreceptors CD4 and CD8 to form double positive (DP) immature thymocytes (Germain, 2002). Further differentiation to $CD4^+$ or $CD8^+$ T cells is regulated by both negative and positive selection events (Germain, 2002). During positive selection, immature DP T cells interact with thymic epithelial cells expressing self-MHC molecules complexes and are induced to differentiate into either $CD4^+$ or $CD8^+$ single-positive (SP) mature T cells (Klein et al., 2014). For negative selection, SP and DP thymocytes interact with DCs and epithelial cells of the thymic medulla engaging with a great variety of self-MHC complexes. Thymocytes that express TCRs with high affinity for self-antigens are eliminated or in some cases programmed to develop into T regulatory cells (Tregs) (Klein et al., 2014).

4.1.2 Signaling

Naïve T cell activation exclusively takes place in secondary lymphoid organs and tissues in which they encounter processed foreign peptides presented by MHC molecules. Upon TCR engagement a series of signaling events occurs in the cytosol of T cells leading to differentiation into effector cells (Pennock et al., 2013). The primary signal lies in T cell receptor activation and is provided by CD3 molecules associated with the TCR. Co-stimulation through molecules like CD28 or 4-1BB provide the ‘signal 2’ which enhance T cell effector functions (Bonilla & Oettgen, 2010). The CD3 complex consists of several subunits (γ, δ, ε and ζ) equipped with immunoreceptor tyrosine-based activation (ITAM) motifs which can be phosphorylated (Gorentla & Zhong,

2012). After phosphorylation of tyrosines in the ITAM motifs by the Src family protein tyrosine kinase Lck, which is associated with either CD4 or CD8 molecule, additional adaptor molecules are recruited (Gorentla & Zhong, 2012). The ζ-associated protein, 70 kDa (ZAP-70) binds to phospho-tyrosines of CD3z ITAM motifs via its SH2 domain which triggers phosphorylation by Lck. Association of ZAP-70 with the TCR/CD3 complex leads to recruitment of further adaptor molecules and formation of a signaling complex (Bonilla & Oettgen, 2010; Gorentla & Zhong, 2012). The two key adaptor molecules phosphorylated by ZAP-70 are Linker for activation of T cells (LAT) and SH2-containing leukocyte phosphoprotein of 76 kDa (SLP-76), promoting recruitment of various other factors (Cantrell, 2002). One active signaling enzyme recruited by ZAP-70 and SLP-76 is phospholipase Cγ1 (PLCγ1), which upon phosphorylation mediates hydrolysis of phosphatidylinositol 4,5-bisphosphate (PIP2) to generate the second messengers diacylglycerol (DAG) and inositol trisphosphate (IP3) (Gorentla & Zhong, 2012; Bonilla & Oettgen, 2010; *T Cell Receptor Signaling*, o. J.). Three major signaling pathways, among others, are then activated (Gorentla & Zhong, 2012; Bonilla & Oettgen, 2010): DAG induces the mitogen-activated protein kinase (MAPK) pathway initiated by the recruitment of RasGTP to ultimately induce expression of activator protein 1 (AP-1). DAG also activates the protein kinase C (PKC) later giving rise to the IKK complex permitting the phosphorylation and subsequent degradation of IκB inhibitors, which eventually leads to release of nuclear-factor-κ-B (NF-κB) dimers, activating transcription of their target genes. IP3 initiates release of Ca^{2+} from the ER binding to the protein calmodulin. Calcium-bound calmodulin activates the phosphatase calcineurin, which subsequently dephosphorylates nuclear factor of activated T cells (NFAT) to generate its active form translocating to the nucleus, promoting IL-2 gene transcription. The transcription factors NFAT, NF-κB and AP-1 enter the nucleus and induce transcription of genes essential for T cell proliferation, differentiation, and effector functions (Brownlie & Zamoyska, 2013).

4.1.3 Co-signaling

Co-stimulatory receptors alone cannot promote T cell activation, but significantly amplify or reduce signaling provided by the TCR complex. Full T cell activation needs both signals, signal 1 through the TCR/CD3 complex, and signal 2 through co-stimulatory molecules (Chen & Flies, 2013). In the absence of signal 2, T cells are unresponsive to antigenic stimulation and become anergic (Schwartz, 2003). This study focuses on the co-stimulatory molecules CD28 and 4-1BB (CD137). CD28 is constitutively expressed on naïve T cells whereas other co-stimulatory receptors, such as inducible T-cell costimulator (ICOS) or 4-1BB (CD137) are inducible upon T cell activation (Kroczek et al., 2004). The most prominent co-signaling family is the CD28-B7 superfamily. B7-1 (CD80) and B7-2 (CD86) are ligands present on APCs and can bind both, the co-stimulatory molecule CD28 and the co-inhibitory molecule cytotoxic T-lymphocyte-associated protein 4 (CTLA-4), whose expression is upregulated following T cell activation. Many other receptor-ligand pairs are involved in T cell activation and regulation (Sharpe & Freeman, 2002; Chen & Flies, 2013).

CD28 is regarded as the primary co-stimulatory receptor and provides a crucial signal for T cell growth and survival (Chen & Flies, 2013). Essentially two motifs in the cytoplasmic tail of CD28 are responsible for signaling: the proximal YMNM and distal PYAP motif. YMNM facilitates phosphorylation of Protein kinase B (PKB) through association with phosphatidylinositol 3--kinase (PI3K) via SH2-domain, resulting in activation of various distal molecules, such as NF-κB and NFAT (Chen & Flies, 2013; Riha & Rudd, 2010). PYAP associates with Lck and the adaptor protein growth factor receptor-bound protein 2 (GRB2) through their SH3 domains initiating NFAT signaling, which in turn enhances IL-2 production (Riha & Rudd, 2010; Chen & Flies, 2013). GRB2 also has an SH2-domain and is recruited by YMNM. GRB2 is not only crucially involved in bringing in Protein kinase C (PKC) to the immunological synapse for subsequent activation, but also activates c-Jun N-terminal kinases (JNKs), ultimately leading to formation of AP-1 transcription complex, which acts in concert with NFAT and NF-κB to enhance IL-2 transcription (Riha & Rudd, 2010; Chen & Flies, 2013).

4-1BB, like OX40, HVEM, GITR AND CD27 is a member of the TNF-receptor (TNFR) superfamily, and another strong player in co-stimulation of T cells. The TNFR-Associated-Factor (TRAF) family of adaptor proteins are necessary to induce signaling after formation of a signalosome (Zapata et al., 2018). Upon 4-1BB activation, a

complex network of TRAF homo- and/or heterotrimers with different configurations is formed. Ubiquitination events on different domains on TRAF molecules ultimately induces activation of IKK complex upon phosphorylation by the protein kinase TAK1, which not only results in a signaling cascade activating NF-κB and ERK, but also activation of MAP kinases (Zapata et al., 2018, S. 13).

Many other co-signaling molecules are involved in enhancing or inhibiting T cell proliferation, differentiation, and effector functions. The classic two-signal model in T cell activation as previously described is now viewed as a complex network, as many more molecules, interactions and mechanisms involved in T cell activation have been discovered (Chen & Flies, 2013).

4.2 Cancer immunotherapy

Engaging the immune system has become an emerging and promising angle in treatment against cancer. Unleashing the body's own T cells to fight neoplastic disease has great potential as T cells are believed to play a crucial role in tumor elimination and immunosurveillance (Houot et al., 2015; Waldman et al., 2020). Surgery, chemotherapy, and radiotherapy make up the earliest forms of cancer therapy but they come with several limitations (Arruebo et al., 2011). Quite often not all cancer cells are removed or destroyed after surgery or radiotherapy and metastasized tumor cells can regrow and the patient's life is at best only prolonged (Majeed & Gupta, 2021). Chemotherapy also effects normal cells leading to harm of not only cancer cells (Arruebo et al., 2011). Targeted therapy, using i.e. antibodies against tumor antigens, or immune checkpoint inhibitors to block inhibitory receptors, such as CTLA-4 or PD-1, in T cells and (re)activate T cell immune response in vivo, and immunotherapy have the potential to eliminate cancer cells specifically without harming the patient's tissue (Waldman et al., 2020; Houot et al., 2015). Every tumor differs from another making it near impossible to cure cancer with a single wonder drug. Combinatorial therapy is the most promising, as cancer cells learn how to evade targeted and immunotherapy considering oncogenic driver mutations and tumor microenvironment (Lim & June, 2017; Houot et al., 2015).

4.2.1 Adoptive T cell transfer

T-cell-based therapies show the most promising results in treating cancer among immunotherapies. Adoptive T cell transfer (ACT) is a highly personalized therapy. It relies on autologous T cells being engineered and/or expanded *ex vivo* to acquire antitumor functions. T cells are then reinfused to fight tumor cells essentially functioning as a living drug able to induce long-term protection (Houot et al., 2015). ACT transfusion has shown durable clinical responses of otherwise treatment-refractory cancers (June et al., 2018). Another advantage of ACT is that patients can be manipulated and deprived of endogenous lymphocytes or suppressor cells, such as Tregs, before transfusion to enhance *in vivo* expansion of transferred T cells (Houot et al., 2015; Waldman et al., 2020). Mainly three forms of ACT are used in clinical practice and further developed: tumor-infiltrating lymphocytes (TILs) and T cells genetically engineered to express tumor specific TCRs or chimeric antigen receptor (CAR) T cells (Houot et al., 2015).

4.2.1.1 Tumor-infiltrating lymphocytes

Tumor-infiltrating lymphocytes (TILs) are a heterogenous cell population but mainly consisting of T cells, all residing within neoplastic tissues (Paijens et al., 2021; Houot et al., 2015). The expression of TCRs directed against tumor-associated antigens allows TILs to mediate specific lysis of autologous malignant cells but not normal cells (Houot et al., 2015). To select and expand TILs ex vivo, they have to be isolated from resected tumor. Metastatic melanoma patients show great response in all visceral sites after administration of TILs with prior lymphodepletion and show durable response, even complete regressions (Waldman et al., 2020; Houot et al., 2015). The advantage of endogenous TCRs is that distinct peptides and a variety of tumor-specific mutations can be recognized, which might explain great response rates to tumors with high mutational loads such as melanoma cells (Lim & June, 2017). The use of TILs to treat cancer has its limitations. Patients need to be able to tolerate lymphodepletion for several weeks, throughout the process of expanding antitumor T cells ex vivo with IL-2 (Waldman et al., 2020). Melanoma gives rise to high numbers of T cells specific for malignant cancer cells unlike other cancer types, where treatment with TILs was frequently not effective (Houot et al., 2015). Tumors sensitive to immune checkpoint blockade show potential to TIL treatment, as the quality and magnitude of not only T

cells, but also NK cell and B cells in the tumor microenvironment is superior to TILs from patients not responsive to immune checkpoint blockade (Houot et al., 2015; Paijens et al., 2021).

4.2.1.2 Transgenic T cell receptor (TCR)

The physiological TCR consists of polymorphic α- and β-glycoprotein with variable regions making contact with pMHC. These chains are coupled with a conserved domain noncovalently associated with non-polymorphic protein dimers, CD3 γε, δε and ζζ, through which signaling is mediated (Bonilla & Oettgen, 2010). The antigen-binding domain can be manipulated to be specific for tumor-associated antigens (TAAs), while preserving the conserved domains to ensure T cell response (Manfredi et al., 2020). Tumor regression after treatment with autologous transgenic TCR T cells was observed in several clinical studies and identification of TAAs targeted by TCRs, including MART1, in melanoma (Morgan et al., 2006), NY-ESO 1 (Robbins et al., 2011) expressed on several cancers such as melanoma, carcinoembryonic antigen (CEA) (Parkhurst et al., 2011) against colorectal cancer or MAGE-A3 (Morgan et al., 2013) against synovial carcinoma, show great promise. Transgenic TCR T cells are limited to respond to intracellular antigens presented by the MHC complex of APCs and cannot bind directly to surface antigens, unlike CARs. MHC molecules can be downregulated by tumor cells leaving T cells unable to engage with cancer cells (Guedan et al., 2019). A major problem of transgenic TCRs is on- or off-target toxicity. TAAs, such as MART1 or CEA, are often expressed on healthy tissue cells as TCRs can induce on-target off-tumor toxicity (Houot et al., 2015; Guedan et al., 2019). Higher-avidity TCRs can improve response rates, but frequently also react with healthy cells indicating a small window between efficacy and toxicity (Guedan et al., 2019). Off-target effects were also observed, as TCR-based therapies induced fatal neurotoxicity and cardiotoxicity in two separate clinical trials using anti-MAGE-A3 T-cell receptors -engineered T cells (Cameron et al., 2013; Morgan et al., 2013). Previously unrecognized expression of targeted proteins in other tissues or cross-recognition of an off-target peptide is difficult to predict and can result in severe adverse events in patients (Houot et al., 2015).

4.2.1.3 Chimeric antigen-receptor (CAR)

CARs are artificial receptors engineered to target surface molecules on cancer cells to redirect antigen specificity (June et al., 2018). CARs basically consist of an extracellular antigen-binding domain, usually an antibody-derived single-chain variable fragment (scFv) specific for a surface molecule on a tumor cell, a hinge region to ensure flexibility and improve antigen engagement, a transmembrane domain linked to one or more intracellular signaling domains triggering T cell effector functions (Srivastava & Riddell, 2015; Jensen & Riddell, 2015). Antigen recognition using CARs is independent of peptide processing and presentation on MHC molecules (Houot et al., 2015). Cancer cells downregulating MHC-molecules is a major mechanism of immune evasion (June et al., 2018). CARs can bypass HLA restriction and target a surface molecule of malignant cells (Waldman et al., 2020) leading to an array of possible targets. However, the conserved binding of TCRs to peptide/MHC complexes doesn't need a high number of target molecules, as they can serially engage them and TCRs can cluster to form organized synapses (Jensen & Riddell, 2015). Therefore, not only a higher density of target molecules, but also tailoring the length and composition of extracellular domains to ideally bind on target molecule is needed for optimal CAR activation (Jensen & Riddell, 2015). A major challenge in designing CARs is minimizing toxicity and spare normal tissue while ensuring effective tumor response (Srivastava & Riddell, 2015). CAR T cells targeting CD19 have shown promising results, because of its high-level expression in B cell malignancies (Lim & June, 2017). Healthy B cells expressing CD19 are also targeted, but loss of normal B cell can be well tolerated and treated with antibody therapy (Lim & June, 2017). CD19 CARs induced complete remissions in several studies treating chemotherapy-refractory diffuse large B-cell lymphoma (DLBCL) (Kochenderfer et al., 2015), chronic lymphocytic leukemia (CLL) (Porter et al., 2014), and relapsed or refractory acute lymphoblastic leukemia (ALL) (Maude et al., 2014). Additional challenges arise in solid tumors, as CARs have not been very successful targeting these tumors (Houot et al., 2015). Several attempts on targets which are overexpressed in cancer cells have been done often leading to fatal off-target toxicities caused by recognition and killing of healthy cells (June et al., 2018). The immunosuppressive tumor microenvironment can directly interfere with the responses of T cells, including engineered CAR T cells. Generally, the tumor microenvironment is excluding T cells from the vicinity of cancer cells by several

mechanisms, such as lack of cytokine stimulation, lack of T cell help, vascularity defects, expression of inhibitory ligands of tumor stroma, or presence of suppressive immune cells (Lim & June, 2017; Joyce & Fearon, 2015). Target-antigen loss by the tumor was also observed in some cases, showing another limitation of CAR-T cells (Houot et al., 2015). Furthermore, mild to severe or even life-threatening cytokine release syndrome (CRS) and neurotoxicity was linked to CAR T cell therapy and issues a major problem in safety and tolerance (June et al., 2018; Waldman et al., 2020).

The first CARs that were developed only had CD3z ITAM domains as a signaling domain and were termed 1st generation CARs (Abate-Daga & Davila, 2016). The first generation of CARs showed T cell activation and target killing *in vitro*, but limited persistence and antitumor efficacy *in vivo* (Abate-Daga & Davila, 2016; Harris & Kranz, 2016). This led to 2nd generation CARs in which a costimulatory domain (mostly CD28 or 4-1BB) was added to the CD3z motif, adding a signal 2 to the signal 1. CARs containing a costimulatory domain showed effective tumor killing and T cell persistence *in vivo*, especially in CD19 CARs, but also led to safety issues (Abate-Daga & Davila, 2016). 3rd generation CARs are conceptually similar to 2nd generation CARs and consist of two costimulatory domains linked to CD3z, mostly combining CD28 with 4-1BB or OX40 (Rohaan et al., 2019). The possibilities to engineer safer and more effective CAR T cells has led to a great variety of innovations to enhance CARs. Following strategies are used to mitigate toxicities (Rafiq et al., 2020): Combinatorial CARs are designed that one receptor with a signal 1 intracellular domain and a second receptor with a costimulatory domain target two different tumor antigens to ensure full activation upon recognition of both target molecules. Inhibitory CARs contain an inhibitory signaling domain which is activated upon binding to a target molecule expressed on healthy tissues. Synthetic Notch receptors are designed to mediate cell killing only with two antigens present, similar to combinatorial CARs, only that activation of one receptor induces expression of the second receptor. Strategies to overcome tumor escape by loss of antigen expression have also been developed (Rafiq et al., 2020): CARs detecting two different antigens using either two scFvs in one CAR (Tandem CARs) or two separate 2nd generation CARs (Dual CAR). Universal CARs recognize an antibody which will recognize tumor antigens and a consistent ‘switch’ domain allowing targeting of new antigens without reengineering T cells. Armoring CAR T cells with chemokines, cytokines or DC-stimulating receptors (4-

1BBL, IL-12, IL-6) or genes to express inflammatory signals have also been designed (Rafiq et al., 2020).

4.3 Triple parameter reporter (TPR) and NF-κB-reporter cells

TPR and NF-κB-reporter cells are reporter cell lines based on the Jurkat E6.1 cell line established in the lab of Peter Steinberger (Jutz et al., 2016). The human leukemic T cell line Jurkat is well studied and probably the most prominent model system to study T cell functions and signaling *in vitro* (Abraham & Weiss, 2004). TPR cells are engineered to express fluorescent proteins to measure fluorescent intensity upon activation. They comprise of responsive elements for NF-κB, NFAT and AP-1 which are combined with a minimal promoter sequence followed by sequences encoding eCFP, eGFP and mCherry, respectively, allowing simultaneous analysis of these three important transcription factors (Jutz et al., 2016). TPR cells been shown to be activated and express reporter genes upon TCR-complex engagement irrespective of the availability of costimulatory ligands, but an increase of reporter activation after signal 1 can be measured via costimulatory receptor (e.g. CD28-CD80, CD58-CD2,…) signaling (Jutz et al., 2016). NF-κB-reporter cells rely on the same concept as TPR cells, but only contain an NF-κB responsive element combined with an eGFP sequence (Jutz et al., 2017).

5 Aims of the study

5.1 Generation of Dual and single CD19 CAR constructs to study the function of costimulatory signaling domains

Within this thesis various chimeric antigen receptor (CAR) constructs were generated and studied in a reporter-based system. To generate our CARs, the Steinberger laboratory designed a Dual CAR construct, which was synthesized by TWIST Bioscience (Fig. 1). This Dual CAR comprises an extracellular CD19 binding antibody-derived single chain variable fragment (scFv) domain and a transmembrane domain derived from CD28 fused to different intracellular signaling domains. One Dual CAR construct expresses two individual CAR molecules which are separated by a 2A self-cleavage peptide. The main focus of my master thesis was to study the effect of spatial separation of various combinations of intracellular signaling domains using a Dual CAR approach or two simultaneously transduced different single CARs on T cell activation. Intracellular domains derived from CD28, 4-1BB and CD3z were assembled in different combinations to one of the two CD19 CAR molecules in a Dual CAR construct. The Dual CAR also contains a CD8 hinge region to ensure proper binding flexibility and distance to the CD19 antigen on the target cell surface. In addition, they were designed to include a strep-tag and either an V5- or HA-tag which enables detection of both molecules on the cell surface. When stable surface expression was achieved, functional analysis of CD19 CARs in reporter cells and primary T cells was carried out. Finally, not only the activation potential of Dual and single CD19 CARs were compared with each other, but also with endogenous receptors (the TCR/CD3 complex and CD28) of reporter cells and T cells.

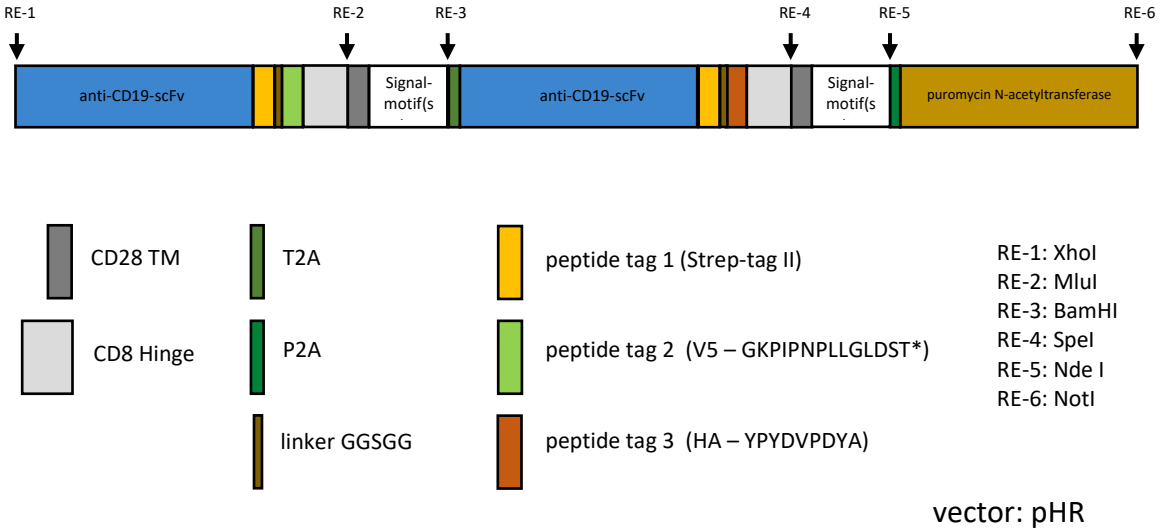

Figure 1: Schematic illustration of synthetized Dual CAR construct; A sequence encoding the anti CD19 single chain variant is fused to two tag sequences followed by sequences encoding a CD8 Hinge domain, a CD28 transmembrane domain, the first signal motif and a self-cleavable peptide. The second part consists of same parts as the first using different base sequences, a different sequence encoding signal motif and at the end a sequence encoding Puromycin-N-acetyltransferase as a selection marker; 6 different restriction sites are placed along the construct; Construct is ligated into a lentiviral pHR vector

5.2 Effect of spatial separation of CD3z and costimulatory signaling domains (CD28 and 4-1BB) in CD19 CARs on T cell activation

Preliminary data in the Steinberger lab showed that 2nd generation CARs harboring CD28 sequences (CD28z) do not induce stronger activating signals than 1st generation CARs (CD3z). This could suggest that CD28 sequences located upstream of CD3z sequence are compromised in their function. To investigate this, we used the Dual CAR system in which one CAR molecule harbors a CD3z signaling domain and another one the CD28 intracellular domain. With this, spatial separation of these two domains is ensured and CD28 domain is not located upstream of CD3z. In the Dual CAR, both molecules with the different signaling domains are encoded in one construct for equal expression. Further, two single CD19 CARs harboring either a CD3z or CD28 signaling domain were separately transduced in T cells or reporter cells and compared to the Dual CAR system. Using V5- and HA-tag sequences encoded in the extracellular part of the CD19 CAR molecule, cell surface expression of each individual CAR can be measured to ensure proper cell surface expression on Jurkat cells or primary T cells.

Furthermore, the Steinberger lab gathered preliminary data in which constitutive NF-κB activation was observed in 2nd generation CARs (41BBz) harboring 4-1BB sequences in absence of the antigen. Therefore, we investigated whether this effect still can be observed when the signaling domains of CD3z and 4-1BB are separated on two CAR molecules.

5.3 Analysis of CD28 signaling motif ‘PYAP’

We wanted to further analyze the ‘PYAP’ motif of the cytoplasmic signaling domain of CD28 to follow up on preliminary data regarding dysfunctional 2nd generation CARs comprising CD28 as costimulatory domain. CD28 contains two major binding motifs, the proximal ‘YMNM’ and the distal ‘PYAP’ motif. We figured that ‘PYAP’ might be sufficient for T cell activation and generated three CD19 CAR constructs in which this motif is incorporated either upstream, within, or downstream of the CD3z motif in a 1st generation CAR. The goal was to show the importance of the ‘PYAP’ motif in T cell activation and its sufficiency providing costimulatory signal. Moreover, we confronted the problem of compromised function regarding CD28 in a 2nd generation CAR (CD28z) as no enhancement in T cell activation was seen compared to 1st generation CARs.

5.4 Cellular model system

For analysis of T cell signaling by CD19 Dual CARs and single CARs, the triple parameter reporter cell line (TPR) and NF-κB-reporter cell line based on the Jurkat E6.1 cell lines were used. These cells are an excellent tool to measure T cell activation upon engagement of a CAR with its antigen counterpart. TPR cells were previously engineered in the laboratory of Peter Steinberger and designed to express three different reporter constructs, namely NFAT-GFP, NF-kB-CFP and AP-1-mCherry. Each reporter construct consists of a responsive element for the transcription factors NFAT, NF-kB or AP-1, respectively, followed by a minimal promoter, which together mediate the expression of the respective reporter gene, GFP, CFP or mCherry (Jutz et al., 2016). Upon stimulation, Jurkat reporter cells are activated, and transcription factor activity can be assessed by flow cytometry. In addition to TPR, we used NF-κB-reporter cells, which only comprise one NF-κB-eGFP reporter construct. To stimulate CD19 CARs on our reporter cells, K562 stimulator cells expressing CD19 were generated. In addition to K562:CD19, K562:CD86, K562:aCD3, K562:CD19:CD86 and K562:aCD3:CD86 were generated, which enables the assessment of CD28 costimulation and endogenous TCR stimulation, respectively. Co-cultures of K562 stimulator cells with reporter cells expressing different CD19 CARs combinations were performed to analyze the functionality of our CARs (Fig. 2).

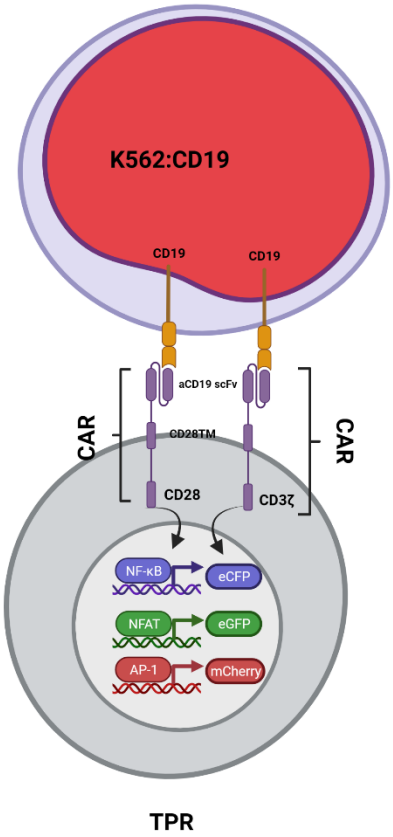

Figure 2: Schematic illustration of K562:CD19 stimulation of TPR cells expressing the aCD19:CD3z-aCD19:CD28 CAR construct, created with Biorender.com

6 Materials and Methods

6.1 Cloning

6.1.1 PCR

PCRs were carried out to create mutations or change restriction sites for different constructs. Primers were designed to align to an insert of interest containing desired sequence differences.

GC or HF reaction buffer, 200 µM dNTPs, 0.5 µM forward and reverse primer, 1 ng template DNA and 0.02 U/µl S7 Fusion Polymerase (Biozym, Germany) were used in a 50 µl reaction. Annealing temperature was set at 60 °C for 20 sec and extension was set to 72 °C 30 – 40 secs depending on the length of samples amplified. Cycles were repeated 30 x. Primers were ordered from ThermoFisher Scientific (Waltham, MA).

6.1.2 Restriction Digest

If preparing a vector or insert, 2 µg DNA were mixed with 2 µl restriction endonucleases, 2 µl 10 x CutSmart Buffer and filled up to 20 µl with ddH_2O. Digest was incubated for 1 - 2 hours.

For control digest of plasmid-DNA (Miniprep), 3 µl plasmid-DNA were mixed with 0.5 µl enzymes, 1 µl CutSmart buffer and 5 µl H_2O and digested for 30 min.

Enzymes and buffer were acquired by NEB (Ipswich, MA). Restriction enzymes used in these experiments are High-Fidelity XhoI, MluI, BamHI, SpeI, NdeI and NotI.

6.1.3 Ligation

Vector and insert were mixed with a molar ratio of 1:3 or 1:1, 1 µl of 10 x T4-DNA-Ligase Buffer and 0.5 µl T4-DNA-ligase were added and filled up to 10 µl with H_2O. The reaction mix was shortly centrifuged and incubated either 1 h at RT or 16 °C o/n. After incubation, ligase was heat-inactivated at 65 °C for 10 minutes. T4-DNA-ligase and DNA-ligase Buffer were acquired from NEB.

6.1.4 Transformation

Bacterial strains used were XL1-Blue and DH5α acquired from Sigma-Aldrich (St. Louis, MO). 45 µl Bacteria, 20 µl 5 x KCM Buffer (500 mM KCl, 150 mM $CaCl_2$ and 250 mM $MgCl_2$) and 2 µl ligation product were mixed and cooled down on ice for 30 min. Heat shock was performed for 45 seconds at 42 °C. Subsequently, the transformation mixture was cooled on ice for 2 minutes and 30 µl of LB medium (w/o ampicillin) was added and put on 37 °C shaking 750 rpm for 1 h. Bacteria were then plated on plates with Ampicillin. Plates were incubated at 37 °C o/n and colonies were inoculated in LB medium with Ampicillin shaking 750 rpm at 37 °C o/n. For plasmid isolation, Thermo Scientific GeneJET Plasmid Miniprep kit was used.

6.1.5 $CaCl_2$-Transfection

HEK-cells were harvested 24 h before transfection and seeded in 24-well plates. 1 h prior to transfection fresh medium is applied. 2 µg of plasmid DNA (pHR-lentiviral expression vector) is mixed with 1 µg VSV and 1 µg PAX helper plasmids and added up to 45 µl H_2O. Afterwards, 5 µl of 2.5M $CaCl_2$ were added and followed by 50 µl of 2 x HBS-Buffer by carefully dripping on DNA while vortexing on low level. This solution was left for 1 min at room temperature to allow formation of DNA-calcium phosphate precipitates and then added on seeded HEK293 cells in 24-well plate. After 16-24 h the medium is replaced and after another 24 h or 48 h the virus-containing supernatant can be harvested.

6.1.6 Transduction

On the day of transduction, 1 x 10^5 reporter cells or K562 cells were seeded in a 48 well plate. 48 h or 72 h post transfection the lentiviral supernatant was harvested, centrifuged to remove remaining HEK293 cells and polybrene was added (final concentration 8 µg/ml). Virus supernatant was then added to reporter cells (1 x 10^5 + 200 ul viral supernatant) and spin infection was performed for 90 min at 30 – 32 °C at 1500 rpm. After 48 h, transduced cells were washed 2 x with fresh medium and transferred to a new plate.

6.2 Constructs

6.2.1 Dual CAR constructs

Based on a previously described CD19 CAR construct (Rydzek et al., 2019), we designed a dual CAR construct with codon optimization which was synthesized by TWIST Bioscience (San Francisco, CA) and contains the following domains:

XhoI::anti-CD19-scFv::Strep-tag::linker::V5-tag::CD8Hinge::MluI::CD28-Transmembrane-domain::signal-motif-1::BamHI::T2A-self-cleavable-peptide::anti-CD19-scFv::Strep-tag::linker::HA-tag::CD8Hinge::SpeI::CD28-Transmembrane-domain::signal-motif-2::NdeI::P2A-self-cleavable-peptide::Puromycin-N-acetyltransferase::NotI (Fig. 1)

Based on this Dual CAR construct and other CARs previously generated by the Steinberger lab (XhoI_X15_scTCR-Strep-CD8S_28-z and XhoI_X15_scTCR-Strep-CD8S_4IBB-zeta_2A_Puro_NotI), 6 Dual CARs with different signaling domain combinations were generated:

- pHR-CD3z-CD28-Puro
- pHR-CD3z-CD3z-Puro
- pHR-CD28z-CD28z-Puro
- pHR-41BBz-41BBz-Puro
- pHR-CD3z-41BB-Puro
- pHR-CD28-CD3z-Puro

To start with, the before mentioned synthesized Dual CAR construct (Fig. 1) was inserted into the lentiviral pHR-SIN-BX-IRES-Emerald vector encoding the puromycin N-acetyl transferase site using restriction enzymes XhoI/NotI (Paster et al., 2013). Based on this pHR plasmid, other Dual CAR combinations with different signaling domains were generated using restriction enzymes and earlier generated constructs from the Steinberger lab. Within the Dual CAR, sequences of individual comprise different codons for each amino acid to avoid interference during transcription.

- pHR-CD3z--CD3z-Puro:

To attain CD3z as the downstream signal motif, PCR was used to insert SpeI/NdeI sites to CD3z signal motif of the XhoI_X15 scTCR-Strep-CD8S_28-z construct.

Oligonucleotide name	Sequence (5'-3')
X15_CD3z_SpeI_Fwd	gcgcccactagtTTCTGGGTTCTGGTTGTTGTTGGTGGGGT CCTTGCATGTTACTCCCTGCTGGTCACCGTAGCTTTTA TCATATTTTGGGTTcgggtgaagttcagcagaag
X15_CD3z_NdeI_Rev	GCGCCCCATATGccttgggggcagggcc

Table 1: Sequences of forward and reverse primer for generation of SpeI and NdeI restriction sites

The sequence encoding the CD28 domain was replaced with a CD3z encoding sequence using SpeI and NdeI restriction sites.

- pHR-CD28-CD3z—CD28-CD3z-Puro:

The downstream CD28z motif was generated using three PCRs. Firstly, CD3z was obtained using a forward primer with a 5' CD28 overhang and reverse primer binding to the 3' end of CD3z flanked with a NdeI restriction site. For the second PCR, the forward primer binds to CD28 transmembrane (CD28TM) sequence flanked with SpeI at the 5' end and reverse primer binds to CD28 sequence containing a 3' CD3z overhang. As template, pHR-CD3z—CD28-Puro was used. After preparation of intermediate DNA products, a final PCR was run to get full CD28z motif using primers 'DC_CD28z_SpeI_Fwd_CD28' as a forward primer binding on CD28TM and 'DC_CD28z_NdeI_Rev_z' as reverse primer binding on 3' end of CD3z. Intermediate DNA products were used as template.

Oligonucleotide name	Sequence (5'-3')
DC_CD28z_Fwd_z	ATTTTGCGGCATATCGATCTAGGGTTAAATTTT CCCGATCTGC
DC_CD28z_NdeI_Rev_z	gcgccccatatgACGGGGTGGAAGTGCTTGC
DC_CD28z_Rev_CD28	GATCGGGAAAATTTAACCCTAGATCGATATGCC GCAAAATCG
DC_CD28z_SpeI_Fwd_CD28	gcgcccactagtTTCTGGGTTCTGGTTGTTGTTG

Table 2: Sequences of forward and reverse primers used to insert SpeI and NdeI restriction sites and obtain desired pHR-CD28-CD3z—CD28-CD3z-Puro construct

This signal motif was then ligated into pHR-CD3z-x-Puro vector to obtain an intermediate pHR-CD3z—CD28z-Puro plasmid. This intermediate construct and XhoI_X15 scTCR-Strep-CD8S_28-z were cut with MluI/BamHI to obtain a pHR-x—CD28z-Puro vector and a CD28z insert. Vector and insert were then ligated together generating the desired pHR-CD28z—CD28z-Puro construct.

- pHR-4-1BB-CD3z—4-1BB-CD3z-Puro:

This construct was generated by three PCRs to insert SpeI and NdeI restriction sites for the downstream signal motif. The second CD28TM domain was flanked with a different 4-1BB base sequence overhang compared to the upstream 4-1BB motif to avoid recombination effects between both domains, using a reverse primer. Forward primer was also flanked with a 4-1BB overhang upstream of CD3z sequence complementary to the reverse primer overhang in 34 base pairs. For first two PCRs pHR-CD3z—CD28-Puro was used as template DNA. Other primers are the same as used for pHR-CD28z—CD28z-Puro and bind to CD28TM domain and CD3z signal motif with flanked by SpeI/NdeI.

Oligonucleotide name	Sequence (5'-3')
DC_CD3z+4-1BB_Fwd	tgaggcctgtacagacaacgcaggaagaggacgggtgcagttgtc gtttccctgaggaggaggagggtggctgcgagctcAGGGTTAA ATTTTCCCGATCTGC
DC_CD28TM+4-1BB_Rev	Ccgtcctcttcctgcgttgtctgtacaggcctcatgaaaggctgcttaa aaatgtagagcagctttttcctcccgcgcttAACCCAAAATAT GATAAAAGCTACGG
DC_CD28z_NdeI_Rev_z	gcgccccatatgACGGGGTGGAAGTGCTTGC
DC_CD28z_SpeI_Fwd_CD28	gcgcccactagtTTCTGGGTTCTGGTTGTTGTTG

Table 3: Sequences of forward and reverse primers used to insert SpeI and NdeI restriction sites to obtain desired pHR-4-1BB-CD3z—4-1BB-CD3z-Puro construct

With the third PCR, overhangs were used to generate the 4-1BBz signal motif flanked with SpeI/NdeI restriction sites using products of first two PCRs as template DNA. This insert was ligated into the vector pHR-CD3z—x-Puro, which was then cut using MluI/BamHI to remove CD3z domain and insert 4-1BBz signal motif of XhoI_X15 scTCR-Strep-CD8S_4IBB-zeta_2A_Puro_NotI construct.

- pHR-CD3z-41BB-Puro:

The insert 4-1BBz of the downstream signal motif of pHR-41BBz—41BBz-Puro was used as template to produce 4-1BB as a signal motif. Primers bind to CD28TM and 4-1BB sequence flanked with SpeI and NdeI restriction sites, respectively. 4-1BB insert was then ligated to pHR-CD3z—x-Puro vector and transformed using DH5α.

Oligonucleotide name	Sequence (5'-3')
4-1BB_altered_Nde_Rev	GCGCCCCATATGgagctcgcagccaccctc
DC_CD28z_SpeI_Fwd_CD28	gcgcccactagtTTCTGGGTTCTGGTTGTTGTTG

Table 4: Sequences of forward and reverse primer used to insert SpeI and NdeI restriction sites and obtain 4-1BB motif

- pHR-CD28-CD3z-Puro:

CD28 with restriction sites MluI/BamHI was generated using PCR and XhoI_X15 scTCR-Strep-CD8S_28-z construct as template DNA. Forward primer contains a MluI site and anneals on CD28TM base sequence. Forward primer is designed to alter CD28TM base pair sequence to avoid interaction with downstream CD28TM sequence. Reverse primer binds on CD28 signal motif 3' end flanked by a NdeI site. pHR-CD3z—CD3z-Puro was cut with MluI/BamHI and CD28 PCR product ligated into the vector pHR-x—CD3z-Puro.

Oligonucleotide name	Sequence (5'-3')
X15_CD28_MluI_F	gcgcccacgcgtTCTGGGTATTGGTAGTCGTAGGTGGAGT CCTCGCATGTTATTCACTCTTGGTAACAGTTGCATTTA TTATTTTCT GGGTCAGGAGTAAGAGGAGCAGGCT
X15_CD28_BamHI_B	gcgcccggatccGGAGCGATAGGCTGCGAAG

Table 5: Sequences of forward and reverse primer inserting MluI and BamHI restriction sites to the attained CD28 motif

6.2.2 Single CAR Constructs

Furthermore, 5 single CAR constructs were inserted into the lentiviral pHR-vector. Two of them have a Puromycin and three a Blasticidin selection marker.

- pHR-CD3z-Puro
- pHR-CD28z-Puro
- pHR-41BB-bla
- pHR-CD28-bla
- pHR-CD28z-bla

Restriction sites XhoI and BamHI were used to generate an insert with antiCD19 scFv, CD8 hinge domain, CD28 transmembrane domain and desired signal motif, as both lentiviral vectors, pHR-x-Puro and pHR-x-bla, have XhoI and BamHI restriction sites.

- pHR-CD3z-Puro

This construct was produced using a pHR-x-Puro vector with restriction sites XhoI and BamHI. pHR-CD3z—CD28-Puro was cut with XhoI/BamHI generating an insert with CD3z signaling domain with CD28 transmembrane domain, CD8hinge domain and the scFv antiCD19, as the XhoI restriction site is upstream of the antiCD19 sequence. Vector and insert were ligated and transformation with XL1 Blue was carried out.

- pHR-CD28z-Puro

The same vector, pHR-x-Puro, was used as for pHR-CD3z-Puro. pHR-CD28z—CD28z was cut with XhoI and BamHI to produce desired insert with the antiCD19 and CD28-CD3z signaling domain. After ligation, transformation was carried out using XL1 Blue bacteria.

- pHR-41BB-bla

With PCR the downstream 4-1BB signal motif of pHR-41BBz—41BBz-Puro construct was produced using a forward primer binding on the downstream antiCD19 scFv sequence and reverse primer binding on 4-1BB flanked with a BamHI site. After PCR, the insert was ligated into the pHR-x-bla vector and transformed using XL1 Blue bacteria.

Oligonucleotide name	Sequence (5'-3')
CD19-2_XhoI_Fwd	gcgcccctcgagATGTTGTTGCTGGTCACTAGCT
41BB-2_BamHI_Rev	gcgcccggatccGAGCTCGCAGCCACCCTC

Table 6: Sequences of forward and reverse primer to insert XhoI and BamHI restriction sites to 4-1BB signal motif

- pHR-CD28-bla

Again, PCR was used to generate an insert consisting of antiCD19 scFv, CD8 hinge, CD28 transmembrane and CD28 signal motif. The construct pHR-CD3z—CD28-Puro as template and primers binding to the scFv and CD28 with XhoI/BamHI restriction sites were used. After ligation to the pHR-x-bla vector, transformation with XL1 Blue bacteria was performed.

Oligonucleotide name	Sequence (5'-3')
CD19-2_XhoI_Fwd	gcgcccctcgagATGTTGTTGCTGGTCACTAGCT
CD28-2_BamHI_Rev	gcgcccggatccAGATCGATATGCCGCAAAATCG

Table 7: Sequences of forward and reverse primer to insert XhoI and BamHI restriction sites to CD28 signal motif

- pHR-CD28z-bla

Lastly, pHR-CD28z-bla was generated using the same principles. The reverse primer flanked with BamHI however, anneals on CD3z domain, as the second motif of pHR-CD28z—CD28z-Puro was used as template for PCR. Ligation to pHR-x-bla was carried out and plasmids were transformed in XL1 Blue bacteria.

Oligonucleotide name	Sequence (5'-3')
CD19-2_XhoI_Fwd	gcgcccctcgagATGTTGTTGCTGGTCACTAGCT
CD3zDC-2_BamHI_Rev	gcgcccggatccACGGGGTGGAAGTGCTTGC

Table 8: Sequences of forward and reverse primer to insert XhoI and BamHI restriction sites to CD28z signal motif

Additionally, all single CAR constructs were inserted into a lentiviral vector without a Puromycin or Blasticidin resistance gene. This vector contains a XhoI restriction site in the MCS site followed by a BamHI site, followed by a stop codon, TAA.

Furthermore, CD19 CAR constructs (termed X variant aCD19-CARs) having the same amino acid sequence, but different codons were produced, using a CAR as template already generated in the Steinberger lab. CD28TM and signaling domains were also used from different constructs of the Steinberger lab having the same amino acid sequence, but different codons compared to CARs described above. HA-tag and V5-tag sequences were added to these constructs using PCR. Primers were designed to bind on CD28TM and CD8 Hinge region of X variant aCD19-CARs with HA-tag and V5-tag included.

Oligonucleotide name	Sequence (5'-3')
ST19_Xho_FW	gcgcccCTCGAGACCATGCTGCTGC
ST19_Strep_linker_HA_Rev1	TGGTGGGCGCCGGTGTTGGTGGTCGCGGCGCTGGCGTCGTGGTGGGAGCATAATCTGGGACATCATACGGATAACCACCACTGCCACCCTTCTCGAACTGGGGGTGGC
ST19_Strep_linker_HA_Rev2_CD8	gcgcccacgcgtCCAGCCCCCTCGTGTGCACTGCGCCCCCCGCCGCTGGCCGGGACGCCTCTGGGCGCAGGGACAGGGGCTGCGACGCGATGGTGGGCGCCGGTGTTGGT
ST19_Strep_linker_V5_Rev1	GGTGGGCGCCGGTGTTGGTGGTCGCGGCGCTGGCGTCGTGGTGGGAGTACTATCCAAACCGAGGAGTGGATTAGGTATTGGTTTCCCACCACTACCGCCCTTCTCGAACTGGGGGTGGC

Table 9: Sequences of forward and reverse primer to insert HA-, and V5-tag sequences to X variant aCD19-CARs.

Additionally, 3 X variant aCD19-CD3z constructs with part of CD28 signaling domain added in front of, within, or at the end of the CD3z intracellular sequence were created (termed aCD19-PYAP X). The PYAP motif is found at the downstream end of CD28 intracellular sequence. Sequences of all constructs are shown in the Appendix.

6.3 Functional Assays

6.3.1 Cell Culture

Triple parameter reporter cells (TPR), NFκB-reporter cells, both based on the Jurkat E6.1 cell line, and the human myelogenous leukemia cell line K562 were split every two to three days by changing RPMI medium supplemented with 10% heat-inactivated fetal calf serum (FCS), 100 µg/mL streptomycin and 100 U/mL penicillin (RPMI++). HEK293T cells were cultured in full IMDM medium (10% heat-inactivated fetal calf serum (FCS), X glutamine, 100 µg/mL streptomycin, and 100 U/mL penicillin) and split every three to four days.

Blood samples were obtained from healthy donors where peripheral blood mononuclear cells (PBMCs) were isolated via standard gradient density centrifugation using Lymphoprep® solution (Technoclone, Austria). PBMCs were depleted for $CD14^+$ cells (MagniSort™ Human CD14 Positive Selection Kit, Thermo Fisher).

6.3.2 Flow Cytometry

Conjugated fluorescent primary labeled antibodies and two primary biotinylated antibodies combined with a fluorochrome labeled secondary antibody were used for detection of CARs in the reporter and K562 cells after transduction. (Table 10)

Antigen	**Label**	**Final concentration**	**Company**	**Clone**
HA-tag	AF647	1:200	Cell Signaling Technology	6E2
V5-tag	PE-Cy7	1:200	eBioscience	TCM5
HA	Biotin	1:50	Roche	3F10
Strep-tagII	Biotin	1:200 (2.5µg/ml)	Genscript	5A9F9
CD14	PE	1:200	BioLegend	63D3
CD19	BV421	1:200	BioLegend	HIB19
CD25	PE-Cy7	1:200	BioLegend	M-A251
CD86	PE	1:200	BioLegend	IT2.2
CD4	BV421	1:200	BioLegend	OKT4
CD8	PerCP	1:200	BioLegend	HIT8a

Table 10: Table showing antibodies used for detection of CARs and receptors on reporter and K562 cells.

Cells were counted, harvested, and washed with FACS buffer solution (0,5 % FCS, 0,05 % NaN3 1x PBS) by pipetting cells up and down. Tubes were centrifuged, and supernatant removed. An appropriate amount of FACS buffer was added and 5 x 10^4 TPR cells in a volume of 50 µl were added to a round bottom FACS tubes. Antibody solutions were prepared (see table above) and added to the tubes. Tubes were spun, vortexed and put on 4 °C in the dark for 30 min. 500 µl FACS buffer were added to tubes, cells spun down (5 min, 1500 rpm), and buffer removed until 10 - 20 µl are left. To detect the binding of the Strep-TagII antibody (THE™ NWSHPQFEK Tag Antibody (Biotin), mAb, Mouse), ordered from GenScript (Piscataway, NJ), Phycoerythrin-labelled (PE-labelled) streptavidine was used ordered from BD Bioscience (San Jose, CA). FACS tubes were again centrifuged (5 min, 1500 rpm), vortexed, and put on 4 °C in the dark for 30 min. 500 µl FACS buffer were added, and tubes spun to wash cells. Buffer solution was removed and tubes vortexed, if necessary and not enough FACS buffer is in the tubes, add 10 - 20 µl FACS buffer. Measurements were carried out using Fortessa LSRII flow cytometer from BD (BD Bioscience, Franklin Lakes, NJ) and data was analyzed using FlowJo software (version 10.4.1, Tree Star, Ashland, OR).

6.3.3 Stimulation Assay

Jurkat reporter cells expressing CD19 CAR constructs and stimulator cells (K562 or BW cells) were counted using cell counter Beckman Coulter. 5 x 10^4 reporter cells were co-cultured with 2 x 10^4 stimulator cells in 96-well flat bottom plates for 24 h at 37 °C in an incubator (in a humidified atmosphere of 5% CO_2). Subsequently, cells were harvested and analyzed for eGFP, eCFP and mCherry expression using flow cytometry. K562 cells were engineered to constantly express a red fluorescent protein (RFP). Geometric mean of fluorescence intensity of viable reporter cells (RFP or mCD45.2 negative) was used for further analysis. LSR Fortessa flow cytometer from BD was used for measurements. Analysis was carried out using FlowJo software.

6.3.4 Cell sorting

Reporter or K562 cells were harvested and stained with the previously mentioned antibodies (Table 10). After 30 min incubation, cells were washed with FACS-buffer. Afterwards, the pellet was taken up in 200 - 800 µl FACS-buffer, depending on pellet size, and passaged through a cell strainer to obtain a single cell solution. Cell sorting was carried out with Sony SH800 cell sorter. After sorting, cells were washed and full RPMI++ medium was added.

6.3.5 Assay with CD14-depleted PBMCs

PBMCs from healthy donors were thawed and monocytes were depleted using Invitrogen MagniSort Human CD14 Positive Selection Kit. CD14-depleted PBMCs were then stimulated with Dynabeads (ThermoFisher Scientific) coated with aCD3 (OKT3) and aCD28 (CD28.2) antibodies (each 1 ug/ml) + TC medium (RPMI++ medium including 100 U/ml IL-2). After 48 h, cells were transduced with viral supernatant of desired constructs using spin infection (90min at 30 – 32 °C at 1500 rpm). The following day, medium was exchanged with fresh TC medium. 8 - 10 days later, cells positive for aCD19 were sorted with the Sony SH800 cell sorter. Afterwards, 1 x 10^5 sorted cells were seeded in 96-well round bottom plate. 5 x 10^5 K562 stimulator cells expressing different stimulatory ligands were incubated for 30 min at 37 °C with mitomycin-C (final 20 ug/ml in 1x PBS) to induce cell cycle arrest and prevent proliferation. Afterwards, stimulatory cells were washed 3x with 1 ml 1x PBS and 2 x 10^4 cells added to the sorted primary cells. After 24 h incubation at 37 °C, cells were harvested and stained with CD4-BV421, CD8-PerCP and CD25-PeCy7 antibodies ordered from BioLegend (San Diego, CA). Measurement was done on a Fortessa LSRII flow cytometer from BD. Prior to staining, supernatant was harvested for cytokine measurement.

7 Results

7.1 Overview of constructs

Throughout this study various combinations of CARs, which differ by their codon-usage, were established in a lentiviral pHR vector system (Table 11). All CAR constructs comprise a strep-tag domain and an additional tag (HA- or V5-tag). Mainly two different CAR sequences were used, one originating from the Dual CAR aCD19:CD3z-aCD19:CD28 synthesized for this study, termed ‘DC’ variant. The second one, from earlier studies in the lab, originates from the single CARs aCD19:CD3z (X), aCD19:CD28z (X) and aCD19:41BBz (X), termed X variants. Several cloning steps have been used to generate desired Dual and single CAR constructs with sequences from the synthesized Dual CAR. From the X variant only single CAR constructs were generated. Throughout this study the histograms of cell surface expression of Dual CAR originated molecules are colored in blue and those from X variants are colored in red. The spelling for e.g., ‘aCD19:CD3z-aCD19:CD28’ refers to Dual CAR, whereas ‘aCD19:CD3z/aCD19:CD28’ refers to single CARs simultaneously transduced with aCD19:CD3z and aCD19:CD28.

CAR Construct	Selection marker	Sequence origin	Dual/Single CAR	Tag
aCD19:CD3z-aCD19:CD28	Puro	DC-DC	Dual CAR	V5 + HA
aCD19:CD3z-aCD19:CD28		DC-DC	Dual CAR	V5 + HA
aCD19:CD3z-aCD19:41BB	Puro	DC-DC	Dual CAR	V5 + HA
aCD19:41BBz-aCD19:41BBz	Puro	X-DC	Dual CAR	V5 + HA
aCD19:CD3z	Puro	DC	Single CAR	V5
aCD19:CD28	Bla	DC	Single CAR	HA
aCD19:CD3z/aCD19:CD28	Puro + Bla	DC-DC	Single CARs	V5 + HA
aCD19:CD28z	Puro	DC	Single CAR	V5
aCD19:41BB	Bla	DC	Single CAR	HA
aCD19:CD3z/aCD19:41BB	Puro + Bla	DC-DC	Single CARs	V5 + HA
aCD19:41BBz	Bla	DC	Single CAR	HA
aCD19:CD3z		DC	Single CAR	V5
aCD19:CD28		DC	Single CAR	HA
aCD19:CD3z/aCD19:CD28		DC-DC	Single CARs	V5 + HA
aCD19:CD28z		DC	Single CAR	V5
aCD19:41BB		DC	Single CAR	HA
aCD19:CD3z/aCD19:41BB		DC-DC	Single CARs	V5 + HA
aCD19:41BBz		DC	Single CAR	HA
aCD19:CD3z	Puro	X	Single CAR	HA
aCD19:CD28	Puro	X	Single CAR	V5
aCD19:CD3z/aCD19:CD28	Puro + Puro	X-X	Single CARs	HA + V5
aCD19:CD28z	Puro	X	Single CAR	HA
aCD19:41BB	Puro	X	Single CAR	V5
aCD19:CD3z/aCD19:41BB	Puro + Puro	X-X	Single CARs	HA + V5
aCD19:41BBz	Puro	X	Single CAR	HA
aCD19:CD3z_PYAP-1	Puro	X	Single CAR	
aCD19:CD3z_PYAP-2	Puro	X	Single CAR	
aCD19:CD3z_PYAP-3	Puro	X	Single CAR	

Table 11: Overview of all constructs used throughout this study. Puromycin is abbreviated with 'Puro' and Blasticidin with 'Bla'.

7.2 Detection of surface expression of Dual CAR constructs

To analyze and compare different intracellular signaling domains of our CD19 CAR constructs, we used a Jurkat NF-κB-eGFP reporter cell line as well as the triple parameter reporter cells line (TPR). Following lentiviral transduction, cell surface expression of the various CAR constructs was determined via flow cytometry. Surface expression of the Dual CAR constructs transduced in these cells was determined through staining of Strep-tag antibody followed by streptavidine-PE (Fig. 3). Staining was performed of all constructs except for aCD19:CD3z-aCD19:CD28 (w/o puromycin) after puromycin selection. For some constructs the puromycin resistance marker was removed in an attempt to increase the expression of the CAR molecules.

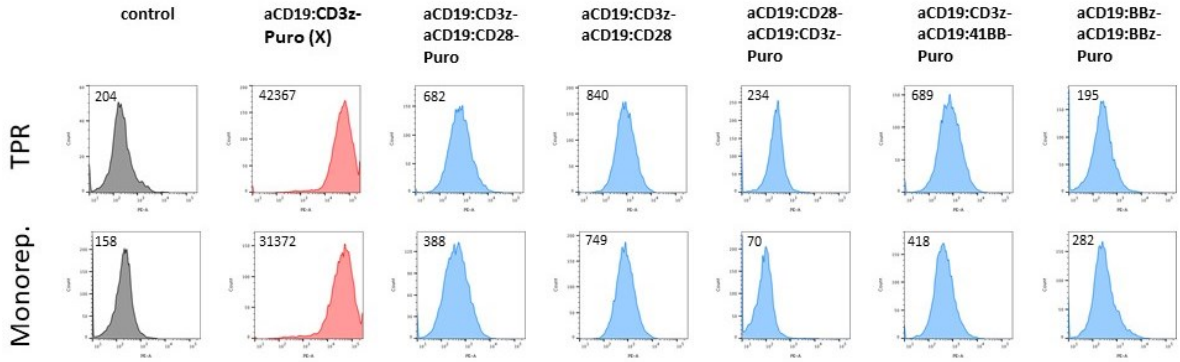

Figure 3: Cell surface expression of CD19 Dual CAR constructs on Jurkat Triple parameter reporter (TPR) and NF-κB-reporter cells. Detection was performed via a NWSHPQFEK Tag-bio (Strep-tag) antibody followed by streptavidine-PE. Numbers in histograms indicate geometric mean of fluorescent intensity. Blue histograms show CAR constructs representing the sequences originated from the synthesized CAR construct. Red histograms show CAR constructs aCD19:CD3z (X) consisting of different codons (X variant) originating from earlier studies. Grey histograms are non-transduced reporter cells as controls.

We observed a high expression of the aCD19:CD3z (X) variant in comparison to the Dual CAR constructs, which showed very low or no cell surface expression (Fig. 3). Expression of aCD19:CD3z-aCD19:CD28 (w/o puromycin) was slightly higher than that of the Dual CAR construct containing the selection marker. Results attained are similar for both, TPR and NF-κB-reporter cells.

7.3 Cell surface expression of aCD19 single CAR constructs

To achieve better cell surface expression of CAR constructs compared to Dual CARs we separated the CAR constructs to single CARs harboring one intracellular domain. Simultaneous transduction of CARs with a CD3z intracellular domain and a costimulatory domain (CD28 or 4-1BB) was performed to attain signal 1 and 2 in the same cell through aCD19 signaling. Following lentiviral transduction, cell surface expression of the various CAR constructs was determined via flow cytometry. To distinguish between single CARs, each CAR was equipped with a specific tag fused to fluorescent label (V5-PECy7 or HA-AF647) in addition to the strep-tag and either a puromycin or blasticidin resistance marker was added. Surface expression was determined through staining of strep-tag antibody followed by streptavidine-PE or V5-PECy7 and HA-AF647 antibodies, respectively (Fig. 4). V5-PECy7 and HA-AF647 antibodies were used to concurrently detect expression of simultaneously transduced CARs. Staining was performed after puromycin/blasticidin selection.

We observed a high expression of aCD19:CD3z of both variants (X and DC), with even higher expression of the X variant, especially in TPR. Constructs with an CD28 domain show high surface expression, whereas constructs containing 4-1BB in their intracellular domain show weak surface expression. aCD19:41BBz was not detectable on the cell surface in TPR cells (Fig. 4). Results are similar in both TPR and NF-κB-reporter cells, but HA staining of aCD19:CD3z/aCD19:CD28 expressed CARs in NF-κB-reporter cells resulted in much weaker or even absent signals compared to the TPR equivalent, which might be due to experimental issues. Unfortunately, HA and V5 stainings did not lead to satisfying results.

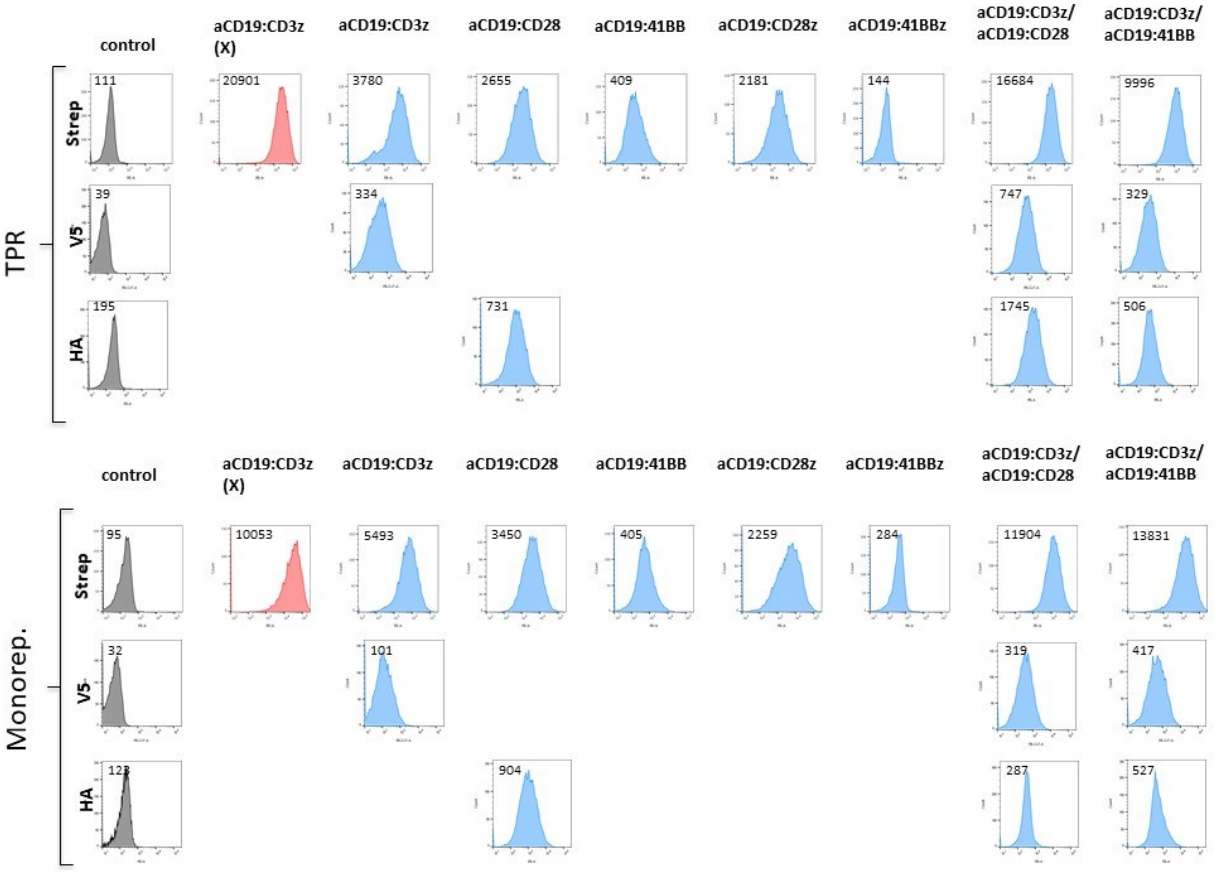

Figure 4: Cell surface expression of CD19 CAR constructs on Jurkat Triple parameter reporter (TPR) (upper panel) and NF-κB-reporter cells (lower panel). Detection was performed via a NWSHPQFEK Tag-bio (Strep-tag) antibody followed by streptavidine-PE antibody, a V5-PECy7 antibody and an HA-AF647 antibody. V5 and HA tags were used to concurrently detect CARs with CD3z and a costimulatory domain. Numbers in histograms indicate geometric mean of fluorescent intensity. Blue histograms show CAR constructs representing the sequences originated from the synthesized CAR construct (DC). Red histograms show CAR constructs aCD19:CD3z (X) consisting of different codons (X variant). Grey histograms are non-transduced reporter cells as controls.

7.4 Functional comparison and evaluation of CD19-expressing stimulator cells

For stimulation of the CD19 CARs, we first compared two different cell lines, specifically the human K562 and the murine BW5147 cell line. TPRs harboring either the Dual CAR construct aCD19:CD3z-aCD19:CD28 or a single CAR, aCD19:CD3z or aCD19:CD3z (X), were co-cultured with control K562, K562:CD19, control BW and BW:CD19 cells (Fig. 5). CD19 surface expression on K562 and BW cells is depicted (Fig. 5, upper panel). NF-κB-eCFP, NFAT-eGFP and AP-1-mCherry activation were assessed using flow cytometry.

We observed activation of all transcription factors upon stimulation of reporter cells expressing CAR constructs with the CD19 stimulatory domain. However, we noticed a lower activation with BW:CD19 cells than with K562:CD19. Noteworthy, K562 cells endogenously express CD58 on the cell surface which interacts with CD2 on reporter cells. Overall, reporter cells expressing the Dual CAR construct were less activated in comparison to reporter cells expressing constructs encoding single CARs, which might be due to their weak cell surface expression. The single CARs both resulted in high activation of reporter cells after stimulation with CD19. The DC variant showed better stimulation of NF-κB and NFAT than the X variant.

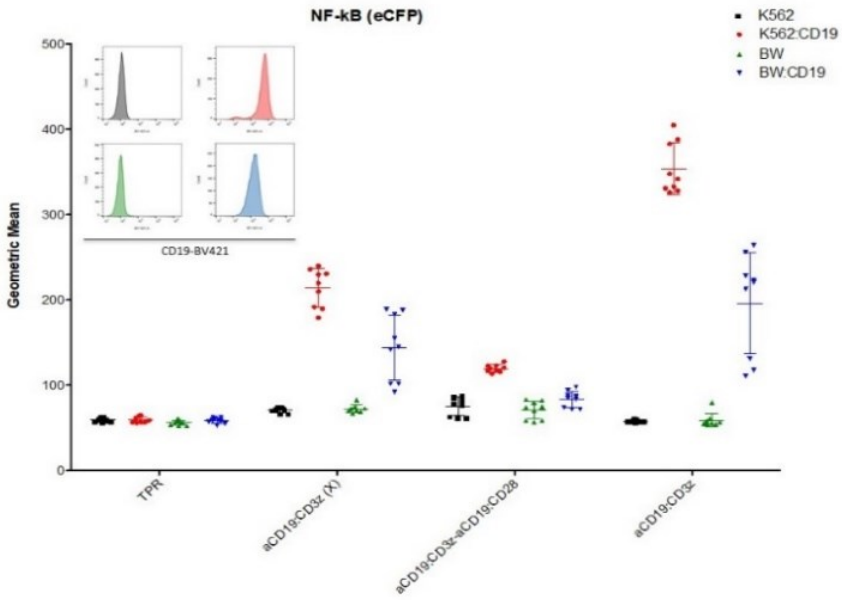
NF-kB (eCFP)
K562
K562:CD19
BW
BW:CD19
Geometric Mean
CD19-BV421
TPR
aCD19:CD3z (X)
aCD19:CD3z-aCD19:CD28
aCD19:CD3z

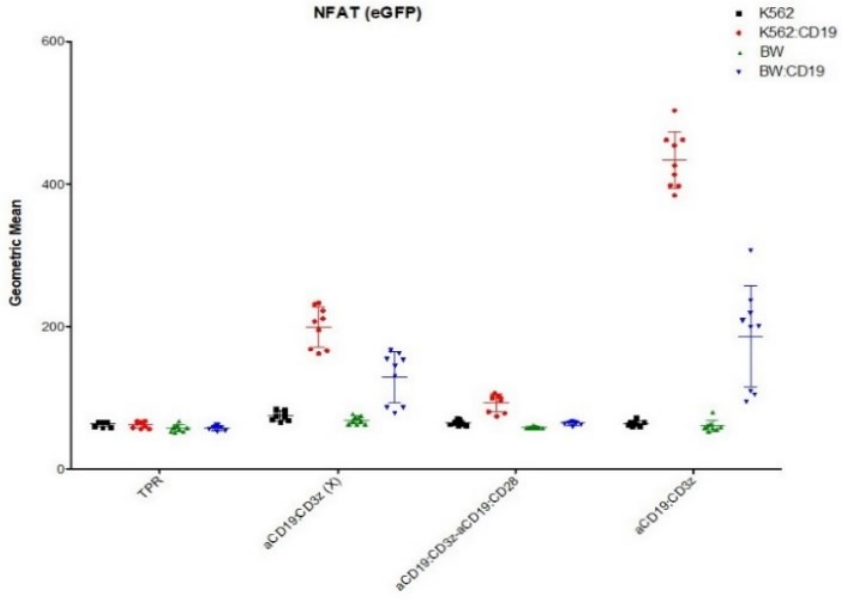
NFAT (eGFP)
K562
K562:CD19
BW
BW:CD19
Geometric Mean
TPR
aCD19:CD3z (X)
aCD19:CD3z-aCD19:CD28
aCD19:CD3z

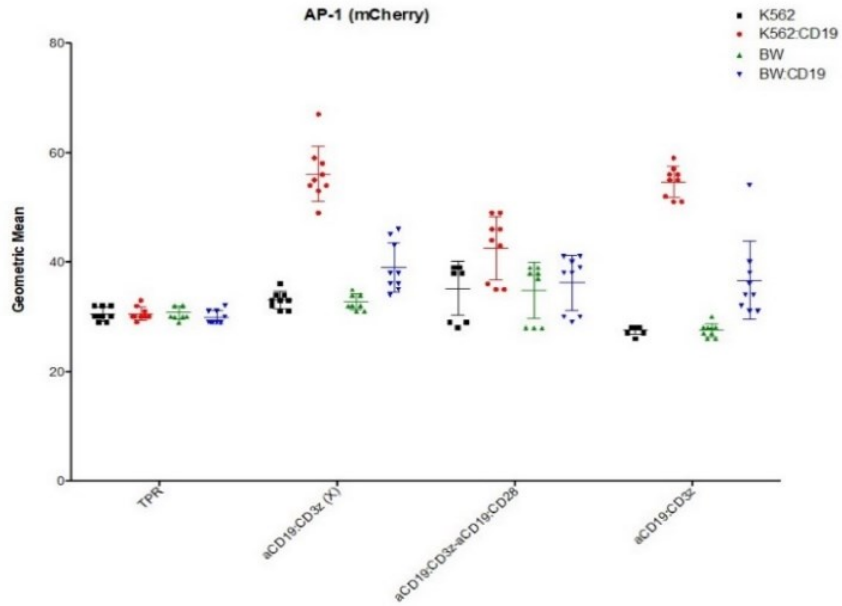
AP-1 (mCherry)
K562
K562:CD19
BW
BW:CD19
Geometric Mean
TPR
aCD19:CD3z (X)
aCD19:CD3z-aCD19:CD28
aCD19:CD3z

Figure 5: Functional comparison of CARs expressed from constructs encoding single CARs and from a Dual CAR construct in Triple parameter reporter (TPR) cells with different stimulator cells, K562:CD19 and BW:CD19. TPR control and TPR expressing aCD19 CAR variants were co-cultured with K562, K562:CD19, BW and BW:CD19. Geometric mean indicates reporter activation. Upper panel shows activation of NF-κB-eCFP and cell surface expression of CD19 in K562 and BW, middle panel NFAT-eGFP and lower panel AP-1-mCherry. Activation of CAR constructs was measured via flow cytometry. Results of 3 independent experiments performed in triplicates are depicted. Mean (SD) values are shown.

Since K562:CD19 induced higher activation of transcription factors than BW:CD19 when co-cultured with TPR in this experiment, we decided to proceed with the K562 cell line as stimulators. In addition to K562:CD19, we generated the following stimulator cells: K562:aCD3, K562:aCD3:CD86, K562:CD19, K562:aCD3:CD19 and K562:CD19:CD86 (Fig. 6). The ‘aCD3’ refers to an anti-human CD3 single chain fragment fused to a human CD14 stem (CD5L-OKT3scFv-CD14), which enables the engagement and activation of the TCR-CD3 complex on the Jurkat cells. CD86 interacts with CD28 and is used to provide costimulation of Jurkat cells.

Following lentiviral transduction, we generated single cell clones of each K562 construct to ensure stable expression of stimulatory ligands. Cell surface expression was determined through staining with ligand-specific PE- or BV421 labeled antibodies via flow cytometry (Fig. 6). K562 stimulator cells are engineered to constantly express a red fluorescent protein (RFP).

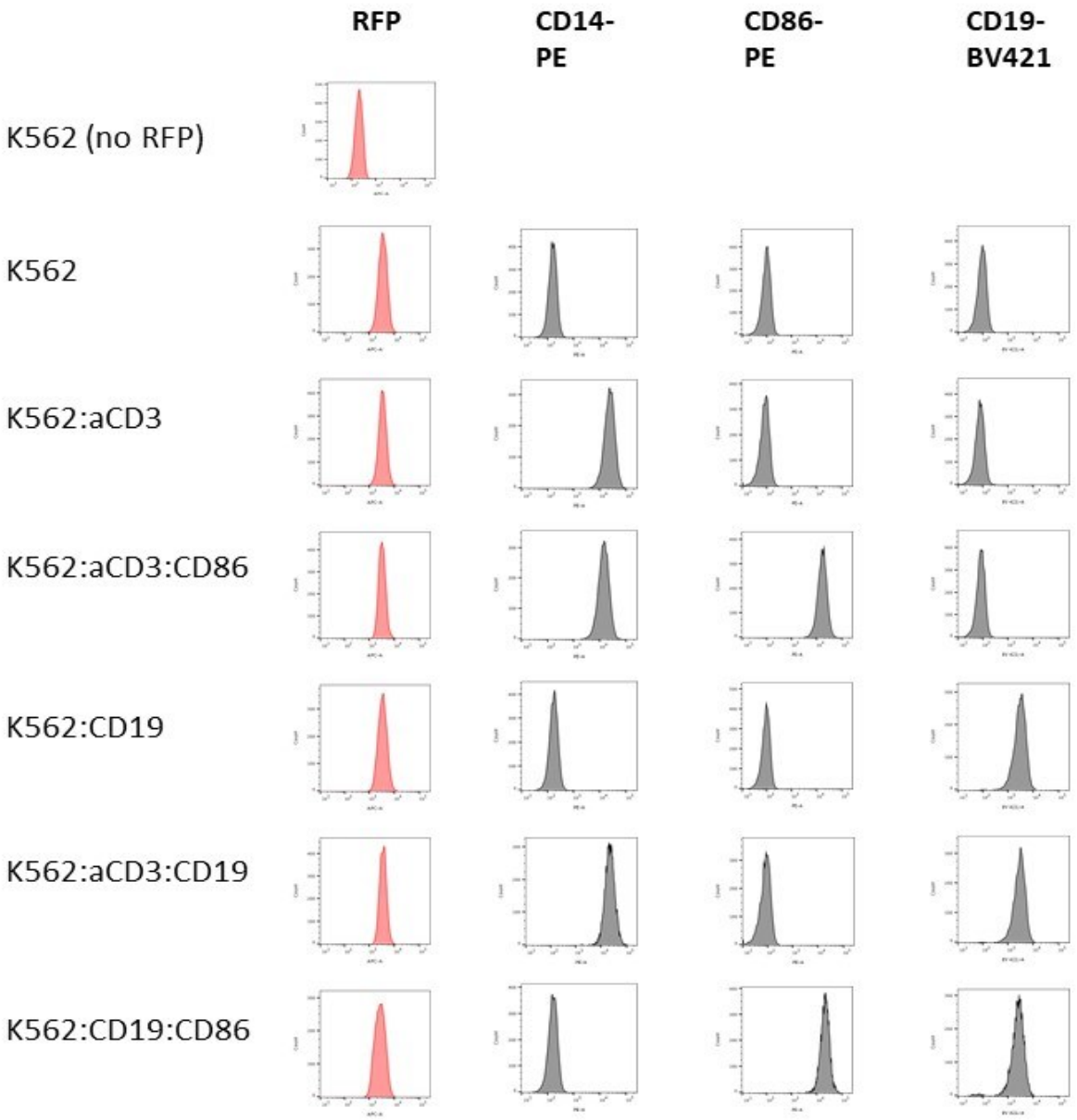

Figure 6: Cell surface expression of stimulatory ligands on K562 cells. K562 stimulator cells were engineered to constantly express a red fluorescent protein (RFP) shown with red histograms. Cells were analyzed for cell surface expression of aCD3, CD86 and CD19 by using CD14-PE, CD86-PE and CD19-BV421 antibodies. Analysis was performed using flow cytometry.

7.5 Functional comparison of aCD19 Dual CARs in TPR and NF-κB-reporter cells

After cell surface expression of CD19 CARs and K562 stimulators was determined, we co-cultured TPR and NF-κB-reporter cells harboring different CAR constructs with either K562, K562:aCD3, K562:CD19 or K562:CD19:CD86 cells and assessed NF-κB, NFAT and AP-1 activation upon stimulation (Fig. 7, 8).

K562:aCD3 cells stimulate Jurkat cells via its endogenous TCR, while K562:CD19 stimulate cells via the aCD19 domain on the CAR construct. To compare the costimulation of the CAR and the endogenously expressed CD28 receptor on the Jurkat cells, we co-cultured the cells transduced with a CAR with K562:CD19:CD86.

CD19 stimulation of single CAR constructs aCD19:CD3z and aCD19:CD3z (X) induced stronger activation of NF-κB than stimulation via K562:aCD3 in the NF-κB-reporter system (Fig. 7, left panel). In TPR, the effect of CD19 CAR activation compared to the endogenous TCR was similar for the X variant and lower for the DC variant (Fig. 8, left panel). K562:aCD19:CD86 enhanced the activation of NF-κB compared to CD19 stimulation alone (Fig. 7, 8a).

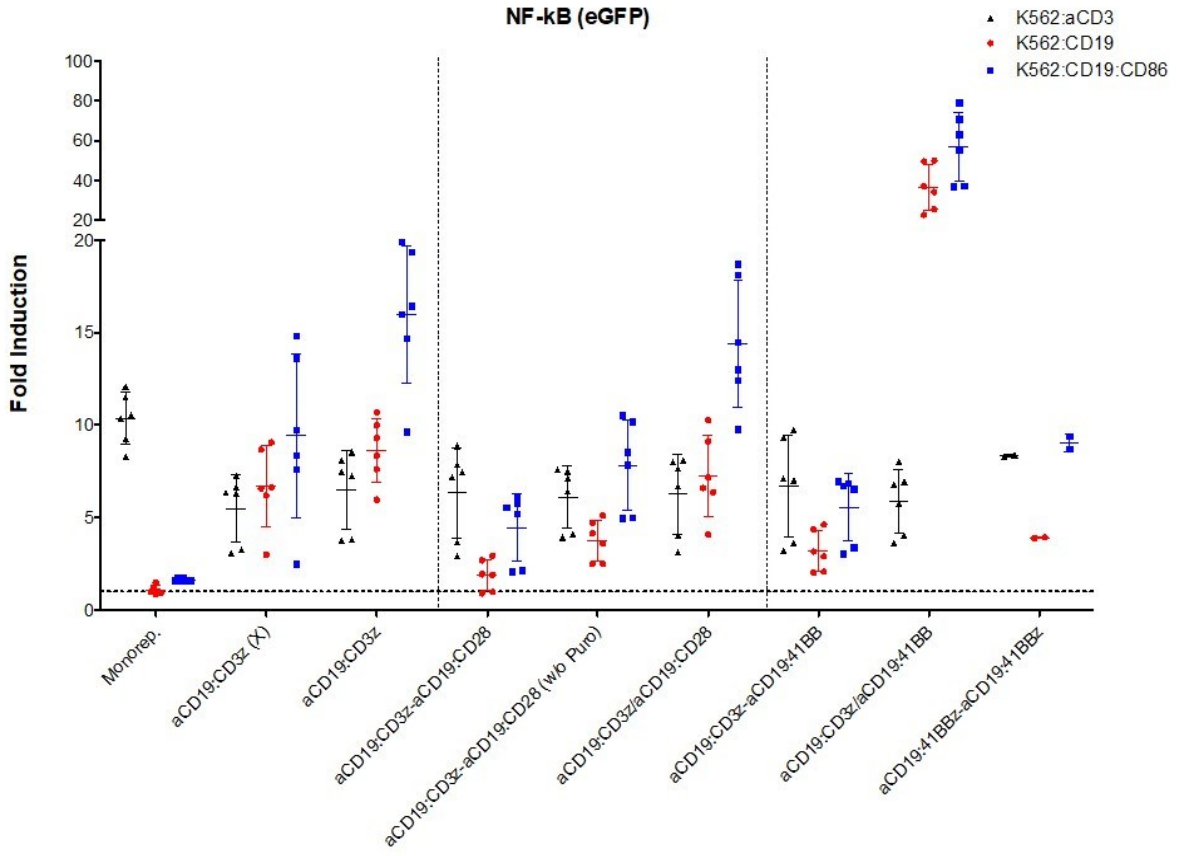

Figure 7: Functional comparison of different aCD19 CARs harboring various signaling domains in an NF-κB-reporter system. NF-κB-reporter cells not expressing CD19-CARs served as controls. Jurkat NF-κB-eGFP control and Jurkat NF-κB-eGFP expressing aCD19 CAR variants were left unstimulated or co-cultured with K562, K562:aCD3, K562:CD19 and K562:CD19:CD86. Reporter activation (NF-κB-eGFP) is shown as fold induction (gMFI of K562-ligand stimulated reporter cells/K562 control stimulated reporter cells). Left panel shows control reporter cells and 1st generation CARs. Middle panel shows stimulation of Dual CARs containing CD28 signaling domains. Right panel shows stimulation of Dual CARs containing 4-1BB signaling domains. Activation of CAR constructs was measured via FACS analysis. Results of 3 independent experiments performed in duplicates are depicted. Only one experiment was carried out with aCD19:41BBz-aCD19:41BBz CAR construct. Mean (SD) values are depicted.

Stimulation of reporter cells transduced with Dual CAR constructs containing CD28 signaling domains aCD19:CD3z-aCD19:CD28 (with or w/o Puromycin resistance marker) did lead to lower induction of NF-κB (Fig. 7, 8a, middle panels), NFAT and AP-1 reporter genes (Fig. 8b and c, middle panels) compared to single CARs. However, reporter cells expressing aCD19:CD3z-aCD19:CD28 (w/o puromycin) resulted in higher activation of NF-κB (Fig. 7, 8a, middle panels) upon stimulation with K562:CD19 when compared to aCD19:CD3z-aCD19:CD28 (with Puromycin resistance marker) correlating with higher surface expression. In addition to the Dual CARs, we generated single CARs which are based on the Dual CAR constructs (DC variants). To obtain Jurkat cells expressing aCD19:CD3z/aCD19:CD28, the cells were simultaneously

transduced with aCD19:CD3z and aCD19:CD28. Surface expression of single CARs and simultaneously double transduced single CARs is shown in Figure 4.

Dual CARs with 4-1BB as costimulatory domain (Fig. 7, 8, right panels) show similar but slightly better activation of NF-κB than the Dual CARs with CD28 as costimulatory domain. For the aCD19:41BBz-aCD19:41BBz Dual CAR only one experiment was carried out. Stimulation of NF-κB-reporter cells expressing the two single CARs aCD19:CD3z/aCD19:41BB (aCD19:CD3z and aCD19:41BB) with K562:CD19 resulted in a significant increase in NF-κB activation in comparison to the other CARs (Fig. 7). In comparison, the TPR cells show a similar effect in NF-κB, but not as profound as it was observed with the NF-κB-reporter cells (Fig. 8a, right panel). 4-1BB did not have a strong enhancing effect on NFAT signaling, as stimulation via K562:CD19 and K562:CD19:CD86 resulted in lower activation than K562:aCD3 (Fig. 8b, right panel).

Overall, stimulation of reporter cells expressing single CARs, or two single CARs resulted in increased activation of NF-κB in comparison to Dual CARs. Nevertheless, this may be due to the difficulties to express these Dual CARs on reporter cells.

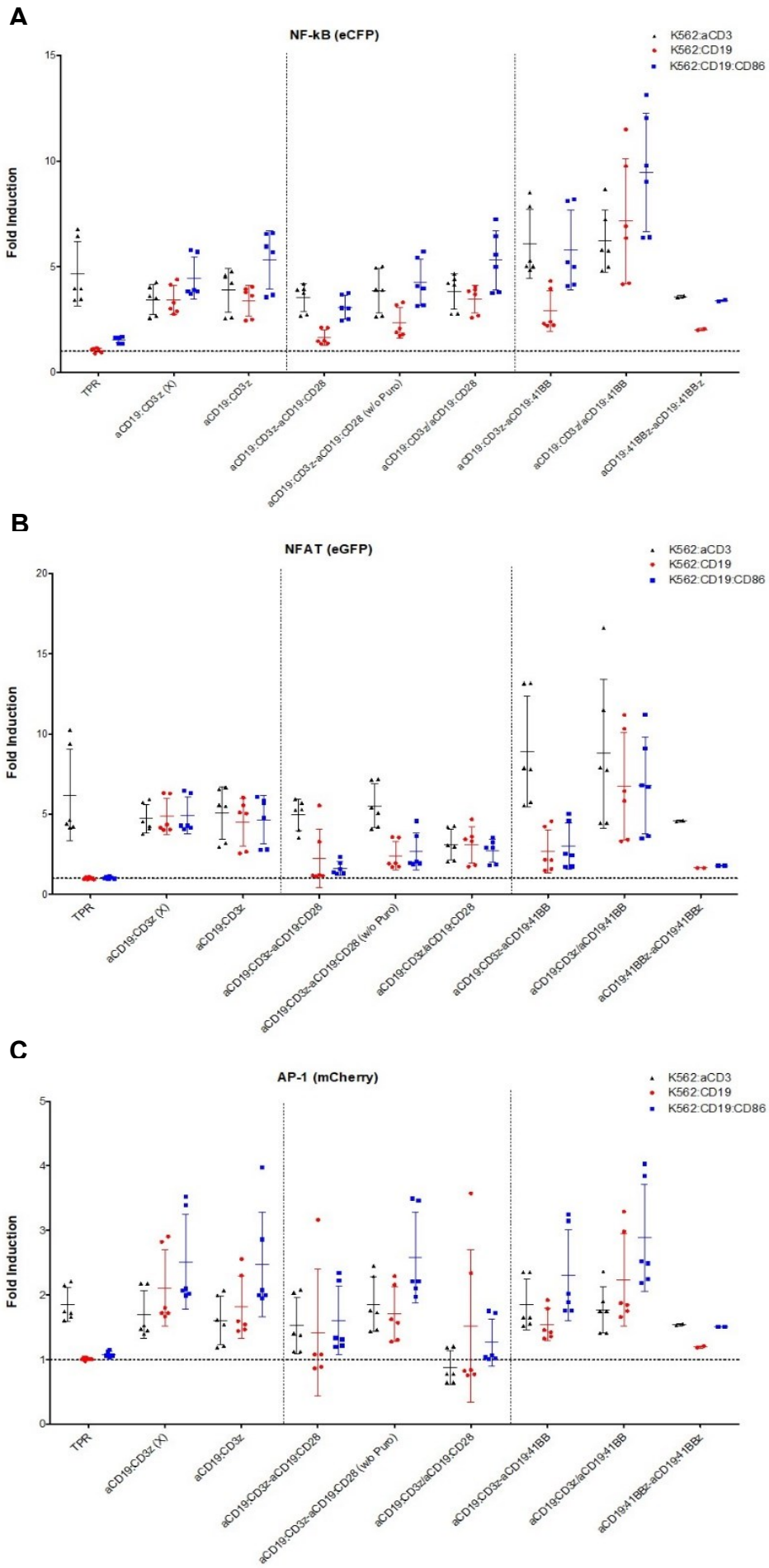
A
NF-kB (eCFP)
K562:aCD3
K562:CD19
K562:CD19:CD86
Fold Induction
TPR
aCD19:CD3z (X)
aCD19:CD3z
aCD19:CD3z-aCD19:CD28
aCD19:CD3z-aCD19:CD28 (w/o Puro)
aCD19:CD3z/aCD19:CD28
aCD19:CD3z-aCD19:41BB
aCD19:CD3z/aCD19:41BB
aCD19:41BBz-aCD19:41BBz
B
NFAT (eGFP)
K562:aCD3
K562:CD19
K562:CD19:CD86
Fold Induction
TPR
aCD19:CD3z (X)
aCD19:CD3z
aCD19:CD3z-aCD19:CD28
aCD19:CD3z-aCD19:CD28 (w/o Puro)
aCD19:CD3z/aCD19:CD28
aCD19:CD3z-aCD19:41BB
aCD19:CD3z/aCD19:41BB
aCD19:41BBz-aCD19:41BBz
C
AP-1 (mCherry)
K562:aCD3
K562:CD19
K562:CD19:CD86
Fold Induction
TPR
aCD19:CD3z (X)
aCD19:CD3z
aCD19:CD3z-aCD19:CD28
aCD19:CD3z-aCD19:CD28 (w/o Puro)
aCD19:CD3z/aCD19:CD28
aCD19:CD3z-aCD19:41BB
aCD19:CD3z/aCD19:41BB
aCD19:41BBz-aCD19:41BBz

Figure 8: Functional comparison of different aCD19 CARs harboring various signaling domains in a triple parameter reporter system (TPR). TPR cells served as controls. TPR control and TPR expressing aCD19 CAR variants were left unstimulated or co-cultured with K562, K562:aCD3, K562:CD19 and K562:CD19:CD86. Reporter activation is shown as fold induction (gMFI of K562-ligand stimulated reporter cells/K562 control stimulated reporter cells). ***A)*** *indicates NF-κB-eCFP activation* ***B)*** *indicates NFAT-eGFP and* ***C)*** *indicates AP-1-mCherry activation.). Left panel shows control reporter cells and 1st generation CARs. Middle panel shows stimulation of Dual CARs containing CD28 signaling domains. Right panel shows stimulation of Dual CARs containing 4-1BB signaling domains. Activation of CAR constructs was measured via FACS analysis. Results of 3 independent experiments performed in duplicates are depicted. Only one experiment was carried out with aCD19:41BBz-aCD19:41BBz CAR construct. Mean (SD) values are depicted.*

7.6 Functional comparison of aCD19 Single CARs in NF-κB-reporter cells

After cell surface expression of the CD19 single CARs was determined on reporter cells, we co-cultured reporter cells with either K562, K562:aCD3, K562:CD19 or K562:aCD3:CD19 cells and assessed NF-κB activation upon stimulation (Fig. 9, Fig. 4). To assess CD28 and 4-1BB costimulatory effects of CAR constructs upon stimulation via endogenous TCR, K562:aCD3:CD19 cells were used for co-cultivation. CD19 stimulation of reporter cells harboring single CAR constructs aCD19:CD3z or aCD19:CD3z (X) induced higher activation of NF-κB than stimulation via the TCR with K562:aCD3 (Fig 7 right panel). The X variant of aCD19:CD3z resulted in higher expression of NF-κB upon stimulation via K562:CD19 than the DC variant correlating with surface expression levels (Fig. 4). Costimulation of the TCR via aCD3 and the CAR via CD19 led to marginal increase in NF-κB expression for aCD19:CD3z and the aCD19:CD28 CARs in comparison to K562:CD19, or K562:aCD3 stimulation (Fig. 9, left and middle panels). Stimulation of aCD19:CD28z or aCD19:CD3z/ aCD19:CD28 CAR yielded similar NF-κB activation compared to aCD19:CD3z (Fig. 9, left and middle panels).

Again, CARs containing 4-1BB domains resulted in strong NF-κB expression in reporter cells upon stimulation with K562:CD19. aCD19:41BB activation was strongly enhanced through K562:aCD3:CD19 by simultaneously triggering the endogenous TCR and the CAR (Fig. 9, right panels). Profound NF-κB activation was achieved for aCD19:CD3z/aCD19:41BB when stimulated with K562:CD19. The effect was increased upon K562:aCD3:CD19 stimulation (Fig. 9, right panels). K562:aCD3:CD19 stimulation of reporter cells comprising aCD19:41BBz (X) led to marginal higher NF-κB activation compared to stimulation with K562:aCD19. Both stimulatory cell lines resulted in increased induction of NF-κB compared to K562:aCD3. Surface expression of aCD19:41BBz (X) is shown in Figure 10. Similar to aCD19:CD28z, costimulatory

effects of aCD19:41BBz (X) through CD19 CAR did not enhance signal 1 via the TCR, which might be due to steric hindrance of costimulatory domain upon successive arrangement of CD3z and costimulatory domains intracellularly.

aCD19:41BBz caused tonic signaling of reporter cells, for aCD19:CD28z this effect also can be seen however in much lower levels (Fig. 9b). Tonic signaling for reporter cells with high surface expression of CARs containing a 4-1BB signaling domain can be seen throughout this study (Supplementary Fig. 6).

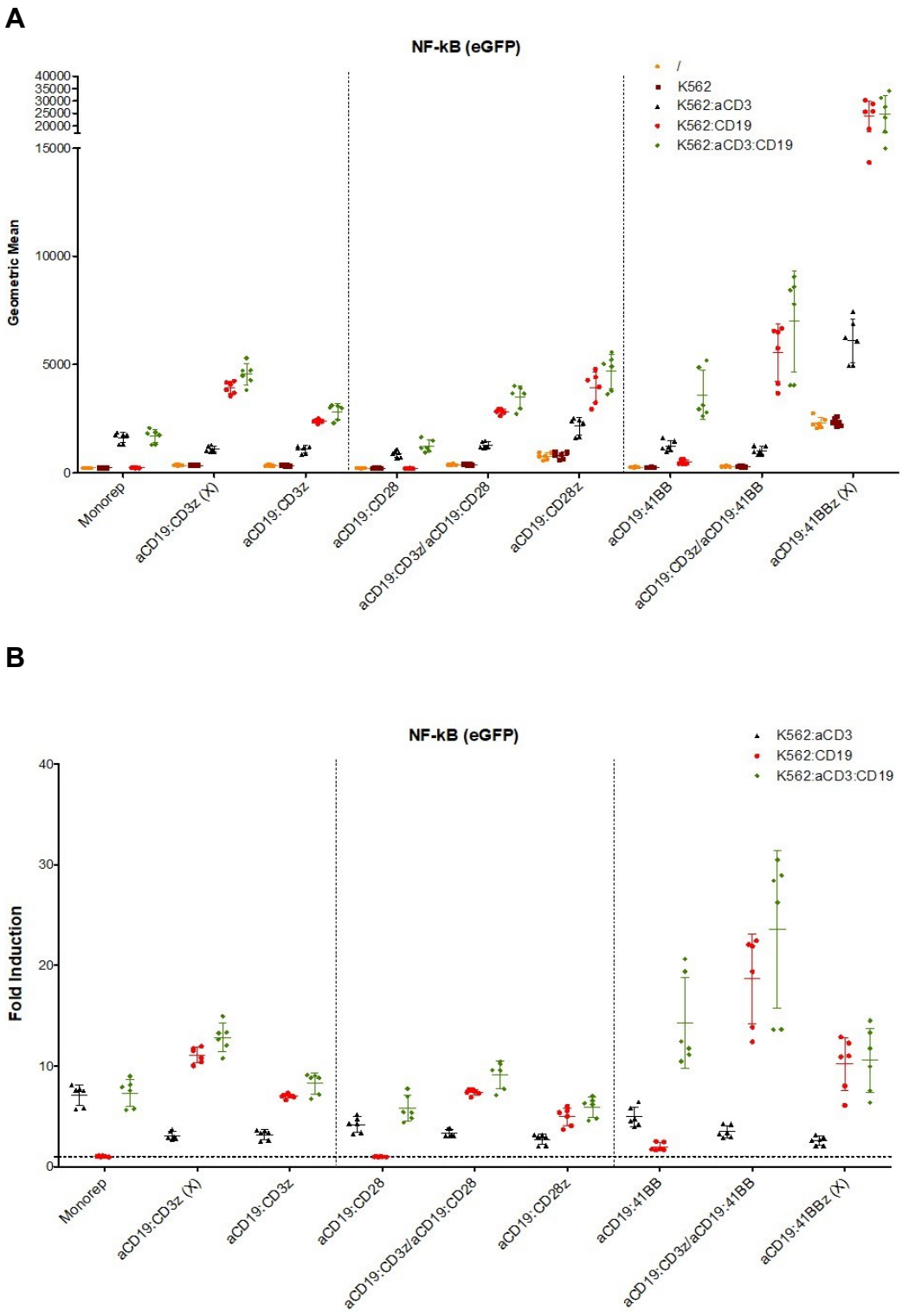

*Figure 9: Functional comparison of different aCD19 CARs harboring various signaling domains in an NF-κB-reporter system. NF-κB-reporter control and NF-κB-reporter expressing aCD19 CAR variants were left unstimulated or co-cultured with K562, K562:aCD3, K562:CD19 and K562:aCD3:CD19. Reporter activation (NF-κB-eGFP) is shown as **A)** gMFI and **B)** fold induction (gMFI of K562-ligand stimulated reporter cells/K562 control stimulated reporter cells). Left panel shows control reporter cells and 1st generation CARs. Middle panel shows stimulation of CARs containing CD28 signaling domains. Right panel shows stimulation of CARs containing 4-1BB signaling domains. Activation of CAR constructs was measured via FACS analysis. Results of 3 independent experiments performed in duplicates are depicted. Mean (SD) values are depicted.*

7.7 Cell surface expression of aCD19 single CAR constructs w/o puromycin/blasticidin resistance markers

To reduce size of the vector containing the CAR construct and gain better surface expression, we removed the puromycin/blasticidin resistance markers of single CAR (DC) constructs. Following lentiviral transduction, cell surface expression of the various CAR constructs was determined via flow cytometry. Analysis of surface expression was performed through staining of strep-tag antibody followed by streptavidine-PE, aV5-PECy7 and aHA-biotin followed by streptavidine-PE antibodies (Fig. 10).

We observed high surface expression of all constructs containing an intracellular CD28 or 41BB domain. aV5 and aHA antibodies were used to concurrently detect the expression of simultaneous transduced CARs, but V5 staining did not attain expression values as expected, due to experimental difficulties. For aCD19:41BBz and aCD19:41BBz-bla cell surface expression, only low levels could be detected. Therefore, aCD19:41BBz (X), which harbors a puromycin resistance marker, was used for further experiments. TPR and NF-κB-reporter cells with an aCD19:41BBz CAR construct were later sorted for better expression (data not shown). Overall, expression of CAR constructs was higher in NF-κB reporter cells than TPR.

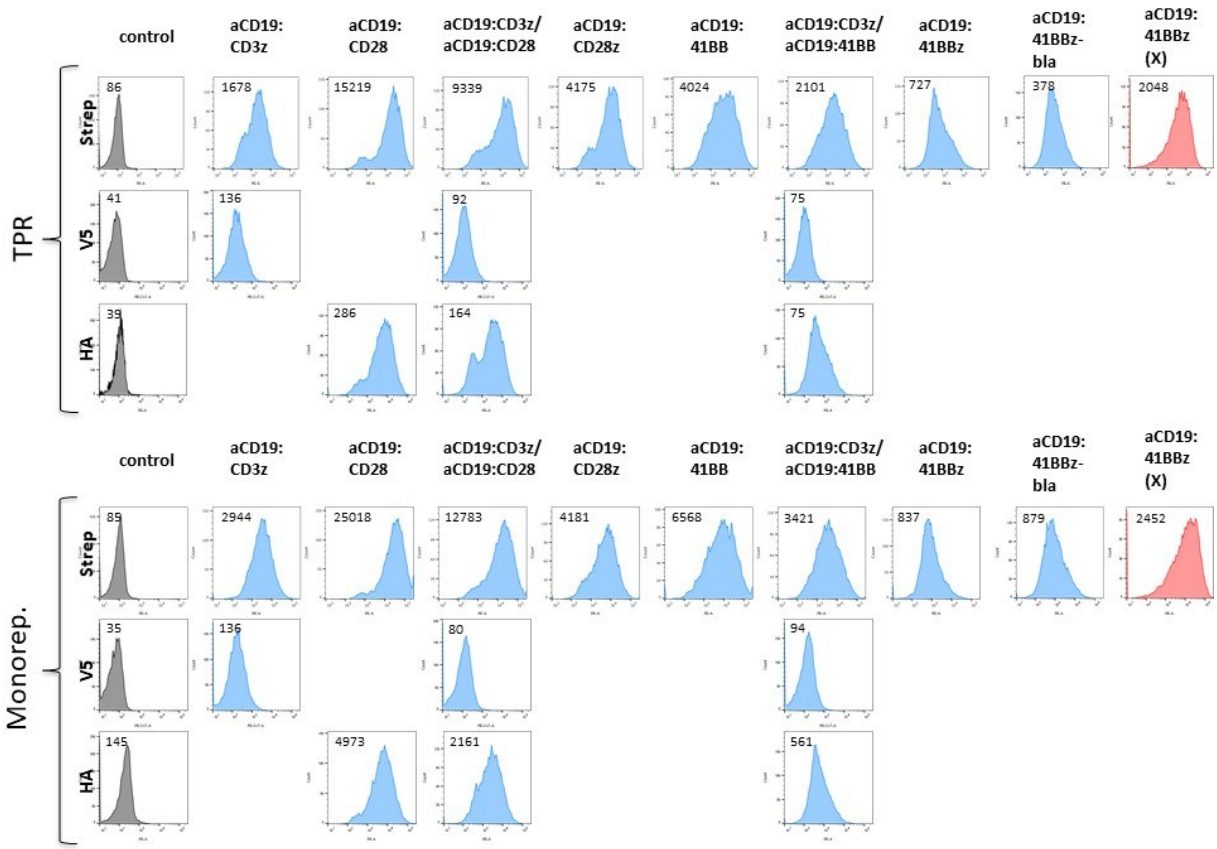

Figure 10: Cell surface expression of aCD19 CAR constructs w/o puromycin or blasticidin resistance marker on Jurkat Triple parameter reporter (TPR) (upper panel) and NF-κB-reporter cells (lower panel). Detection was performed via a NWSHPQFEK Tag-bio (Strep-tag) antibody followed by streptavidine-PE antibody, a V5-PECy7 antibody and an HA-AF647 antibody. V5 and HA tags were used to concurrently detect CARs with CD3z and a costimulatory domain as intracellular signaling domains. Numbers in histograms indicate geometric mean of fluorescent intensity. Blue histograms show CAR constructs representing the sequences originated from the synthesized CAR construct (DC). Red histograms show CAR construct aCD19:41BBz (X) consisting of different codons (X variant). Grey histograms are non-transduced reporter cells as controls.

7.8 Functional comparison of aCD19 Single CARs w/o puromycin/blasticidin in TPR

We co-cultured the TPR cells, each comprising one CAR construct, with either control K562, K562:CD19, K562:CD19:CD86, K562:aCD3, K562:aCD3:CD19 or K562:aCD3:CD86 to assess activation of transcription factors NF-κB, NFAT and AP-1 upon stimulation (Fig. 11). Stimulation through CD19 achieved lower activation levels for transcription factors NF-κB and NFAT than stimulation via K562:aCD3 in cells transduced with aCD19:CD3z CAR. Induction via K562:CD19:CD86 cells led to increased NF-κB activation (Fig. 11a, left panel). For AP-1, equally high activation was reached (Fig. 11c, left panel).

Costimulation via aCD19:CD28 CAR through K562:aCD3:CD19 resulted in almost equally high activation compared to stimulation via the endogenous CD28 receptor through K562:aCD3:CD86 for NF-κB transcription factor (Fig. 11a, middle panel). Higher activation levels were reached for AP-1 (Fig. 11c, middle panel). Stimulation of aCD19:CD3z/aCD19:CD28 and aCD19:CD28z did not reach the same activation levels via CD19 stimulation compared to endogenous TCR stimulation with K562:aCD3 (Fig. 11a, left panel). Upon stimulation via K562:aCD19:CD86, costimulatory effects through the endogenous CD28 receptor resulted in higher activation of NF-κB compared to CD19 stimulation alone, but activation was not as high as upon stimulation via K562:aCD3:CD86. aCD19:CD3z/aCD19:CD28 resulted in lower NF-κB upon activation in reporter cells upon K562:CD19 or K562:CD19:CD86 stimulation than cells harboring the single CAR construct aCD19:CD28z. (Fig 9a, middle panel). Stimulation via K562:CD19:CD86 resulted in equally high AP-1 activation compared to stimulation via K562:aCD3:CD86 (Fig. 11c, middle panel).

A

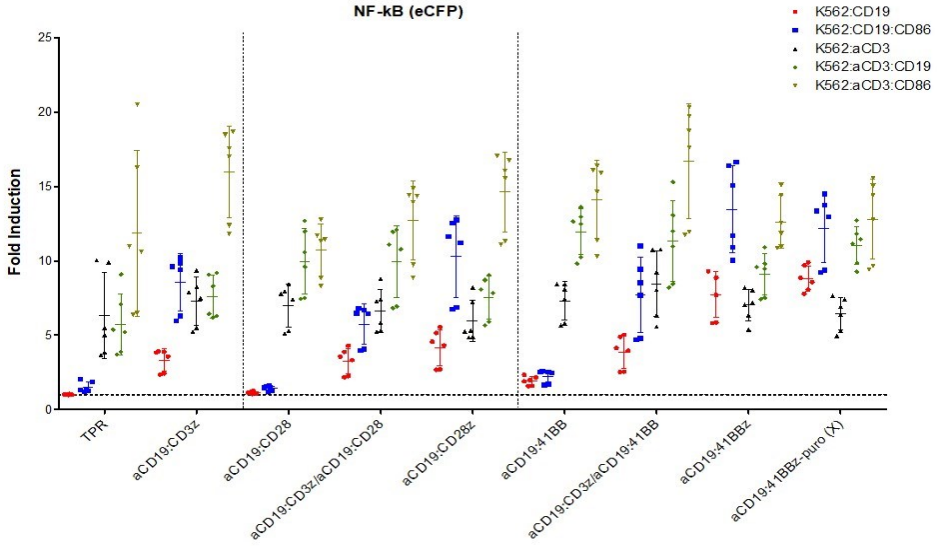
NF-kB (eCFP)
K562:CD19
K562:CD19:CD86
K562:aCD3
K562:aCD3:CD19
K562:aCD3:CD86
Fold Induction
25
20
15
10
5
0
TPR
aCD19:CD3z
aCD19:CD28
aCD19:CD3z/aCD19:CD28
aCD19:CD28z
aCD19:41BB
aCD19:CD3z/aCD19:41BB
aCD19:41BBz
aCD19:41BBz-puro (X)

B

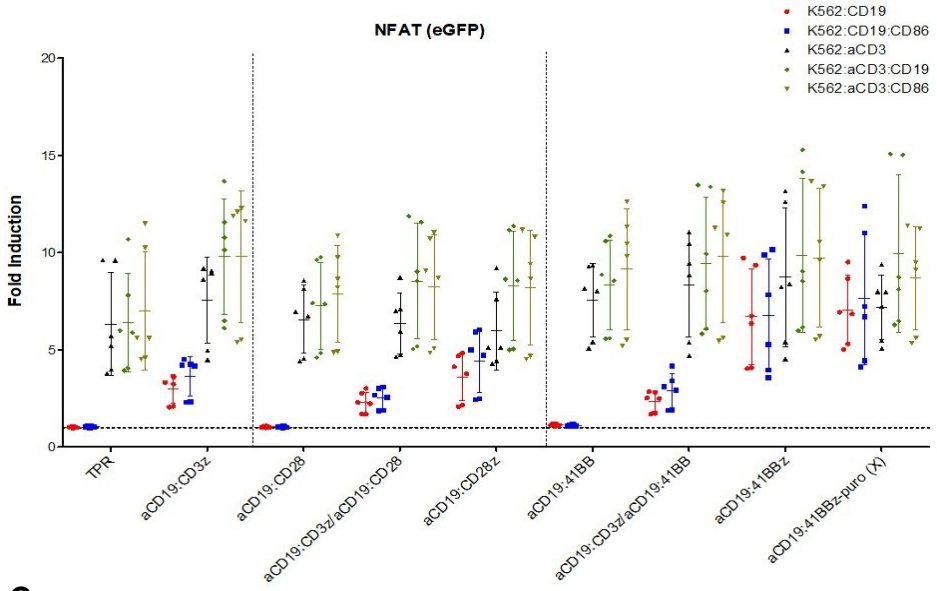
NFAT (eGFP)
K562:CD19
K562:CD19:CD86
K562:aCD3
K562:aCD3:CD19
K562:aCD3:CD86
Fold Induction
20
15
10
5
0
TPR
aCD19:CD3z
aCD19:CD28
aCD19:CD3z/aCD19:CD28
aCD19:CD28z
aCD19:41BB
aCD19:CD3z/aCD19:41BB
aCD19:41BBz
aCD19:41BBz-puro (X)

C

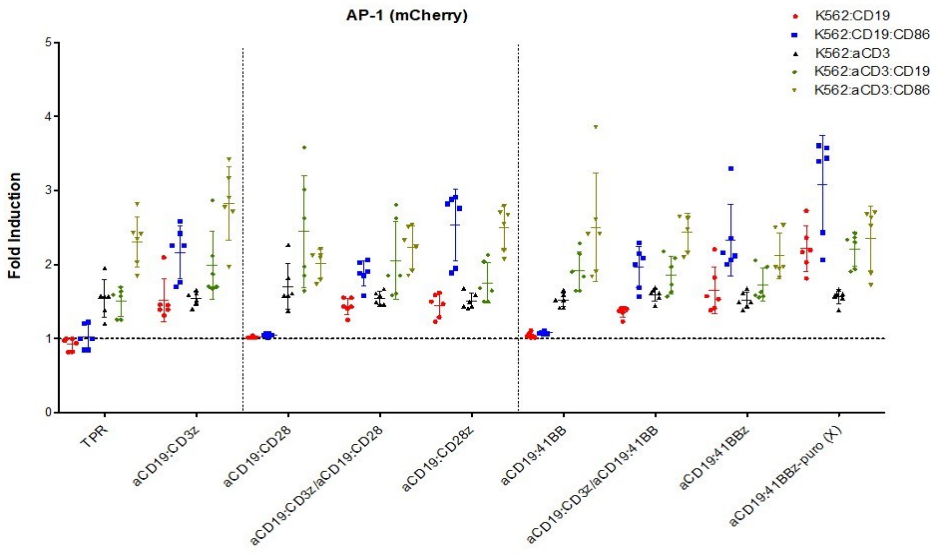
AP-1 (mCherry)
K562:CD19
K562:CD19:CD86
K562:aCD3
K562:aCD3:CD19
K562:aCD3:CD86
Fold Induction
5
4
3
2
1
0
TPR
aCD19:CD3z
aCD19:CD28
aCD19:CD3z/aCD19:CD28
aCD19:CD28z
aCD19:41BB
aCD19:CD3z/aCD19:41BB
aCD19:41BBz
aCD19:41BBz-puro (X)

Figure 11: Functional comparison of different aCD19 CARs harboring various signaling domains and no puromycin or blasticidin resistance marker in a triple parameter reporter system (TPR). TPR cells served as controls. TPR control and TPR expressing aCD19 CAR variants were left unstimulated or co-cultured with K562, K562:CD19, K562:CD19:CD86, K562:aCD3, K562:aCD3:CD19 and K562:aCD3:CD86. Reporter activation is shown as fold induction (gMFI of K562-ligand stimulated reporter cells/K562 control stimulated reporter cells). ***A)*** *indicates NF-κB-eCFP activation* ***B)*** *indicates NFAT-eGFP and* ***C)*** *indicates AP-1-mCherry activation. Left panel shows control reporter cells and 1st generation CAR. Middle panel shows stimulation of CARs containing CD28 signaling domains. Right panel shows stimulation of CARs containing 4-1BB signaling domains. aCD19:41BBz (X) harbors a puromycin resistance marker. Activation of CAR constructs was measured via FACS analysis. Results of 3 independent experiments performed in duplicates are depicted. Mean (SD) values are depicted.*

Costimulation of endogenous TCR through aCD19:41BB resulted in high NF-κB and AP-1 activation in reporter cells. Interaction of reporter cells expressing aCD19:CD3z/aCD19:41BB or aCD19:41BBz (X and DC variant) with K562:CD19 resulted in increased activation of NF-κB and AP-1, while the signal was amplified upon additional CD28-CD86 stimulation. Stimulation of reporter cells expressing these constructs via K562:CD19:CD86 and K562:aCD3:CD19 resulted in higher activation compared to CD19 stimulation alone, showing functionality for signal 1 and signal 2 (Fig. 11a, 11c, right panels). For the double transduced aCD19:CD3z/aCD19:41BB TPR cells, activation levels of NF-κB and AP-1 did not reach same levels as aCD19:41BBz constructs upon CD19 stimulation.

NFAT signaling is not affected by 4-1BB costimulation (Jutz et al., 2016), which is also shown in this study (Fig. 11b, right panel). Stimulation via K562:CD19 and K562:CD19:CD86 did result in only weak NFAT activation of TPR cells expressing aCD19:CD3z, aCD19:CD3z/aCD19:CD28, aCD19:CD28z and aCD19:CD3z/aCD19:41BB (Fig. 11b).

In summary, TPR cells harboring a costimulatory domain in addition to the signal 1 yielded higher activation of transcription factors. Cells expressing 4-1BB led to more induction than cells expressing CD28, especially aCD19:41BBz which might be due to its high expression levels (Fig. 10).

7.9 Cell surface expression of aCD19 single CAR constructs (X variant)

Because cell surface expression of our Dual CAR constructs was always challenging, we decided to proceed with single CARs based on the X variant. All constructs comprise either a puromycin or blasticidin selection marker. After lentiviral transduction of the X variant single CARs in TPR and NF-κB-reporter cells, cell surface expression was determined via flow cytometry. Detection of surface expression was again achieved through staining with a strep-tag and aHA-biotin antibody followed by streptavidine-PE or aV5-PECy7 antibody (Fig. 12). aV5 and aHA antibodies were used to concurrently detect expression of simultaneously transduced CARs. We detected high cell surface expression for all CARs (single and double transduced) with only lower expression for aCD19:41BB (X) with the strep-tag, HA and V5 antibodies. Reporter cells that were double transduced with aCD19:CD3z (X) and aCD19:CD28 (X) or aCD19:41BB (X) showed high expression when stained for both V5 (CD28, 41BB CAR-specific) and HA (CD3z CAR-specific).

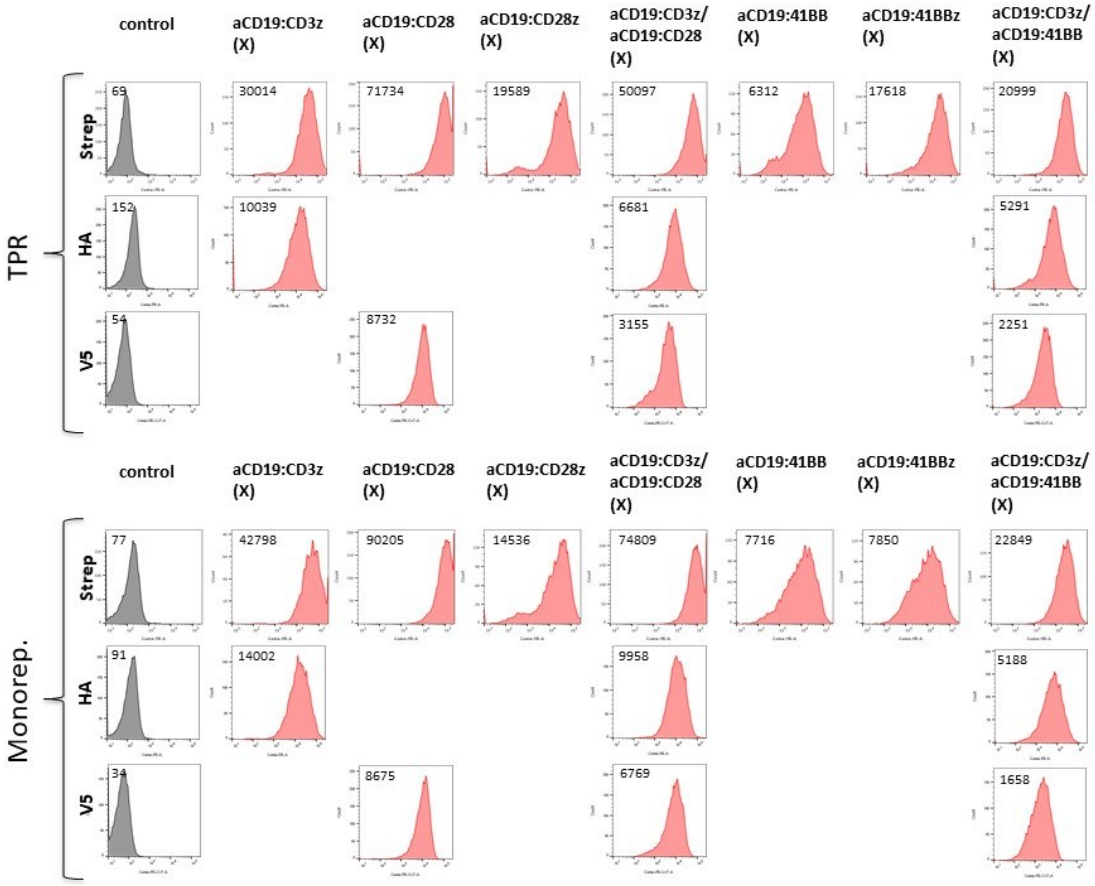

Figure 12: Cell surface expression of aCD19 CAR constructs on Jurkat Triple parameter reporter (TPR) (upper panel) and NF-κB-reporter cells (lower panel). Detection was performed via a NWSHPQFEK Tag-bio (Strep-tag) antibody followed by streptavidine-PE antibody, a V5-PECy7 antibody and an HA-AF647 antibody. V5 and HA tags were used to concurrently detect CARs with CD3z and a costimulatory domain as intracellular signaling domains. Numbers in histograms indicate geometric mean of fluorescent intensity. Red histograms show CAR construct consisting of X variant codons. Grey histograms are non-transduced reporter cells as controls.

7.10. Functional comparison of aCD19 Single CAR constructs (X)

We co-cultured the TPR cells, each comprising one CAR construct of X variant, with either control K562, K562:CD19, K562:CD19:CD86, K562:aCD3, K562:aCD3:CD19 or K562:aCD3:CD86 to assess activation of transcription factors NF-κB, NFAT and AP-1 (Fig. 13).

Stimulation of TPR cells expressing aCD19:CD3z (X) through K562:CD19 resulted in equal activation levels of NF-κB (Fig. 13a, left panel), and slightly higher activation of NFAT and AP-1 (Fig. 13b and c, left panels) compared to stimulation through K562:aCD3. Co-stimulation by K562:CD19:CD86 yields slightly lower activation of NF-κB in comparison to stimulation via the endogenous TCR and CD28 with K562:aCD3:CD86. For AP-1, stimulation of TPR cells with K562:CD19:CD86 resulted in higher activation than with K562:aCD3:CD86 and no increase upon endogenous CD28 costimulation can be seen for NFAT (Fig. 13, left panels). Stimulation of the endogenous TCR and CD19 CAR of aCD19:CD3z (X) via K562:aCD3:CD19 resulted in slightly higher activation of TPR cells compared to stimulation through K562:aCD3 or K562:CD19 for NFAT and AP-1, but not NF-κB (Fig. 13, left panels).

Co-stimulation of aCD19:CD28 (X) with K562:aCD3:CD19 resulted in enhanced NF-κB and AP-1 expression in comparison to solely TCR triggering with K562:aCD3 and endogenous CD86 with K562:aCD3:CD86. (Fig. 13a&c, middle panels). Double transduced TPR cells harboring the aCD19:CD3z/aCD19:CD28 (X) CARs, yielded similar NF-κB and AP-1 activation levels compared to aCD19:CD3z (X) via aCD19. K562:CD19:CD86 stimulation of double transduced TPR cells led to lower NF-κB and AP-1 activation levels compared to aCD19:CD3z (X) (Fig. 13a&c, middle panels).

Stimulation of TPR cells harboring aCD19:CD28z (X) yielded low activation for all three transcription factors NF-κB, NFAT and AP-1. Interestingly, stimulation of aCD19:CD28z CARs through endogenous receptors, K562aCD3 and K562:aCD3:CD86, led to diminished activation levels for NF-κB, NFAT and AP-1 (Fig. 13, middle panels).

For NFAT, costimulation through CD28 did not lead to higher activation of transcription factors than signal 1 alone, as activation levels were similarly high for all stimulation variations (Fig. 13 middle panel), except for aCD19:CD28z (X) via K562:aCD3:CD19, as the z-domain possibly leads to increased activation.

A

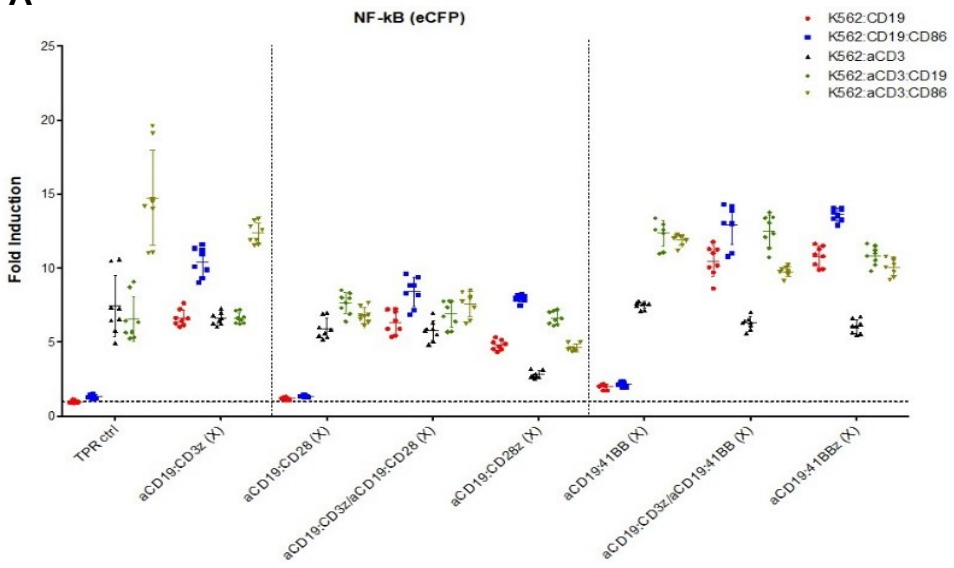
NF-kB (eCFP)
K562:CD19
K562:CD19:CD86
K562:aCD3
K562:aCD3:CD19
K562:aCD3:CD86
Fold Induction
25
20
15
10
5
0
TPR ctrl
aCD19:CD3z (X)
aCD19:CD28 (X)
aCD19:CD3z/aCD19:CD28 (X)
aCD19:CD28z (X)
aCD19:41BB (X)
aCD19:CD3z/aCD19:41BB (X)
aCD19:41BBz (X)

B

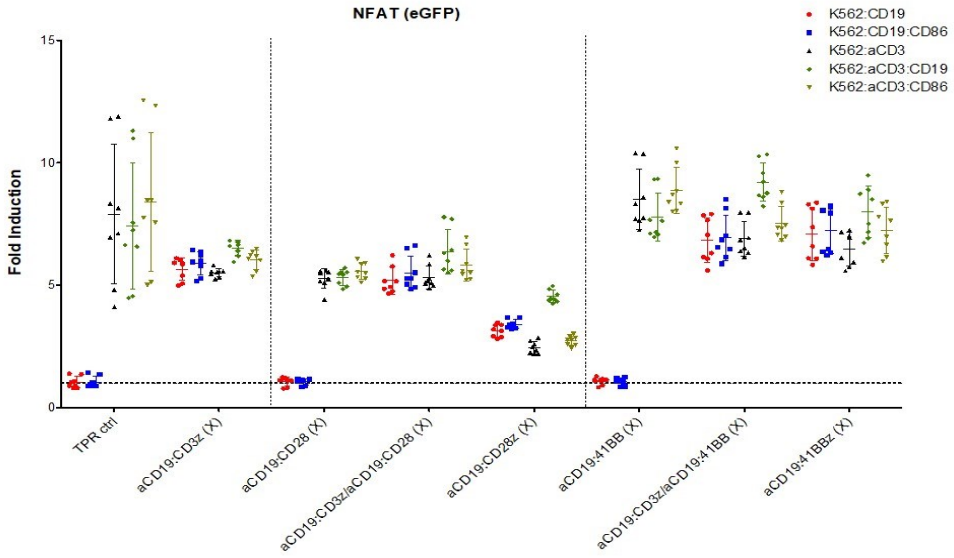
NFAT (eGFP)
K562:CD19
K562:CD19:CD86
K562:aCD3
K562:aCD3:CD19
K562:aCD3:CD86
Fold Induction
15
10
5
0
TPR ctrl
aCD19:CD3z (X)
aCD19:CD28 (X)
aCD19:CD3z/aCD19:CD28 (X)
aCD19:CD28z (X)
aCD19:41BB (X)
aCD19:CD3z/aCD19:41BB (X)
aCD19:41BBz (X)

C

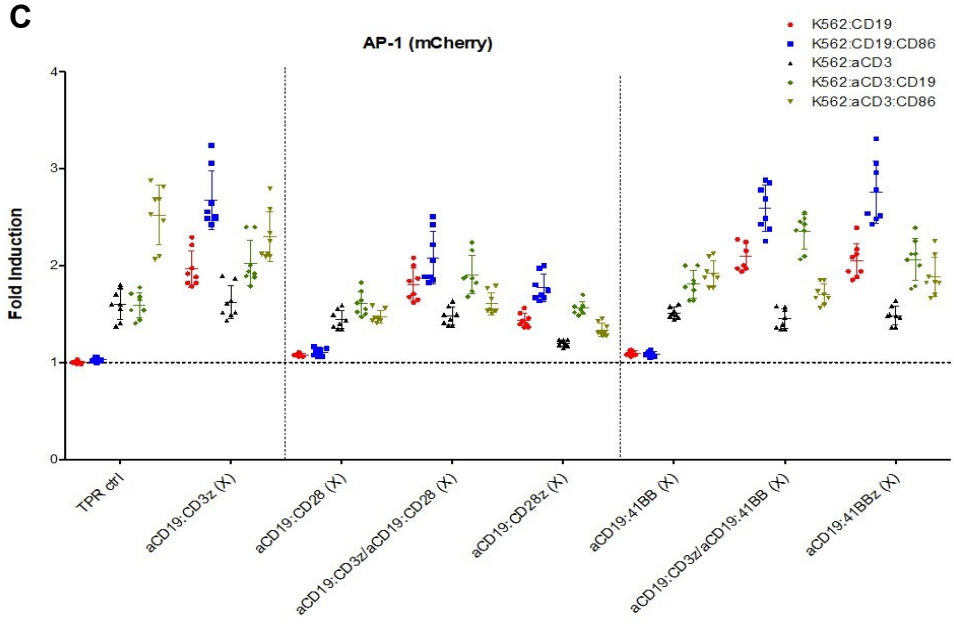
AP-1 (mCherry)
K562:CD19
K562:CD19:CD86
K562:aCD3
K562:aCD3:CD19
K562:aCD3:CD86
Fold Induction
4
3
2
1
0
TPR ctrl
aCD19:CD3z (X)
aCD19:CD28 (X)
aCD19:CD3z/aCD19:CD28 (X)
aCD19:CD28z (X)
aCD19:41BB (X)
aCD19:CD3z/aCD19:41BB (X)
aCD19:41BBz (X)

*Figure 13: Functional comparison of different aCD19 CARs (X) harboring various signaling domains in a triple parameter reporter system (TPR). TPR cells served as controls. TPR control and TPR expressing aCD19 CAR X variants were left unstimulated or co-cultured with K562, K562:CD19, K562:CD19:CD86, K562:aCD3, K562:aCD3:CD19 and K562:aCD3:CD86. Reporter activation is shown as fold induction (gMFI of K562-ligand stimulated reporter cells/K562 control stimulated reporter cells). **A)** indicates NF-κB-eCFP activation **B)** indicates NFAT-eGFP and **C)** indicates AP-1-mCherry activation. Left panel shows control reporter cells and 1st generation CAR. Middle panel shows stimulation of CARs containing CD28 signaling domains. Right panel shows stimulation of CARs containing 4-1BB signaling domains. All CAR constructs harbor a puromycin or blasticidin resistance marker. Activation of CAR constructs was measured via FACS analysis. Results of 4 independent experiments performed in duplicates are depicted. Mean (SD) values are depicted.*

In addition to CD28, we assessed costimulation of the 41BB domain in our reporter system (Fig. 13, right panels). Stimulation of TPR cells via aCD19:41BB (X) with K562:aCD3:CD19 resulted in higher activation in comparison to aCD19:CD28 (X). We compared single and double transduced CARs and observed similar activation levels of NF-κB and AP-1 for the aCD19:CD3z/aCD19:41BB (X) and aCD19:41BBz (X) CAR expressing cells. This effect could be enhanced by stimulating with K562:CD19:CD86 as the cells endogenously express CD28.

For NF-κB and AP-1, CD19 CAR stimulation of reporter cells transduced with aCD19:CD3z/aCD19:41BB (X) and aCD19:41BBz (X) yielded significantly higher activation levels of NF-κB and AP-1 than stimulation through K562:aCD3 and even slightly stronger activation compared to stimulation through K562:aCD3:CD86. (Fig. 13a and c, right panels). The only major difference between aCD19:CD3z/aCD19:41BB (X) and aCD19:41BBz (X) could be observed via stimulation with K562:aCD3:CD19. Stimulation of TPR cells comprising aCD19:CD3z/aCD19:41BB (X) showed enhanced activation compared to aCD19:41BBz (X), as activation levels of aCD19:41BBz (X) via K562:aCD3:CD19 were equal to those stimulated via K562:CD19 (Fig. 13a&c, right panels).

For NFAT, aCD19:41BB (X) TPR cells did not enhance activation of signal 1 through co-culture with K562:aCD3:CD19, but even reduced activation levels (Fig. 13b, right panel). Activation levels were similar upon all combinations of stimulatory cells and CAR constructs. However, endogenous signals yielded stronger activation in TPR cells transduced with aCD19:41BB (X) compared to other 4-1BB variants. Stimulation of TPR cells harboring aCD19:CD3z/aCD19:41BB (X) and aCD19:41BBz (X) via K562:aCD3:CD19 resulted in enhanced activation compared to K562:aCD3 in contrast to aCD19:41BB (X) (Fig. 13b, right panels).

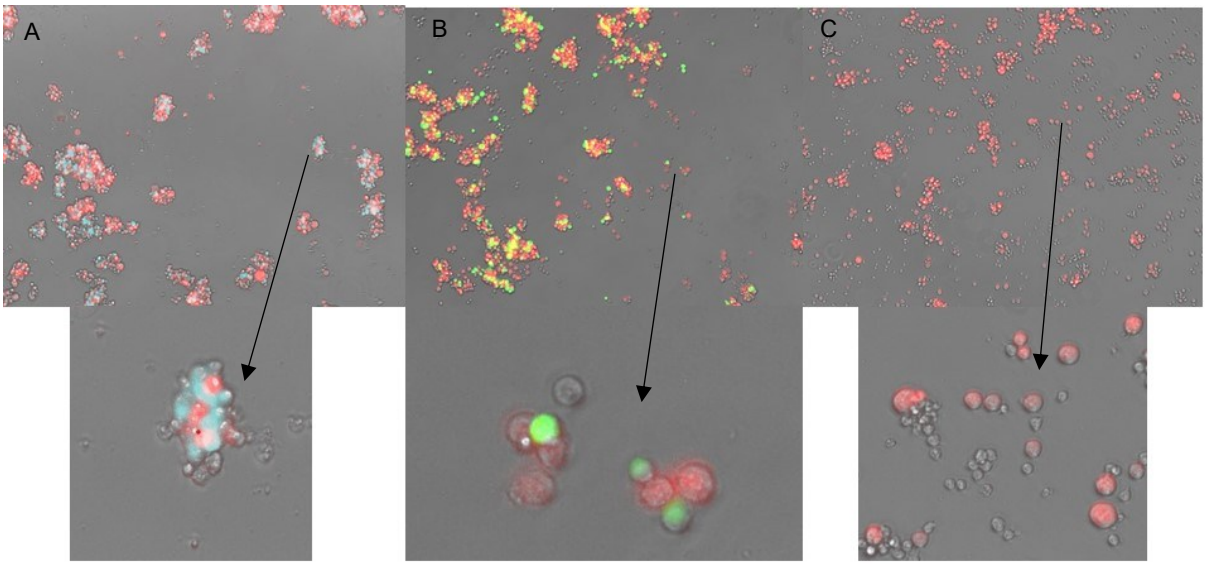

*Figure 14: Fluorescece microscopic images of co-culture of aCD19:CD3z (X) expressing cells with K562:CD19 taken with EVOS M500 microscope. TPR expressing NF-κB-eCFP **(A)** and NF-κB-reporter expressing NF-κB-eGFP **(B)** containing aCD19:CD3z (X) were co-cultured for 24 h with K562:CD19, which endogenously express a red fluorescent protein (RFP). NF-κB-reporter cells containing aCD19:CD3z (X) were co-cultured with control K562 cells **(C)** and served as control. NF-κB-eCFP is shown in blue, NF-κB-eGFP is shown in green and K562 cells are shown in red. Arrows indicate zoomed in locations.*

Representative images taken with EVOS M500 are shown in Figure 14. TPR and NF-κB reporter cells transduced with aCD19:CD3z (X) were co-cultured with K562:CD19 and form clusters upon CAR engagement. Activation of NF-κB of reporter cells can be seen in blue (TPR, NF-κB-eCFP, left panel) and green (NF-κB reporter cells, NF-κB-eGFP, middle panel), stimulator cells appear red via the red fluorescent protein (RFP) in image (Fig. 14). As control, NF-κB reporter cells expressing aCD19:CD3z (X) were co-cultured with control K562 cells (Fig. 14, right panel).

7.11 Cell surface expression of an aCD19:CD3z CAR construct harboring a CD28 PYAP motif

CD28 is an important molecule in the TCR-mediated signaling pathway. Within the cytoplasmic tail two regions have been described namely the YMNM and the PYAP motif. In this study, we were interested if the PYAP motif added to the CD3z signaling domain is sufficient to enhance activation. For this, we generated three different constructs. The PYAP motif was appended either upstream, in the middle, or downstream of the CD3z signaling domain and expressed in our reporter system. The X variant of aCD19:CD3z containing a puromycin resistance marker was used for the following experiments. After lentiviral transduction of CARs in TPR and NF-κB-reporter cells, cell surface expression was determined via flow cytometry (Fig. 15). Detection of surface expression was performed through staining with a strep-tag antibody followed by streptavidine-PE (Fig. 15). We observed high cell surface expression for all constructs. As control, aCD19:PD1$_{1\text{-}17aa}$ was used, which is a CD19 CAR containing only the first 17 amino acids of the intracellular region of PD-1.

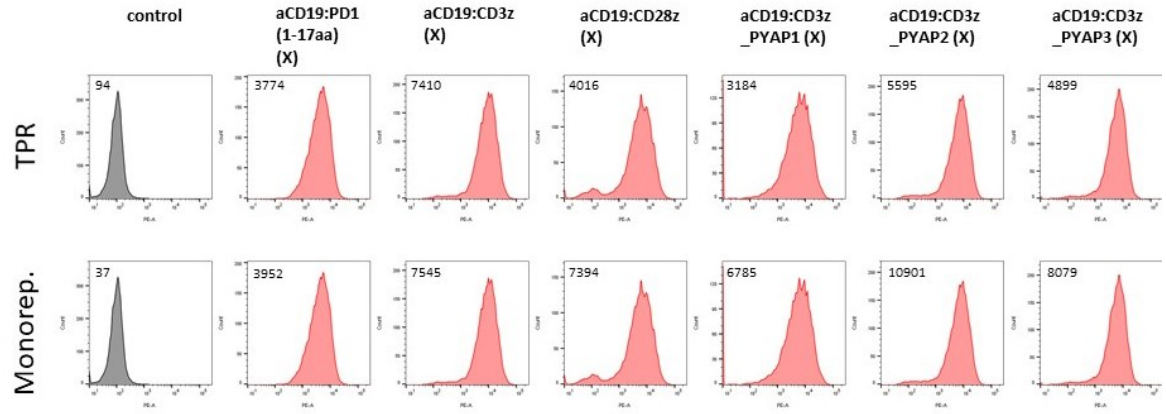

Figure 15: Cell surface expression of aCD19 CAR constructs on Jurkat Triple parameter reporter (TPR) (upper panel) and NF-κB-reporter cells (lower panel). Constructs comprise of a CD3z domain with a PYAP motif appended. As control an established construct, aCD19:PD1$_{1\text{-}17}$, aCD19:CD3z and aCD19:CD28z were used. Detection was performed via a NWSHPQFEK Tag-bio (Strep-tag) antibody followed by streptavidine-PE antibody. Numbers in histograms indicate geometric mean of fluorescent intensity. Red histograms show CAR construct consisting of X variant codons. Grey histograms are non-transduced reporter cells as controls.

7.12 Evaluation and functional comparison of aCD19:CD3z_PYAP single CAR constructs (X variant)

TPR cells expressing different CAR constructs were co-cultured with either K562, K562:CD19, K562:CD19:CD86, K562:aCD3 or K562:aCD3:CD86 to assess activation of transcription factors NF-κB, NFAT and AP-1 upon stimulation (Fig. 15 and 16).

Expression of all three transcription factors (NF-κB-eCFP, NFAT-eGFP and AP-1-mCherry) was higher for aCD19:CD3z (X) compared to aCD19:CD28z (X) when reporter cells were stimulated with K562:CD19 or K562:CD19:CD86 (Fig. 16, left panels).

For control aCD19:PD1$_{1-17}$, no activation can be seen upon CD19 stimulation. Interestingly, TPR cells comprising of aCD19:CD28z (X) CAR showed decreased expression levels for all transcription factors in comparison to aCD19:CD3z independent of the stimulator cell. This can also be seen in experiments carried out earlier (Fig. 13, middle panels).

A

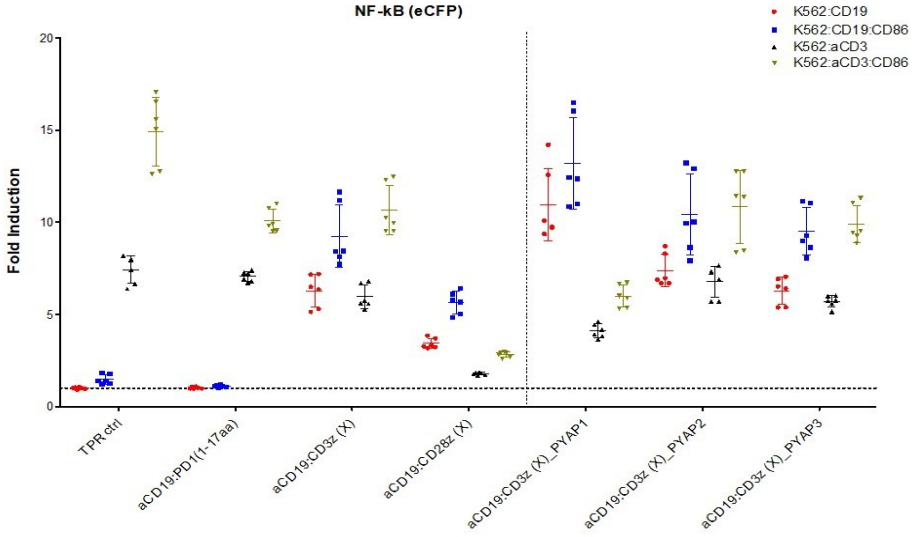
NF-kB (eCFP)
K562:CD19
K562:CD19:CD86
K562:aCD3
K562:aCD3:CD86
Fold Induction
20
15
10
5
0
TPR ctrl
aCD19;PD1(1-17aa)
aCD19;CD3z (X)
aCD19;CD28z (X)
aCD19;CD3z (X)_PYAP1
aCD19;CD3z (X)_PYAP2
aCD19;CD3z (X)_PYAP3

B

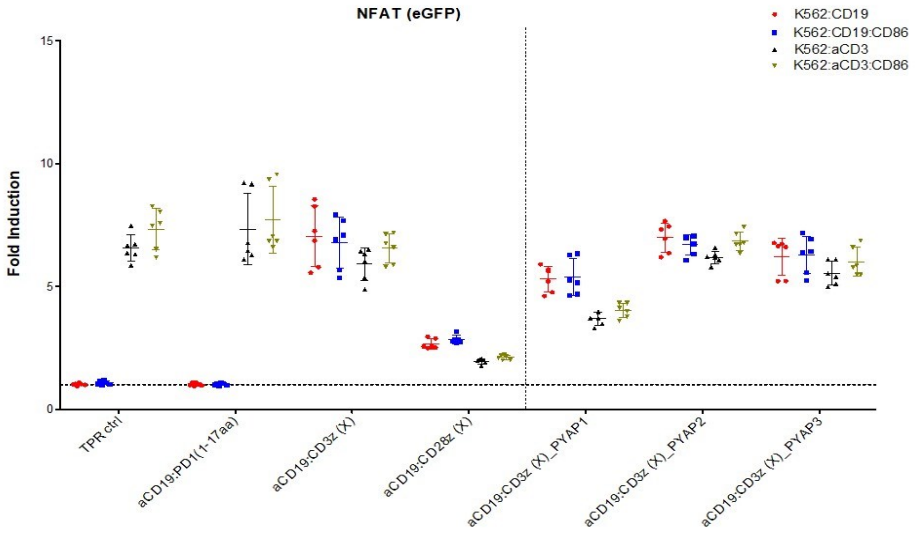
NFAT (eGFP)
K562:CD19
K562:CD19:CD86
K562:aCD3
K562:aCD3:CD86
Fold Induction
15
10
5
0
TPR ctrl
aCD19;PD1(1-17aa)
aCD19;CD3z (X)
aCD19;CD28z (X)
aCD19;CD3z (X)_PYAP1
aCD19;CD3z (X)_PYAP2
aCD19;CD3z (X)_PYAP3

C

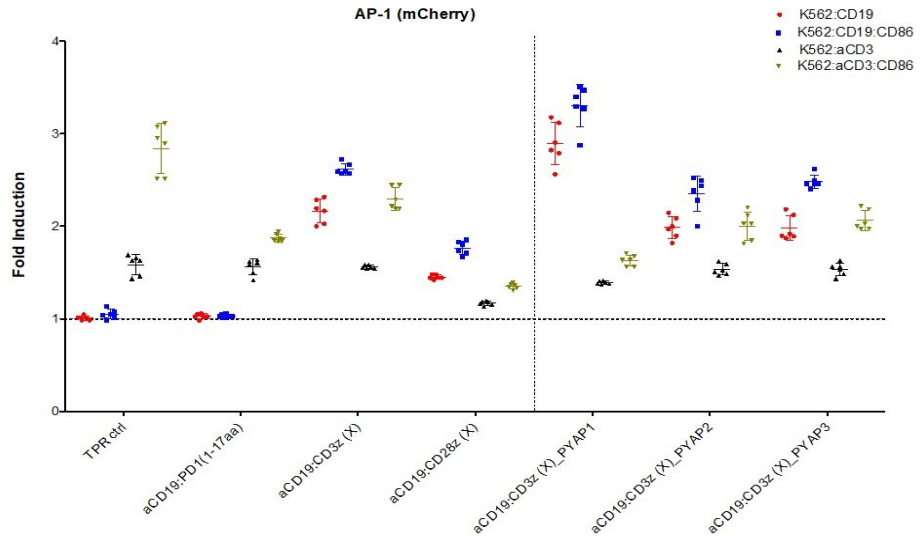
AP-1 (mCherry)
K562:CD19
K562:CD19:CD86
K562:aCD3
K562:aCD3:CD86
Fold Induction
4
3
2
1
0
TPR ctrl
aCD19;PD1(1-17aa)
aCD19;CD3z (X)
aCD19;CD28z (X)
aCD19;CD3z (X)_PYAP1
aCD19;CD3z (X)_PYAP2
aCD19;CD3z (X)_PYAP3

Figure 16: Functional comparison of different aCD19 CAR (X) constructs on triple parameter reporter (TPR) cells harboring various signaling domains. Constructs comprise of a CD3z domain with a PYAP motif appended. As controls, aCD19:PD1$_{1\text{-}17aa}$, aCD19:CD3z, aCD19:CD28z and non-transduced TPR cells were used. TPR control and TPR expressing aCD19 CAR X variants were left unstimulated or co-cultured with K562, K562:CD19, K562:CD19:CD86, K562:aCD3 or K562:aCD3:CD86. Reporter activation is shown as fold induction (gMFI of K562-ligand stimulated reporter cells/K562 control stimulated reporter cells). ***A)*** *indicates NF-κB-eCFP activation* ***B)*** *indicates NFAT-eGFP and* ***C)*** *indicates AP-1-mCherry activation.). Left panel shows control reporter cells. Right panel shows stimulation of CARs containing a PYAP motif. All CAR constructs harbor a puromycin resistance marker. Activation of CAR constructs was measured via FACS analysis. Results of 3 independent experiments performed in duplicates are depicted. Mean (SD) values are depicted.*

Comparing CD3z_PYAP to CD3z CARs, we observed particularly for the construct harboring the PYAP1 motif a significant increase in NF-κB and AP-1 activation (Fig. 16, right panels). aCD19:CD3z_PYAP-2 (X) and aCD19:CD3z_PYAP-3 (X) showed similar activation levels for all three transcription factors in regard to aCD19:CD3z (X) CAR upon stimulation of TPR cells with all K562 cells. Thus, these data clearly indicate that the PYAP motif upstream of CD3z in a single CAR can enhance the activation of NF-κB and AP-1 in comparison to CD3z alone.

Interestingly, the same decreased activation effects for all transcription factors upon K562:aCD3 and K562:aCD3:CD86 stimulation seen for aCD19:CD28z (X) are present in a weakened form for TPR cells transduced with the aCD19:CD3z_PYAP-1 (X) CAR (Fig. 16, right panels).

7.13 Cell surface expression of aCD19 single CAR constructs (X variant) in primary T cells

To further test and evaluate our CAR constructs, we transduced the X variant CAR constructs in CD14-depleted peripheral blood mononuclear cells (PBMCs). For this, PBMCs were isolated from healthy donors and were further separated from $CD14^+$ cells by using MagniSort Human CD14 Positive Selection Kit (eBioscience). Prior to lentiviral transduction, separated PBMCs were activated for 2 days with IL-2 for higher transduction efficiency. Lentiviral transduction was performed the same way as with Jurkat reporter cells (Fig. 17).

Detection of surface expression was achieved through staining of strep-tag and aHA-biotin antibody followed by streptavidine-PE and an aV5-PECy7 antibody (Fig. 17). aV5 (specific for aCD19:CD28 (X) CAR) and aHA (specific for aCD19:CD3z (X) CAR) antibodies were used to concurrently detect expression of simultaneously transduced CARs. aCD19:$PD1_{1\text{-}17aa}$, aCD19:CD3z and constructs containing an intracellular CD28 motif show a transduction efficiency of 20-30%. PBMCs transduced with CARs comprising of a 4-1BB motif showed weak expression levels of around 15%.

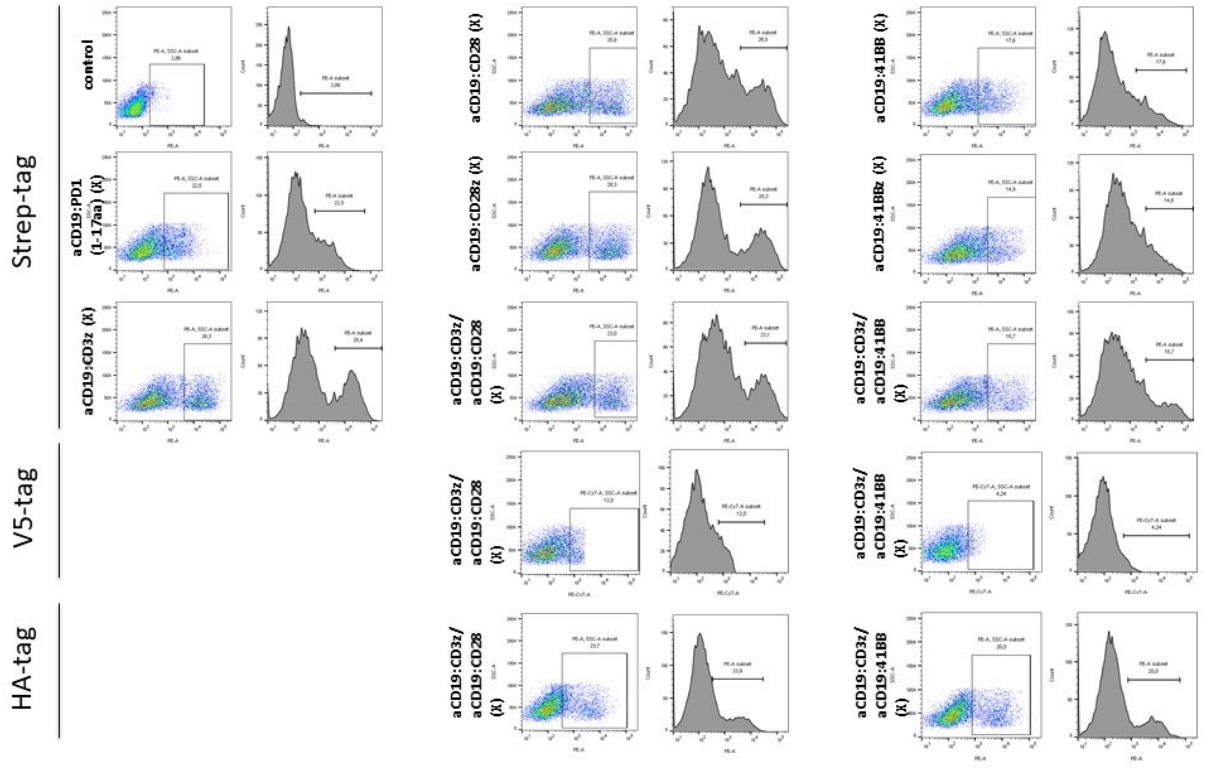

Figure 17: Cell surface expression of aCD19 CAR constructs on CD14 negative-selected peripheral blood mononuclear cells (PBMCs). Non-transduced PBMCs and aCD19:PD1$_{1\text{-}17aa}$ (X) construct are used as controls. Detection was performed via a NWSHPQFEK Tag-bio (Strep-tag) antibody followed by streptavidine-PE antibody, a V5-PECy7 antibody and an HA-PE antibody followed by streptavidine-PE antibody. V5 and HA tags were used to concurrently detect CARs with CD3z and a costimulatory domain as intracellular signaling domains. Numbers and lines in histograms indicate percentage of transduced cells. Dot plot and histograms are shown

Double transduced PBMCs (aCD19:CD3z/aCD19:CD28 (X) and aCD19:CD3z/aCD19:41BB (X)) showed similar expression as single transduced CARs upon strep-tag and HA-tag staining, but cell surface detection upon aV5 antibody resulted in low percentage of positive cells for aCD19:CD3z/aCD19:41BB (X). Prior to functional evaluation, CD14-negative selected PBMCs expressing CD19 CARs were sorted.

7.14 Functional comparison of aCD19 single CAR constructs (X variant) in primary T cells

To assess CAR function in CD14-negative selected PBMCs, we co-cultured the cells with either K562, K562:aCD3 or K562:CD19 or left them unstimulated. After 24h, we monitored the activation of T cells by determining the cell surface expression of the activation marker CD25 on CD4+ and CD8+ T cell subsets. Only one representative experiment is shown (Fig. 18).

As expected, the control CAR construct aCD19:PD1$_{(1\text{-}17aa)}$ (X) showed no activation upon co-culture with K562:CD19, K562 or when left unstimulated. K562:aCD3 resulted in strong activation of both CD4+ and CD8+ T cells (Fig. 18).

aCD19:CD3z (X) transduced T cells resulted in high expression of CD25 upon stimulation with K562:CD19, which was even higher by stimulating via the TCR with K562:aCD3. Unstimulated aCD19:CD3z (X) T cells have shown same basal activation levels as T cells transduced with the aCD19:PD1$_{(1\text{-}17aa)}$ (X) CAR (Fig. 18). Similar results were obtained for T cells harboring the aCD19:41BBz construct.

Interestingly, CD4+ and CD8+ T cells comprising an aCD19:CD28z (X) CAR yielded high activation levels of CD25 when left unstimulated or with control K562. Nevertheless, activation marker CD25 could be enhanced upon CD19 stimulation.

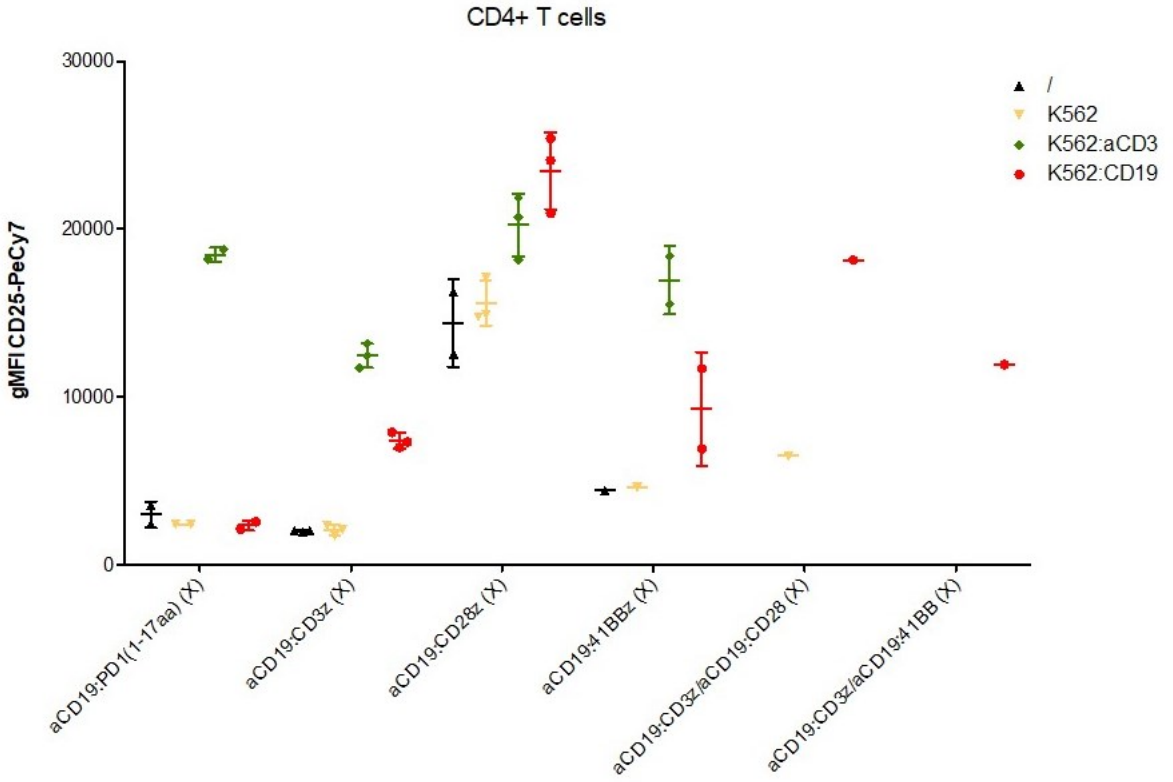
CD4+ T cells
gMFI CD25-PeCy7
30000
20000
10000
0
/
K562
K562:aCD3
K562:CD19
aCD19:PD1(1-17aa) (X)
aCD19:CD3z (X)
aCD19:CD28z (X)
aCD19:41BBz (X)
aCD19:CD3z/aCD19:CD28 (X)
aCD19:CD3z/aCD19:41BB (X)

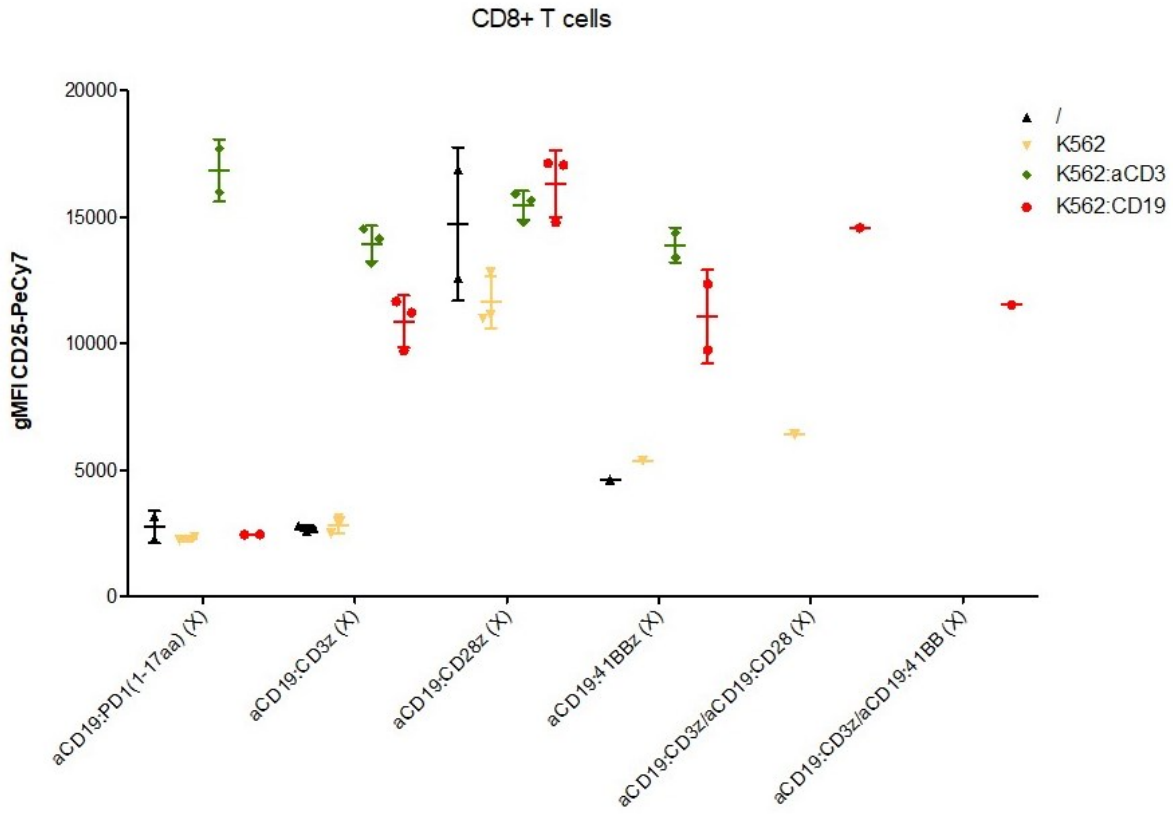
CD8+ T cells
gMFI CD25-PeCy7
20000
15000
10000
5000
0
/
K562
K562:aCD3
K562:CD19
aCD19:PD1(1-17aa) (X)
aCD19:CD3z (X)
aCD19:CD28z (X)
aCD19:41BBz (X)
aCD19:CD3z/aCD19:CD28 (X)
aCD19:CD3z/aCD19:41BB (X)

Figure 18: Functional comparison of different aCD19 CARs (X) harboring various signaling domains in primary CD4+ and CD8+ T cells. Prior to stimulation of cells, T cells expressing aCD19 CARs were sorted. T cells expressing aCD19 CAR X variants were left unstimulated or co-cultured with K562, K562:CD19 or K562:aCD3. T cell activation in the CD4+ and CD8+ T cell subsets is shown as geometric mean upon staining with the T cell activation marker CD25 with a CD25-PeCy7 antibody. ***A)*** *shows activation of CD4+ T cells and* ***B)*** *shows activation of CD8+ T cells. When enough cells were harvested, experiments in triplicates were performed, otherwise duplicates or single wells. Activation of CAR constructs was measured via FACS analysis. Mean (SD) values are depicted.*

Unfortunately, due to low expression efficiency of the double transduced CARs aCD19:CD3z/aCD19:CD28 (X) or aCD19:CD3z/aCD19:41BB (X) only a few cells could be sorted. Still, we observed upon stimulation with K562:CD19 an increase in activation marker CD25 for both, $CD4^+$ and $CD8^+$ T cells.

Unstimulated and co-cultured with K562 cells caused moderate activation of T cells when transduced with aCD19:41BBz (X) CAR, but much less compared to T cells with aCD19:CD28z (X). CAR stimulation via K562:CD19 resulted in activation of T cells, but not as strong as stimulation through the endogenous TCR. $CD8^+$ T cells were stronger activated than CD4+ T cells (Fig. 18). Stimulation of T cells harboring aCD19:CD3z/aCD19:41BB (X) CARs resulted in similar activation levels as aCD19:41BBz (X) transduced T cells.

All in all, further experiments with more donors and optimized protocols need to be performed for more valuable conclusions.

8 Discussion

8.1 Evaluating expression of CAR constructs in TPR and NF-κB-reporter cells and the effect of spatial separation of intracellular signaling domains

Traditional 2nd generation CARs basically consist of an extracellular antigen-binding domain, a transmembrane domain and intracellular signaling domains comprising a membrane-distal CD3z and a membrane-proximal costimulatory (CD28, 4-1BB,…) domain. The extracellular domain, an antibody-derived single-chain variable fragment (scFv), allows CARs to engage with potentially any surface antigen target on tumor cells (Srivastava & Riddell, 2015; Jensen & Riddell, 2015). Because CD19 CARs treating B-cell malignancies showed great promise already in earlier studies (Kochenderfer et al., 2015; Porter et al., 2014) and are in general well studied, we decided to use CD19 CARs to analyze signaling effects of costimulatory domains CD28 and 4-1BB using a Jurkat-based triple parameter reporter (TPR) cell line and an NF-κB-reporter cell line.

The goal of my master thesis was to analyze if superior activation of Jurkat reporter cells and T cells mediated through spatial separation of intracellular signaling domains using a Dual CAR system is achieved, as preliminary data in our lab showed impaired costimulatory effects when CD28 sequence is located upstream of CD3z domain. Based on the Dual CAR construct designed by Peter Steinberger (synthesized by TWIST Bioscience), expression constructs encoding CARs with various signaling domain combinations were created (Fig. 1). However, expression levels of these Dual CARs were very low compared to single CARs (X variant) from earlier studies in the lab (Fig. 3). Therefore, we thought that the Dual CAR constructs may be too big (3.5 kb) to be effectively transduced and subsequently separated them into single CARs. The single CARs still were not as highly expressed as X variant CARs, especially constructs containing a 4-1BB motif, as aCD19:41BBz showed no expression at all. Expression efficiency was enhanced by removing puromycin and blasticidin resistance markers to further reduce the size, but surface expression still greatly varied among CAR constructs (Fig. 10). We hypothesize that codon usage may play a major role in CAR expression efficacy as the DC and X variant of the aCD19:CD3z CAR constructs have the exact same amino acid sequence but consist of different codons for each

amino acid (Komar, 2016; Quax et al., 2015), yet expression varies. Codons were designed to encode human sequences, which are altered to prevent recurrence of identical sequences. Dual CARs must comprise different codons for each domain to prevent transcriptional interference. Synthesis of repetitive sequences can be difficult, and recombination of similar sequences can occur in such constructs. We later decided to proceed with single CARs of the X variant which showed stable expression of all constructs generated on reporter cells.

When comparing stimulation levels of Dual CARs with single CARs in our reporter cells, we observed that aCD19:CD3z CARs yielded higher activation than all Dual CARs (Fig. 7), which might be due to the higher expression level of this CAR (Fig. 4). Stimulation of reporter cells through double transduced single CARs aCD19:CD3z/aCD19:CD28 resulted in same activation levels as single CD3z CARs upon CD19 stimulation and aCD19:CD3z/aCD19:41BB yielded higher activation levels. Presence of the intracellular sequence of CD28 did not enhance signal 1 despite being expressed on TPR and NF-κB-reporter cells, but 4-1BB led to a strong increase in activation, although 4-1BB was less prominent on reporter cell surface. In further experiments regarding DC variant single CARs, similar effects can be seen (Fig. 9). CD28 costimulation upon CD19 CAR engagement did not result in higher activation of reporter cells than aCD19:CD3z CARs alone, no matter if intracellular domains are separated or not. For 4-1BB, costimulation through CD19 CAR led to increased activation levels, especially when intracellular domains are separately transduced (Fig. 9B). Similar effects are observed for NF-κB-eCFP in TPR cells when resistance markers are removed from the constructs (Fig. 11A).

Regarding expression levels of the X variants of our CAR constructs, CARs containing 4-1BB were still weaker expressed on the cell surface of reporter cells than aCD19:CD3z (X) or CARs containing a CD28 domain, but still high expression levels were achieved (Fig. 12). CD28 domains did not lead to increased activation upon CD19 stimulation of neither NF-κB-eCFP, NFAT-eGFP or AP-1-mCherry, no matter if costimulatory domains are separated or not from the CD3z domain (Fig. 13). Further, we observed an almost two-fold induction for NF-κB-eCFP in TPR cells compared to aCD19:CD3z (X) upon CD19 stimulation when using a CAR harboring a 4-1BB signaling motif is involved, but again using CARs where the costimulatory and the zeta sequences were separated did not result in stronger reporter activation. Interestingly,

our data show when CD28 CARs are present in TPR cells, a reduction of activation of all three transcription factors upon endogenous CD28 stimulation can be seen (Fig. 13 middle panels). For aCD19:CD28z (X), this reduction effect was more prominent than in other CARs containing a CD28 signaling domain. Even stimulation via the TCS/CD3 complex with K562:aCD3 resulted in much lower activation levels for all three transcription factors in comparison to other CARs on reporter cells. Also, CD19 stimulation was not as profound as in other CARs (Fig. 13).

Since CD28 costimulation does appear to be impaired in CAR constructs (when the entire cytoplasmic domain of CD28 was used), we investigated whether the combination of CD3z sequences with isolated CD28 motifs could result in improved CD28 costimulation. The PYAP motif at the downstream end of CD28 is believed to be highly involved in T cell activation, so we created three constructs in which the PYAP motif is either upstream (PYAP1), within (PYAP2), or downstream (PYAP3) of the CD3z domain. As shown in Figure 16, only TPR cells comprising aCD19:CD3z_PYAP1 (X) yielded higher expression levels of NF-κB-eCFP and AP-1-mCherry upon CD19 CAR engagement compared to CD3z stimulation alone or aCD19:CD28z (X) stimulation. This suggests that the PYAP motif alone is sufficient to enhance signal 1 upon CD19 CAR stimulation. The position of this motif is important to be membrane-proximal, as aCD19:CD3z_PYAP2 (X) and aCD19:CD3z_PYAP3 (X) showed no difference in activation levels in comparison to aCD19:CD3z (X). Noteworthy, stimulation of TPR cells comprising ‘PYAP1’ through endogenous receptors (via K562:aCD3 and K562:aCD3:CD86) resulted in lower activation levels compared to TPR cells containing aCD19:CD3z (X), but higher NF-κB expression was observed.

All in all, CD28 costimulation, separated from signal 1 or not, via a 2nd generation CD19 CAR did not lead to an increase in induction of NF-κB, NFAT or AP-1 in reporter cells throughout this study. CD28 CAR costimulation of the endogenous TCR did result in higher activation levels compared to TCR activation alone, but to a much lower degree than endogenous CD28 costimulation. In addition, in aCD19:CD28z the CD28 domain seems to interfere with the CD3z domain as activation of TPR cells is highly reduced. CD19 CAR stimulation of 4-1BB domains resulted in higher expression of NF-κB-eCFP and AP-1-mCherry compared to stimulation through CD3z CAR or endogenous TCR stimulation. 4-1BB does not activate NFAT expression (Jutz et al., 2016).

8.2 Analyzing constitutive NF-κB activation of CD19 CARs in absence of CD19

In preliminary experiments in the Steinberger lab, constitutive activation of NF-κB-reporter cells comprising a CAR with a 4-1BB domain was observed. We hypothesized that this effect could be reduced by separating the intracellular domains of 4-1BB and CD3z. This appeared to be the case in Figure 9 and previous experiments (data not shown), as aCD19:41BBz (X) showed much higher constitutive NF-κB expression than other reporter cells containing a 4-1BB domain. But this was misleading as the expression of the X variant of aCD19:41BBz in NF-κB-reporter cells were always higher than the DC variant CAR constructs containing a 4-1BB domain. Experiments with X variant CARs comprising a 4-1BB domain showed strong NF-κB activation in the absence of stimulatory cells in NF-κB-reporter cells (Supplementary Fig. 6). Also, in TPR cells this effect could be observed on a much smaller scale. This suggests that tonic signaling of reporter cells does not depend on expression of a 2nd generation 4-1BB CAR, but on high expression levels of a CAR comprising a 4-1BB domain. Spatial separation did not appear to lower tonic signaling in reporter cells when CARs are equally expressed (Supplementary Fig. 6).

In Figure 9, aCD19:CD28z (DC) also showed tonic signaling when left unstimulated or co-cultured with control K562 cells. Further, in experiments with the X variant of a 2nd generation CAR comprising a CD28 domain, low constitutive NF-κB activation can be observed in NF-κB-reporter cells (data not shown). Interestingly, when transduced in T cells (Fig. 18), strong activation was measured when T cells were left unstimulated or co-cultured with control K562 cells. But this was only one representative experiment out of two (Supplementary Fig. 5), which needs to be repeated with multiple donors for conclusive data.

8.3 Outlook

TPR and NF-κB-reporter cells provide a great platform to study *in vitro* T cell activation dynamics quantitatively. Because a lot of data can be generated very fast, various combinations of signaling domains can be analyzed.

To further analyze reporter cell activation through CARs, expression of CAR constructs must be optimized to ensure stable and equal expression on reporter cell surface. Varying CAR expression of different construct can lead to wrong conclusions of CAR efficiency. To evaluate the highly different expression levels of X variant and DC variant CARs, hybrid constructs with nucleotide sequences of both variants can be generated. For instance, the extracellular, hinge and transmembrane domain sequences from the X variant and intracellular sequence from DC variant. This might give insight what causes weak expression of DC variant CARs. Further, more experiments with primary T cells can enlighten the understanding of the effect of CARs in T cell activation. Furthermore, optimization of transduction protocols for primary T cells are necessary to achieve higher expression efficiencies. Moreover, the modular system of CARs and fast data generating system of our reporter cells allow to study various CD19 CAR constructs with co-stimulatory or co-inhibitory domains and varying in their nucleotide sequences

Finally, Dual CARs comprising the X variant and other well-expressing sequences can be generated and analyzed for their expression and activation potential in T cells or Jurkat-based reporter cells. To gain optimal expression of CAR constructs on reporter cells and T cells, optimization of transduction protocols must be attained.

9 References

Abate-Daga, D., & Davila, M. L. (2016). CAR models: Next-generation CAR modifications for enhanced T-cell function. *Molecular Therapy Oncolytics*, *3*, 16014. https://doi.org/10.1038/mto.2016.14

Abraham, R. T., & Weiss, A. (2004). Jurkat T cells and development of the T-cell receptor signalling paradigm. *Nature Reviews Immunology*, *4*(4), 301–308. https://doi.org/10.1038/nri1330

Anaya, J.-M., Shoenfeld, Y., Levy, R. A., & Rojas-Villarraga, A. (o. J.). *Autoimmunity: From Bench to Bedside*. El Rosario University Press.

Arruebo, M., Vilaboa, N., Sáez-Gutierrez, B., Lambea, J., Tres, A., Valladares, M., & González-Fernández, Á. (2011). Assessment of the Evolution of Cancer Treatment Therapies. *Cancers*, *3*(3), 3279–3330. https://doi.org/10.3390/cancers3033279

Bonilla, F. A., & Oettgen, H. C. (2010). Adaptive immunity. *Journal of Allergy and Clinical Immunology*, *125*(2), S33–S40. https://doi.org/10.1016/j.jaci.2009.09.017

Brownlie, R. J., & Zamoyska, R. (2013). T cell receptor signalling networks: Branched, diversified and bounded. *Nature Reviews Immunology*, *13*(4), 257–269. https://doi.org/10.1038/nri3403

Cameron, B. J., Gerry, A. B., Dukes, J., Harper, J. V., Kannan, V., Bianchi, F. C., Grand, F., Brewer, J. E., Gupta, M., Plesa, G., Bossi, G., Vuidepot, A., Powlesland, A. S., Legg, A., Adams, K. J., Bennett, A. D., Pumphrey, N. J., Williams, D. D., Binder-Scholl, G., … Jakobsen, B. K. (2013). Identification of a Titin-derived HLA-A1-presented peptide as a cross-reactive target for engineered MAGE A3-directed T cells. *Science Translational Medicine*, *5*(197), 197ra103. https://doi.org/10.1126/scitranslmed.3006034

Cantrell, D. A. (2002). T-cell antigen receptor signal transduction. *Immunology*, *105*(4), 369–374. https://doi.org/10.1046/j.1365-2567.2002.01391.x

Chen, L., & Flies, D. B. (2013). Molecular mechanisms of T cell co-stimulation and co-inhibition. *Nature Reviews Immunology*, *13*(4), 227–242. https://doi.org/10.1038/nri3405

Germain, R. N. (2002). T-cell development and the CD4–CD8 lineage decision. *Nature Reviews Immunology*, *2*(5), 309–322. https://doi.org/10.1038/nri798

Gorentla, B. K., & Zhong, X.-P. (2012). T cell Receptor Signal Transduction in T lymphocytes. *Journal of clinical & cellular immunology*, *2012*(Suppl 12), 005. https://doi.org/10.4172/2155-9899.S12-005

Guedan, S., Ruella, M., & June, C. H. (2019). Emerging Cellular Therapies for Cancer. *Annual review of immunology*, *37*, 145–171. https://doi.org/10.1146/annurev-immunol-042718-041407

Harris, D. T., & Kranz, D. M. (2016). Adoptive T Cell Therapies: A Comparison of T Cell Receptors and Chimeric Antigen Receptors. *Trends in pharmacological sciences*, *37*(3), 220–230. https://doi.org/10.1016/j.tips.2015.11.004

Houot, R., Schultz, L. M., Marabelle, A., & Kohrt, H. (2015). T-cell–based Immunotherapy: Adoptive Cell Transfer and Checkpoint Inhibition. *Cancer Immunology Research*, *3*(10), 1115–1122. https://doi.org/10.1158/2326-6066.CIR-15-0190

Jensen, M. C., & Riddell, S. R. (2015). Designing Chimeric Antigen Receptors to Effectively and Safely Target Tumors. *Current opinion in immunology*, *33*, 9–15. https://doi.org/10.1016/j.coi.2015.01.002

Joyce, J. A., & Fearon, D. T. (2015). T cell exclusion, immune privilege, and the tumor microenvironment. *Science*, *348*(6230), 74–80. https://doi.org/10.1126/science.aaa6204

June, C. H., O'Connor, R. S., Kawalekar, O. U., Ghassemi, S., & Milone, M. C. (2018). CAR T cell immunotherapy for human cancer. *Science*, *359*(6382), 1361–1365. https://doi.org/10.1126/science.aar6711

Jutz, S., Hennig, A., Paster, W., Asrak, Ö., Dijanovic, D., Kellner, F., Pickl, W. F., Huppa, J. B., Leitner, J., & Steinberger, P. (2017). A cellular platform for the evaluation of immune checkpoint molecules. *Oncotarget*, *8*(39), 64892–64906. https://doi.org/10.18632/oncotarget.17615

Jutz, S., Leitner, J., Schmetterer, K., Doel-Perez, I., Majdic, O., Grabmeier-Pfistershammer, K., Paster, W., Huppa, J. B., & Steinberger, P. (2016). Assessment of costimulation and coinhibition in a triple parameter T cell reporter line: Simultaneous measurement of NF-κB, NFAT and AP-1. *Journal of Immunological Methods*, *430*, 10–20. https://doi.org/10.1016/j.jim.2016.01.007

Klein, L., Kyewski, B., Allen, P. M., & Hogquist, K. A. (2014). Positive and negative selection of the T cell repertoire: What thymocytes see (and don't see). *Nature Reviews Immunology*, *14*(6), 377–391. https://doi.org/10.1038/nri3667

Kochenderfer, J. N., Dudley, M. E., Kassim, S. H., Somerville, R. P. T., Carpenter, R. O., Stetler-Stevenson, M., Yang, J. C., Phan, G. Q., Hughes, M. S., Sherry, R. M., Raffeld, M., Feldman,

S., Lu, L., Li, Y. F., Ngo, L. T., Goy, A., Feldman, T., Spaner, D. E., Wang, M. L., … Rosenberg, S. A. (2015). Chemotherapy-Refractory Diffuse Large B-Cell Lymphoma and Indolent B-Cell Malignancies Can Be Effectively Treated With Autologous T Cells Expressing an Anti-CD19 Chimeric Antigen Receptor. *Journal of Clinical Oncology*, *33*(6), 540–549. https://doi.org/10.1200/JCO.2014.56.2025

Komar, A. A. (2016). The Yin and Yang of codon usage. *Human Molecular Genetics*, *25*(R2), R77–R85. https://doi.org/10.1093/hmg/ddw207

Kroczek, R. A., Mages, H. W., & Hutloff, A. (2004). Emerging paradigms of T-cell co-stimulation. *Current Opinion in Immunology*, *16*(3), 321–327. https://doi.org/10.1016/j.coi.2004.03.002

Lieberman, J. (2003). The ABCs of granule-mediated cytotoxicity: New weapons in the arsenal. *Nature Reviews Immunology*, *3*(5), 361–370. https://doi.org/10.1038/nri1083

Majeed, H., & Gupta, V. (2021). Adverse Effects Of Radiation Therapy. In *StatPearls*. StatPearls Publishing. http://www.ncbi.nlm.nih.gov/books/NBK563259/

Manfredi, F., Cianciotti, B. C., Potenza, A., Tassi, E., Noviello, M., Biondi, A., Ciceri, F., Bonini, C., & Ruggiero, E. (2020). TCR Redirected T Cells for Cancer Treatment: Achievements, Hurdles, and Goals. *Frontiers in Immunology*, *11*. https://doi.org/10.3389/fimmu.2020.01689

Maude, S. L., Frey, N., Shaw, P. A., Aplenc, R., Barrett, D. M., Bunin, N. J., Chew, A., Gonzalez, V. E., Zheng, Z., Lacey, S. F., Mahnke, Y. D., Melenhorst, J. J., Rheingold, S. R., Shen, A., Teachey, D. T., Levine, B. L., June, C. H., Porter, D. L., & Grupp, S. A. (2014). Chimeric antigen receptor T cells for sustained remissions in leukemia. *The New England Journal of Medicine*, *371*(16), 1507–1517. https://doi.org/10.1056/NEJMoa1407222

Morgan, R. A., Chinnasamy, N., Abate-Daga, D. D., Gros, A., Robbins, P. F., Zheng, Z., Feldman, S. A., Yang, J. C., Sherry, R. M., Phan, G. Q., Hughes, M. S., Kammula, U. S., Miller, A. D., Hessman, C. J., Stewart, A. A., Restifo, N. P., Quezado, M. M., Alimchandani, M., Rosenberg, A. Z., … Rosenberg, S. A. (2013). Cancer regression and neurologic toxicity following anti-MAGE-A3 TCR gene therapy. *Journal of immunotherapy (Hagerstown, Md. : 1997)*, *36*(2), 133–151. https://doi.org/10.1097/CJI.0b013e3182829903

Morgan, R. A., Dudley, M. E., Wunderlich, J. R., Hughes, M. S., Yang, J. C., Sherry, R. M., Royal, R. E., Topalian, S. L., Kammula, U. S., Restifo, N. P., Zheng, Z., Nahvi, A., de Vries, C. R., Rogers-Freezer, L. J., Mavroukakis, S. A., & Rosenberg, S. A. (2006). Cancer Regression in

Patients After Transfer of Genetically Engineered Lymphocytes. *Science*, *314*(5796), 126–129. https://doi.org/10.1126/science.1129003

Mosmann, T. R., Cherwinski, H., Bond, M. W., Giedlin, M. A., & Coffman, R. L. (1986). Two types of murine helper T cell clone. I. Definition according to profiles of lymphokine activities and secreted proteins. *The Journal of Immunology*, *136*(7), 2348–2357.

Paijens, S. T., Vledder, A., de Bruyn, M., & Nijman, H. W. (2021). Tumor-infiltrating lymphocytes in the immunotherapy era. *Cellular & Molecular Immunology*, *18*(4), 842–859. https://doi.org/10.1038/s41423-020-00565-9

Parkhurst, M. R., Yang, J. C., Langan, R. C., Dudley, M. E., Nathan, D.-A. N., Feldman, S. A., Davis, J. L., Morgan, R. A., Merino, M. J., Sherry, R. M., Hughes, M. S., Kammula, U. S., Phan, G. Q., Lim, R. M., Wank, S. A., Restifo, N. P., Robbins, P. F., Laurencot, C. M., & Rosenberg, S. A. (2011). T cells targeting carcinoembryonic antigen can mediate regression of metastatic colorectal cancer but induce severe transient colitis. *Molecular Therapy: The Journal of the American Society of Gene Therapy*, *19*(3), 620–626. https://doi.org/10.1038/mt.2010.272

Paster, W., Brockmeyer, C., Fu, G., Simister, P. C., Wet, B. de, Martinez-Riaño, A., Hoerter, J. A. H., Feller, S. M., Wülfing, C., Gascoigne, N. R. J., & Acuto, O. (2013). GRB2-Mediated Recruitment of THEMIS to LAT Is Essential for Thymocyte Development. *The Journal of Immunology*, *190*(7), 3749–3756. https://doi.org/10.4049/jimmunol.1203389

Pennock, N. D., White, J. T., Cross, E. W., Cheney, E. E., Tamburini, B. A., & Kedl, R. M. (2013). T cell responses: Naïve to memory and everything in between. *Advances in Physiology Education*, *37*(4), 273–283. https://doi.org/10.1152/advan.00066.2013

Porter, D. L., Frey, N. V., Melenhorst, J. J., Hwang, W.-T., Lacey, S. F., Shaw, P., Chew, A., Grupp, S. A., Capobianchi, J., Gilmore, J., Kalos, M., Litchman, M., Lledo, L., Loren, A. W., Mahnke, Y., Marcucci, K. T., McConville, H., Shen, A., Wood, P. A., … June, C. H. (2014). Randomized, Phase II Dose Optimization Study of Chimeric Antigen Receptor Modified T Cells Directed Against CD19 (CTL019) in Patients with Relapsed, Refractory CLL. *Blood*, *124*(21), 1982. https://doi.org/10.1182/blood.V124.21.1982.1982

Quax, T. E. F., Claassens, N. J., Söll, D., & van der Oost, J. (2015). Codon Bias as a Means to Fine-Tune Gene Expression. *Molecular cell*, *59*(2), 149–161. https://doi.org/10.1016/j.molcel.2015.05.035

Rafiq, S., Hackett, C. S., & Brentjens, R. J. (2020). Engineering strategies to overcome the current roadblocks in CAR T cell therapy. *Nature Reviews Clinical Oncology*, *17*(3), 147–167. https://doi.org/10.1038/s41571-019-0297-y

Riha, P., & Rudd, C. E. (2010). CD28 co-signaling in the adaptive immune response. *Self Nonself*, *1*(3), 231–240. https://doi.org/10.4161/self.1.3.12968

Robbins, P. F., Morgan, R. A., Feldman, S. A., Yang, J. C., Sherry, R. M., Dudley, M. E., Wunderlich, J. R., Nahvi, A. V., Helman, L. J., Mackall, C. L., Kammula, U. S., Hughes, M. S., Restifo, N. P., Raffeld, M., Lee, C.-C. R., Levy, C. L., Li, Y. F., El-Gamil, M., Schwarz, S. L., … Rosenberg, S. A. (2011). Tumor Regression in Patients With Metastatic Synovial Cell Sarcoma and Melanoma Using Genetically Engineered Lymphocytes Reactive With NY-ESO-1. *Journal of Clinical Oncology*, *29*(7), 917–924. https://doi.org/10.1200/JCO.2010.32.2537

Rohaan, M. W., Wilgenhof, S., & Haanen, J. B. A. G. (2019). Adoptive cellular therapies: The current landscape. *Virchows Archiv*, *474*(4), 449–461. https://doi.org/10.1007/s00428-018-2484-0

Rydzek, J., Nerreter, T., Peng, H., Jutz, S., Leitner, J., Steinberger, P., Einsele, H., Rader, C., & Hudecek, M. (2019). Chimeric Antigen Receptor Library Screening Using a Novel NF-κB/NFAT Reporter Cell Platform. *Molecular Therapy*, *27*(2), 287–299. https://doi.org/10.1016/j.ymthe.2018.11.015

Schwartz, R. H. (2003). T Cell Anergy. *Annual Review of Immunology*, *21*(1), 305–334. https://doi.org/10.1146/annurev.immunol.21.120601.141110

Sharpe, A. H., & Freeman, G. J. (2002). The B7–CD28 superfamily. *Nature Reviews Immunology*, *2*(2), 116–126. https://doi.org/10.1038/nri727

Srivastava, S., & Riddell, S. R. (2015). Engineering CAR-T Cells: Design Concepts. *Trends in immunology*, *36*(8), 494–502. https://doi.org/10.1016/j.it.2015.06.004

T Cell Receptor Signaling. (o. J.). Cell Signaling Technology. Abgerufen 11. Dezember 2021, von https://www.cellsignal.com/pathways/t-cell-receptor-signaling

Waldman, A. D., Fritz, J. M., & Lenardo, M. J. (2020). A guide to cancer immunotherapy: From T cell basic science to clinical practice. *Nature Reviews Immunology*, *20*(11), 651–668. https://doi.org/10.1038/s41577-020-0306-5

Wucherpfennig, K. W., Gagnon, E., Call, M. J., Huseby, E. S., & Call, M. E. (2010). Structural Biology of the T-cell Receptor: Insights into Receptor Assembly, Ligand Recognition, and Initiation of

Signaling. *Cold Spring Harbor Perspectives in Biology*, *2*(4), a005140. https://doi.org/10.1101/cshperspect.a005140

Zapata, J. M., Perez-Chacon, G., Carr-Baena, P., Martinez-Forero, I., Azpilikueta, A., Otano, I., & Melero, I. (2018). CD137 (4-1BB) Signalosome: Complexity Is a Matter of TRAFs. *Frontiers in Immunology*, *9*, 2618. https://doi.org/10.3389/fimmu.2018.02618

Zúñiga-Pflücker, J. C. (2004). T-cell development made simple. *Nature Reviews Immunology*, *4*(1), 67–72. https://doi.org/10.1038/nri1257

10 Figures and Tables

11 List of abbreviations

41BBz	4-1BB-CD3ζ
ACT	Adoptive T cell therapy
AF647	Alexa fluor 647
ALL	Acute lymphoblastic leukemia
AP-1	Activator protein 1
APCs	Antigen presenting cells
BV421	Blue violet 421
Ca2+	Calcium
CAR	Chimeric antigen receptor
CD3	Cluster of differentiation 3
CD3z	CD3ζ
CD4	Cluster of differentiation 4
CD8	Cluster of differentiation 8
CD19	Cluster of differentiation 19, B cell marker
CD28	Cluster of differentiation 28
CD28TM	CD28 transmembrane
CD28z	CD28-CD3ζ
CD80	Cluster of differentiation 80, B7-1
CD86	Cluster of differentiation 86, B7-2
CD137	Cluster of differentiation 137, 4-1BB
CEA	Carcinoembryonic antigen
CFP	Cyan fluorescent protein
CLL	Chronic lymphocytic leukemia
CRS	Cytokine release syndrome
CTA	Cancer-testis antigen
CTLA-4	Cytotoxic T-lymphocyteassociated Protein 4
CTL	Cytotoxic T lymphocytes
DAG	Diacylglycerol
DCs	Dendritic cells
DLBCL	Diffuse large B-cell lymphoma
DN	Double negative
DNA	Desoxyribonucleic acid
DP	Double positive
FACS	Fluorescence-activated cell sorting

FCS	Fetal calf serum
gMFI	Geometric mean fluorescence intensity
GFP	Green fluorescent protein
GRB2	Growth factor receptor-bound protein 2
HA	Hemagglutinin
HLA	Human leukocyte antigen
HSC	Hematopoietic stem cells
ICOS	Inducible T-cell costimulator
IL-x	Interleukin x
IP3	Inositol trisphosphate
ITAM	immunoreceptor tyrosine-based activation motif
JNK	C-Jun N-terminal kinase
LAT	Linker for activation of T cells
LB	Lysogeny broth
Lck	Lymphocyte-specific protein tyrosine kinase
MAPK	Mitogen-activated protein kinase
MCS	Multiple cloning site
MHC	Major histocompatibility complex
NFAT	Nuclear factor of activated T cells
NF-κB	Nuclear factor κB
NK	Natural Killer cells
O/n	Overnight
PBMCs	Peripheral Blood Mononuclear Cells
PD1	Programmed cell death protein 1
PE	Phycoerythrin
PE-Cy7	Phycoerythrin-Cyanine 7
PerCP	Peridinin-Chlorophyll-protein
PI3K	Phosphatidylinositol 3-kinase
PIP2	Phosphatidylinositol 4,5-bisphosphate
PKB	Protein kinase B
PKC	Protein kinase C
PLCγ1	Phospholipase Cγ1
RFP	Red fluorescent protein
scFv	Single-chain antibody fragment
SD	Standard Deviation
SLP-76	SH2-containing leukocyte phosphoprotein of 76 kDa

SP	Single positive
Strep	Streptavidine
TAA	Tumor-associated antigen
TCR	T cell receptor
TNFR	TNF-receptor
T_H	T-Helper cells
TIL	Tumor-infiltrating lymphocytes
TPR	Triple-parameter reporter
Tregs	T regulatory cells
TRAF	TNFR-Associated-Factor
V5	V proteins of the paramyxovirus of the simian virus 5
W/o	Without
ZAP-70	ζ-chain associated protein kinase of 70 kDa

12 Appendix

12.1 Sequences of CD19 CAR constructs

The nucleotide and protein sequences of Dual CARs, single CARs (DC and X variant) are shown here. Moreover, a presentation of the different nucleotide codons used for the extracellular anti-CD19 scFv domain is depicted

Different codons used for same amino acid sequence (aCD19 scFv):

aCD19:CD3z-Puro (DC)

aCD19:CD28-bla (DC)

aCD19:CD3z-Puro (X)

```
 M   L   L   L   V   T   S   L   L   L   C   E   L   P   H   P   A   F   L   L   I
ATG TTG TTG TTG GTT ACT TCA CTC CTC TTG TGT GAA CTT CCT CAT CCG GCA TTC CTT TTG ATT
ATG TTG TTG CTG GTC ACT AGC TTG CTC CTT TGT GAG CTT CCC CAT CCA GCG TTT CTG CTC ATT
ATG CTG CTG CTG GTG ACC AGC CTG CTG CTG TGC GAG CTG CCC CAC CCC GCC TTT CTG CTG ATC

 P   E   Q   K   L   I   S   E   E   D   L   E   Q   K   L   I   S   E   E   D   L
CCT GAA CAA AAG CTC ATT AGT GAG GAA GAT TTG GAG CAA AAG TTG ATT AGT GAA GAG GAC CTC
CCA GAG CAA AAG CTT ATT TCC GAA GAA GAT CTT GAA CAA AAG CTC ATT TCT GAA GAA GAT CTT
CCC GAG CAG AAG CTG ATC TCC GAA GAG GAC CTG GAA CAG AAA CTG ATC AGC GAG GAA GAT CTG

 D   I   Q   M   T   Q   T   T   S   S   L   S   A   S   L   G   D   R   V   T   I
GAT ATA CAA ATG ACG CAA ACA ACG TCT TCA TTG TCC GCA TCC TTG GGA GAT AGG GTC ACA ATT
GAT ATC CAA ATG ACT CAA ACC ACT TCC AGC CTT AGT GCG TCA CTC GGT GAT CGA GTC ACA ATC
GAC ATC CAG ATG ACC CAG ACC ACC TCC AGC CTG AGC GCC AGC CTG GGC GAC CGG GTG ACC ATC

 S   C   R   A   S   Q   D   I   S   K   Y   L   N   W   Y   Q   Q   K   P   D   G
TCA TGT AGA GCG TCC CAA GAT ATT TCA AAA TAC CTC AAT TGG TAC CAA CAA AAG CCA GAT GGA
TCT TGT CGT GCT TCT CAA GAT ATA TCC AAA TAT TTG AAT TGG TAT CAA CAG AAA CCA GAT GGA
AGC TGC CGG GCC AGC CAG GAC ATC AGC AAG TAC CTG AAC TGG TAT CAG CAG AAG CCC GAC GGC

 T   V   K   L   L   I   Y   H   T   S   R   L   H   S   G   V   P   S   R   F   S
ACA GTG AAA TTG TTG ATT TAT CAT ACG AGT AGA CTT CAT TCT GGA GTA CCA TCC CGC TTC TCC
ACT GTT AAA CTC TTG ATC TAC CAT ACT TCT CGT CTT CAT TCT GGC GTC CCG AGT CGC TTT TCA
ACC GTC AAG CTG CTG ATC TAC CAC ACC AGC CGG CTG CAC AGC GGC GTG CCC AGC CGG TTT AGC

 G   S   G   S   G   T   D   Y   S   L   T   I   S   N   L   E   Q   E   D   I   A
GGA TCT GGT TCA GGG ACA GAT TAT TCT CTC ACT ATA TCA AAT TTG GAG CAA GAG GAC ATT GCA
GGA AGC GGG TCA GGG ACT GAT TAT AGT CTC ACC ATA TCT AAT TTG GAA CAA GAA GAT ATT GCA
GGC AGC GGC TCC GGC ACC GAC TAC AGC CTG ACC ATC TCC AAC CTG GAA CAG GAA GAT ATC GCC

 T   Y   F   C   Q   Q   G   N   T   L   P   Y   T   F   G   G   G   T   K   L   E
ACT TAT TTC TGT CAA CAA GGG AAT ACC TTG CCT TAT ACT TTC GGA GGA GGG ACG AAA CTT GAG
ACT TAT TTC TGT CAA CAA GGG AAT ACA CTG CCC TAT ACT TTT GGA GGA GGT ACG AAA TTG GAA
ACC TAC TTT TGC CAG CAG GGC AAC ACA CTG CCC TAC ACC TTT GGC GGC GGA ACA AAG CTG GAA

 I   T   G   S   T   S   G   S   G   K   P   G   S   G   E   G   S   T   K   G   E
ATT ACA GGG TCA ACA TCA GGG TCT GGG AAA CCC GGG TCA GGG GAA GGG TCC ACT AAA GGA GAA
ATT ACT GGA AGT ACA AGT GGG TCT GGA AAG CCT GGT TCC GGT GAG GGG AGC ACT AAA GGA GAG
ATC ACC GGC AGC ACC TCC GGC AGC GGC AAG CCT GGC AGC GGC GAG GGC AGC ACC AAG GGC GAG
```

```
 V   K   L   Q   E   S   G   P   G   L   V   A   P   S   Q   S   L   S   V   T   C
GTA AAA TTG CAA GAG AGT GGA CCC GGT CTT GTC GCT CCT TCC CAA TCC TTG TCA GTC ACT TGT
GTA AAA CTC CAA GAG AGT GGA CCA GGG CTC GTA GCT CCT TCA CAA TCT TTG TCC GTC ACG TGT
GTG AAG CTG CAG GAA AGC GGC CCT GGC CTG GTG GCC CCC AGC CAG AGC CTG AGC GTG ACC TGC

 T   V   S   G   V   S   L   P   D   Y   G   V   S   W   I   R   Q   P   P   R   K
ACT GTC TCC GGA GTC TCT CTC CCG GAT TAT GGG GTT TCC TGG ATT AGA CAA CCA CCA CGG AAA
ACC GTT AGC GGT GTT AGT TTG CCG GAT TAT GGG GTT TCT TGG ATT CGC CAA CCA CCG AGG AAA
ACC GTG AGC GGC GTG AGC CTG CCC GAC TAC GGC GTG AGC TGG ATC CGG CAG CCC CCC AGG AAG

 G   L   E   W   L   G   V   I   W   G   S   E   T   T   Y   Y   N   S   A   L   K
GGA CTG GAG TGG CTC GGA GTC ATT TGG GGT TCT GAA ACG ACT TAT TAT AAT TCC GCT CTC AAA
GGG TTG GAA TGG TTG GGC GTT ATT TGG GGC TCA GAA ACA ACG TAC TAC AAT AGT GCT CTT AAA
GGC CTG GAA TGG CTG GGC GTG ATC TGG GGC AGC GAG ACC ACC TAC TAC AAC AGC GCC CTG AAG

 S   R   L   T   I   I   K   D   N   S   K   S   Q   V   F   L   K   M   N   S   L
AGT CGC TTG ACT ATA ATT AAA GAT AAT TCA AAG AGT CAA GTC TTC TTG AAA ATG AAC TCT CTC
AGC AGG TTG ACC ATA ATT AAA GAC AAT AGC AAA AGC CAA GTT TTC CTC AAG ATG AAT TCA CTT
AGC CGG CTG ACC ATC ATC AAG GAC AAC AGC AAG AGC CAG GTG TTC CTG AAG ATG AAC AGC CTG

 Q   T   D   D   T   A   I   Y   Y   C   A   K   H   Y   Y   Y   G   G   S   Y   A
CAG ACC GAC GAC ACT GCT ATT TAT TAT TGT GCT AAA CAT TAT TAT TAT GGC GGG TCT TAT GCA
CAA ACA GAC GAC ACT GCA ATT TAC TAT TGT GCT AAG CAT TAC TAC TAC GGT GGA AGT TAT GCT
CAG ACC GAC GAC ACC GCC ATC TAC TAC TGC GCC AAG CAC TAC TAC TAC GGC GGC AGC TAC GCC

 M   D   Y   W   G   Q   G   T   S   V   T   V   S   S
ATG GAC TAT TGG GGA CAA GGG ACT TCT GTC ACT GTA TCC TCA
ATG GAT TAC TGG GGT CAA GGC ACG TCA GTT ACT GTA AGT AGT
ATG GAC TAC TGG GGC CAG GGC ACC AGC GTG ACC GTG AGC AGC
```

12.1.1 Dual CARs

aCD19:**CD3z**-aCD19:**CD28**-Puro

Nucleotide sequence:

```
CTCGAGACCATGTTGTTGTTGGTTACTTCACTCCTCTTGTGTGAACTTCCTCATCCGGCATTCCTTTTGATTCCTGAACA
AAAGCTCATTAGTGAGGAAGATTTGGAGCAAAAGTTGATTAGTGAAGAGGACCTCGATATACAAATGACGCAAACAACGT
CTTCATTGTCCGCATCCTTGGGAGATAGGGTCACAATTTCATGTAGAGCGTCCCAAGATATTTCAAAATACCTCAATTGG
TACCAACAAAAGCCAGATGGAACAGTGAAATTGTTGATTTATCATACGAGTAGACTTCATTCTGGAGTACCATCCCGCTT
CTCCGGATCTGGTTCAGGGACAGATTATTCTCTCACTATATCAAATTTGGAGCAAGAGGACATTGCAACTTATTTCTGTC
AACAAGGGAATACCTTGCCTTATACTTTCGGAGGAGGGACGAAACTTGAGATTACAGGGTCAACATCAGGGTCTGGGAAA
CCCGGGTCAGGGGAAGGGTCCACTAAAGGAGAAGTAAAATTGCAAGAGAGTGGACCCGGTCTTGTCGCTCCTTCCCAATC
CTTGTCAGTCACTTGTACTGTCTCCGGAGTCTCTCTCCCGGATTATGGGGTTTCCTGGATTAGACAACCACCACGGAAAG
GACTGGAGTGGCTCGGAGTCATTTGGGGTTCTGAAACGACTTATTATAATTCCGCTCTCAAAAGTCGCTTGACTATAATT
AAAGATAATTCAAAGAGTCAAGTCTTCTTGAAAATGAACTCTCTCCAGACCGACGACACTGCTATTTATTATTGTGCTAA
ACATTATTATTATGGCGGGTCTTATGCAATGGACTATTGGGGACAAGGGACTTCTGTCACTGTATCCTCAGGGAGCAATT
GGAGTCATCCACAATTTGAGAAAGGCGGTAGTGGTGGGAAACCAATACCTAATCCACTCCTCGGTTTGGATAGTACTCCA
ACAACAACTCCTGCCCCTCGGCCCCCAACCCCTGCACCAACTATTGCAAGTCAACCTCTCTCTTTGCGTCCTGAAGCCTC
TCGCCCCGCCGCCGGCGGTGCCGTTCATACACGAGGTCTTGACGCGTTCTGGGTATTGGTAGTCGTAGGTGGAGTCCTCG
CATGTTATTCACTCTTGGTAACAGTTGCATTTATTATTTTCTGGGTCAGGGTTAAATTTTCCCGATCTGCTGATGCGCCA
GCGTATCAACAAGGGCAAAACCAACTTTATAATGAACTTAATTTGGGACGGCGAGAGGAATATGATGTGTTGGACAAACG
ACGAGGACGAGATCCCGAAATGGGTGGAAAACCACGACGCAAGAATCCTCAAGAGGGACTCTACAATGAGCTTCAAAAGG
ATAAAATGGCTGAAGCATATTCCGAAATAGGAATGAAAGGAGAAAGACGGAGAGGTAAAGGGCATGATGGATTGTACCAA
GGTTTGAGCACAGCTACAAAAGACACGTACGATGCACTCCACATGCAAGCACTTCCACCCCGTGGATCCGGAGAAGGTCG
GGGCTCCCTCTTGACATGTGGGGATGTAGAAGAAAATCCTGGGCCTATGTTGTTGCTGGTCACTAGCTTGCTCCTTTGTG
AGCTTCCCCATCCAGCGTTTCTGCTCATTCCAGAGCAAAAGCTTATTTCCGAAGAAGATCTTGAACAAAAGCTCATTTCT
GAAGAAGATCTTGATATCCAAATGACTCAAACCACTTCCAGCCTTAGTGCGTCACTCGGTGATCGAGTCACAATCTCTTG
TCGTGCTTCTCAAGATATATCCAAATATTTGAATTGGTATCAACAGAAACCAGATGGAACTGTTAAACTCTTGATCTACC
ATACTTCTCGTCTTCATTCTGGCGTCCCGAGTCGCTTTTCAGGAAGCGGGTCAGGGACTGATTATAGTCTCACCATATCT
AATTTGGAACAAGAAGATATTGCAACTTATTTCTGTCAACAAGGGAATACACTGCCCTATACTTTTGGAGGAGGTACGAA
ATTGGAAATTACTGGAAGTACAAGTGGGTCTGGAAAGCCTGGTTCCGGTGAGGGGAGCACTAAAGGAGAGGTAAAACTCC
AAGAGAGTGGACCAGGGCTCGTAGCTCCTTCACAATCTTTGTCCGTCACGTGTACCGTTAGCGGTGTTAGTTTGCCGGAT
TATGGGGTTTCTTGGATTCGCCAACCACCGAGGAAAGGGTTGGAATGGTTGGGCGTTATTTGGGGCTCAGAAACAACGTA
CTACAATAGTGCTCTTAAAAGCAGGTTGACCATAATTAAAGACAATAGCAAAAGCCAAGTTTTCCTCAAGATGAATTCAC
TTCAAACAGACGACACTGCAATTTACTATTGTGCTAAGCATTACTACTACGGTGGAAGTTATGCTATGGATTACTGGGGT
CAAGGCACGTCAGTTACTGTAAGTAGTGGGAGCAATTGGAGTCATCCACAATTCGAAAAGGGTGGCAGTGGTGGTTATCC
GTATGATGTCCCAGATTATGCTCCCACAACAACACCTGCTCCAAGACCCCCTACTCCAGCACCCACAATTGCTTCCCAAC
CACTTTCACTCAGGCCAGAAGCGTCACGCCCTGCAGCAGGCGGGGCGGTCCATACACGTGGATTGACTAGTTTCTGGGTT
CTGGTTGTTGTTGGTGGGGTCCTTGCATGTTACTCCCTGCTGGTCACCGTAGCTTTTATCATATTTTGGGTTCGAAGTAA
ACGGTCTAGGCTTCTTCATAGTGATTATATGAATATGACACCACGGCGTCCAGGACCTACGCGCAAACATTATCAACCGT
ATGCACCACCGCGCGATTTTGCGGCATATCGATCTCATATGGGGTCTGGGGCGACAAACTTTTCCCTTTTGAAACAAGCT
GGTGATGTAGAAGAAAATCCTGGACCTATGACGGAATATAAACCAACCGTCAGGCTGGCTACTAGAGATGATGTTCCGCG
CGCAGTTCGGACTTTGGCTGCTGCATTTGCAGATTATCCTGCGACCAGACATACGGTAGACCCTGATCGGCATATTGAAA
GGGTTACTGAACTTCAGGAGCTGTTTCTGACTAGGGTGGGACTGGATATTGGAAAAGTTTGGGTAGCCGATGATGGGGCT
GCAGTTGCCGTTTGGACAACCCCCGAATCTGTCGAGGCTGGCGCAGTATTTGCGGAAATTGGACCTCGAATGGCGGAACT
CTCCGGCTCTAGGTTGGCTGCCCAACAGCAAATGGAAGGATTGCTTGCACCACATAGGCCAAAAGAACCTGCTTGGTTTC
TGGCAACAGTAGGGGTGAGTCCGGATCATCAAGGGAAAGGCTTGGGTTCTGCGGTGGTTCTTCCTGGTGTCGAAGCCGCT
GAACGAGCTGGCGTTCCTGCTTTTCTCGAAACTTCAGCCCCGCGGAATTTGCCATTTTATGAACGACTGGGGTTTACTGT
TACAGCTGATGTGGAAGTACCAGAGGGTCCAAGAACATGGTGTATGACTAGGAAACCAGGGGCATAAGCGGCCGC
```

Features:

XhoI	: [1 : 6]
anti-CD19 scFv	: [10 : 870]
Peptide tag 1 (Strep)	: [871 : 903]
linker GGSG	: [904 : 915]
Peptide tag 2 (V5)	: [916 : 957]
CD8 Hinge	: [958 : 1080]
MluI	: [1082 : 1087]
CD28 TM	: [1090 : 1167]
signal motif 1 CD3z	: [1168 : 1503]
BamHI	: [1504 : 1509]
T2A	: [1510 : 1566]
anti-CD19 scFv	: [1567 : 2427]
Peptide tag 1 (Strep)	: [2428 : 2460]
linker GGSGG	: [2461 : 2475]

Peptide tag 3 (HA) : [2476 : 2502]
CD8 Hinge : [2503 : 2625]
SpeI : [2626 : 2631]
CD28 TM : [2632 : 2712]
CD28cyto : [2713 : 2835]
NdeI : [2836 : 2841]
P2A : [2842 : 2907]
Puromycin N-acetyltransferase : [2908 : 3507]
NotI : [3508 : 3515]

Protein sequence:
LETMLLLVTSLLLCELPHPAFLLIPEQKLISEEDLEQKLISEEDLDIQMTQTTSSLSASLGDRVTISCRASQDISKYLNW
YQQKPDGTVKLLIYHTSRLHSGVPSRFSGSGSGTDYSLTISNLEQEDIATYFCQQGNTLPYTFGGGTKLEITGSTSGSGK
PGSGEGSTKGEVKLQESGPGLVAPSQSLSVTCTVSGVSLPDYGVSWIRQPPRKGLEWLGVIWGSETTYYNSALKSRLTII
KDNSKSQVFLKMNSLQTDDTAIYYCAKHYYYGGSYAMDYWGQGTSVTVSSGSNWSHPQFEKGGSGGKPIPNPLLGLDSTP
TTTPAPRPPTPAPTIASQPLSLRPEASRPAAGGAVHTRGLDAFWVLVVVGGVLACYSLLVTVAFIIFWVRVKFSRSADAP
AYQQGQNQLYNELNLGRREEYDVLDKRRGRDPEMGGKPRRKNPQEGLYNELQKDKMAEAYSEIGMKGERRRGKGHDGLYQ
GLSTATKDTYDALHMQALPPRGSGEGRGSLLTCGDVEENPGPMLLLVTSLLLCELPHPAFLLIPEQKLISEEDLEQKLIS
EEDLDIQMTQTTSSLSASLGDRVTISCRASQDISKYLNWYQQKPDGTVKLLIYHTSRLHSGVPSRFSGSGSGTDYSLTIS
NLEQEDIATYFCQQGNTLPYTFGGGTKLEITGSTSGSGKPGSGEGSTKGEVKLQESGPGLVAPSQSLSVTCTVSGVSLPD
YGVSWIRQPPRKGLEWLGVIWGSETTYYNSALKSRLTIIKDNSKSQVFLKMNSLQTDDTAIYYCAKHYYYGGSYAMDYWG
QGTSVTVSSGSNWSHPQFEKGGSGGYPYDVPDYAPTTTPAPRPPTPAPTIASQPLSLRPEASRPAAGGAVHTRGLTSFWV
LVVVGGVLACYSLLVTVAFIIFWVRSKRSRLLHSDYMNMTPRRPGPTRKHYQPYAPPRDFAAYRSHMGSGATNFSLLKQA
GDVEENPGPMTEYKPTVRLATRDDVPRAVRTLAAAFADYPATRHTVDPDRHIERVTELQELFLTRVGLDIGKVWVADDGA
AVAVWTTPESVEAGAVFAEIGPRMAELSGSRLAAQQQMEGLLAPHRPKEPAWFLATVGVSPDHQGKGLGSAVVLPGVEAA
ERAGVPAFLETSAPRNLPFYERLGFTVTADVEVPEGPRTWCMTRKPGA

aCD19:**CD3z**-aCD19:**41BB**-Puro

Nucleotidee sequence:
CTCGAGACCATGTTGTTGTTGGTTACTTCACTCCTCTTGTGTGAACTTCCTCATCCGGCATTCCTTTTGATTCCTGAACA
AAAGCTCATTAGTGAGGAAGATTTGGAGCAAAAGTTGATTAGTGAAGAGGACCTCGATATACAAATGACGCAAACAACGT
CTTCATTGTCCGCATCCTTGGGAGATAGGGTCACAATTTCATGTAGAGCGTCCCAAGATATTTCAAAATACCTCAATTGG
TACCAACAAAAGCCAGATGGAACAGTGAAATTGTTGATTTATCATACGAGTAGACTTCATTCTGGAGTACCATCCCGCTT
CTCCGGATCTGGTTCAGGGACAGATTATTCTCTCACTATATCAAATTTGGAGCAAGAGGACATTGCAACTTATTTCTGTC
AACAAGGGAATACCTTGCCTTATACTTTCGGAGGAGGGACGAAACTTGAGATTACAGGGTCAACATCAGGGTCTGGGAAA
CCCGGGTCAGGGGAAGGGTCCACTAAAGGAGAAGTAAAATTGCAAGAGAGTGGACCCGGTCTTGTCGCTCCTTCCCAATC
CTTGTCAGTCACTTGTACTGTCTCCGGAGTCTCTCTCCCGGATTATGGGGTTTCCTGGATTAGACAACCACCACGGAAAG
GACTGGAGTGGCTCGGAGTCATTTGGGGTTCTGAAACGACTTATTATAATTCCGCTCTCAAAAGTCGCTTGACTATAATT
AAAGATAATTCAAAGAGTCAAGTCTTCTTGAAAATGAACTCTCTCCAGACCGACGACACTGCTATTTATTATTGTGCTAA
ACATTATTATTATGGCGGGTCTTATGCAATGGACTATTGGGGACAAGGGACTTCTGTCACTGTATCCTCAGGGAGCAATT
GGAGTCATCCACAATTTGAGAAAGGCGGTAGTGGTGGGAAACCAATACCTAATCCACTCCTCGGTTTGGATAGTACTCCA
ACAACAACTCCTGCCCCTCGGCCCCCAACCCCTGCACCAACTATTGCAAGTCAACCTCTCTCTTTGCGTCCTGAAGCCTC
TCGCCCCGCCGCCGGCGGTGCCGTTCATACACGAGGTCTTGACGCGTTCTGGGTATTGGTAGTCGTAGGTGGAGTCCTCG
CATGTTATTCACTCTTGGTAACAGTTGCATTTATTATTTTCTGGGTCAGGGTTAAATTTTCCCGATCTGCTGATGCGCCA
GCGTATCAACAAGGGCAAAACCAACTTTATAATGAACTTAATTTGGGACGGCGAGAGGAATATGATGTGTTGGACAAACG
ACGAGGACGAGATCCCGAAATGGGTGGAAAACCACGACGCAAGAATCCTCAAGAGGGACTCTACAATGAGCTTCAAAAGG
ATAAAATGGCTGAAGCATATTCCGAAATAGGAATGAAAGGAGAAAGACGGAGAGGTAAAGGGCATGATGGATTGTACCAA
GGTTTGAGCACAGCTACAAAAGACACGTACGATGCACTCCACATGCAAGCACTTCCACCCCGTGGATCCGGAGAAGGTCG
GGGCTCCCTCTTGACATGTGGGGATGTAGAAGAAAATCCTGGGCCTATGTTGTTGCTGGTCACTAGCTTGCTCCTTTGTG
AGCTTCCCCATCCAGCGTTTCTGCTCATTCCAGAGCAAAAGCTTATTTCCGAAGAAGATCTTGAACAAAAGCTCATTTCT
GAAGAAGATCTTGATATCCAAATGACTCAAACCACTTCCAGCCTTAGTGCGTCACTCGGTGATCGAGTCACAATCTCTTG
TCGTGCTTCTCAAGATATATCCAAATATTTGAATTGGTATCAACAGAAACCAGATGGAACTGTTAAACTCTTGATCTACC
ATACTTCTCGTCTTCATTCTGGCGTCCCGAGTCGCTTTTCAGGAAGCGGGTCAGGGACTGATTATAGTCTCACCATATCT
AATTTGGAACAAGAAGATATTGCAACTTATTTCTGTCAACAAGGGAATACACTGCCCTATACTTTTGGAGGAGGTACGAA
ATTGGAAATTACTGGAAGTACAAGTGGGTCTGGAAAGCCTGGTTCCGGTGAGGGGAGCACTAAAGGAGAGGTAAAACTCC
AAGAGAGTGGACCAGGGCTCGTAGCTCCTTCACAATCTTTGTCCGTCACGTGTACCGTTAGCGGTGTTAGTTTGCCGGAT
TATGGGGTTTCTTGGATTCGCCAACCACCGAGGAAAGGGTTGGAATGGTTGGGCGTTATTTGGGGCTCAGAAACAACGTA
CTACAATAGTGCTCTTAAAAGCAGGTTGACCATAATTAAAGACAATAGCAAAAGCCAAGTTTTCCTCAAGATGAATTCAC
TTCAAACAGACGACACTGCAATTTACTATTGTGCTAAGCATTACTACTACGGTGGAAGTTATGCTATGGATTACTGGGGT
CAAGGCACGTCAGTTACTGTAAGTAGTGGGAGCAATTGGAGTCATCCACAATTCGAAAAGGGTGGCAGTGGTGGTTATCC
GTATGATGTCCCAGATTATGCTCCCACAACAACACCTGCTCCAAGACCCCCTACTCCAGCACCCACAATTGCTTCCCAAC
CACTTTCACTCAGGCCAGAAGCGTCACGCCCTGCAGCAGGCGGGGCGGTCCATACACGTGGATTGACTAGTTTCTGGGTT
CTGGTTGTTGTTGGTGGGGTCCTTGCATGTTACTCCCTGCTGGTCACCGTAGCTTTTATCATATTTTGGGTTAAGCGCGG
GAGGAAAAAGCTGCTCTACATTTTTAAGCAGCCTTTCATGAGGCCTGTACAGACAACGCAGGAAGAGGACGGGTGCAGTT

GTCGTTTCCCTGAGGAGGAGGAGGGTGGCTGCGAGCTCCATATGGGGTCTGGGGCGACAAACTTTTCCCTTTTGAAACAA
GCTGGTGATGTAGAAGAAAATCCTGGACCTATGACGGAATATAAACCAACCGTCAGGCTGGCTACTAGAGATGATGTTCC
GCGCGCAGTTCGGACTTTGGCTGCTGCATTTGCAGATTATCCTGCGACCAGACATACGGTAGACCCTGATCGGCATATTG
AAAGGGTTACTGAACTTCAGGAGCTGTTTCTGACTAGGGTGGGACTGGATATTGGAAAAGTTTGGGTAGCCGATGATGGG
GCTGCAGTTGCCGTTTGGACAACCCCCGAATCTGTCGAGGCTGGCGCAGTATTTGCGGAAATTGGACCTCGAATGGCGGA
ACTCTCCGGCTCTAGGTTGGCTGCCCAACAGCAAATGGAAGGATTGCTTGCACCACATAGGCCAAAAGAACCTGCTTGGT
TTCTGGCAACAGTAGGGGTGAGTCCGGATCATCAAGGGAAAGGCTTGGGTTCTGCGGTGGTTCTTCCTGGTGTCGAAGCC
GCTGAACGAGCTGGCGTTCCTGCTTTTCTCGAAACTTCAGCCCCGCGGAATTTGCCATTTTATGAACGACTGGGGTTTAC
TGTTACAGCTGATGTGGAAGTACCAGAGGGTCCAAGAACATGGTGTATGACTAGGAAACCAGGGGCATAAGCGGCCGC

Features:

XhoI	:	[1 : 6]
anti-CD19 scFv	:	[10 : 870]
Peptide tag 1 (Strep)	:	[871 : 903]
linker GGSG	:	[904 : 915]
Peptide tag 2 (V5)	:	[916 : 957]
CD8 Hinge	:	[958 : 1080]
MluI	:	[1082 : 1087]
CD28 TM	:	[1090 : 1167]
signal motif 1 CD3z	:	[1168 : 1503]
BamHI	:	[1504 : 1509]
T2A	:	[1510 : 1566]
anti-CD19 scFv	:	[1567 : 2427]
Peptide tag 1 (Strep)	:	[2428 : 2460]
linker GGSGG	:	[2461 : 2475]
Peptide tag 3 (HA)	:	[2476 : 2502]
CD8 Hinge	:	[2503 : 2625]
SpeI	:	[2626 : 2631]
CD28 TM	:	[2632 : 2712]
signal motif 2 4-1BB	:	[2713 : 2838]
NdeI	:	[2839 : 2844]
P2A	:	[2845 : 2910]
Puromycin N-acetyltransferase	:	[2911 : 3510]
NotI	:	[3511 : 3518]

Protein sequence:

LETMLLLVTSLLLCELPHPAFLLIPEQKLISEEDLEQKLISEEDLDIQMTQTTSSLSASLGDRVTISCRASQDISKYLNW
YQQKPDGTVKLLIYHTSRLHSGVPSRFSGSGSGTDYSLTISNLEQEDIATYFCQQGNTLPYTFGGGTKLEITGSTSGSGK
PGSGEGSTKGEVKLQESGPGLVAPSQSLSVTCTVSGVSLPDYGVSWIRQPPRKGLEWLGVIWGSETTYYNSALKSRLTII
KDNSKSQVFLKMNSLQTDDTAIYYCAKHYYYGGSYAMDYWGQGTSVTVSSGSNWSHPQFEKGGSGGKPIPNPLLGLDSTP
TTTPAPRPPTPAPTIASQPLSLRPEASRPAAGGAVHTRGLDAFWVLVVVGGVLACYSLLVTVAFIIFWVRVKFSRSADAP
AYQQGQNQLYNELNLGRREEYDVLDKRRGRDPEMGGKPRRKNPQEGLYNELQKDKMAEAYSEIGMKGERRRGKGHDGLYQ
GLSTATKDTYDALHMQALPPRGSGEGRGSLLTCGDVEENPGPMLLLVTSLLLCELPHPAFLLIPEQKLISEEDLEQKLIS
EEDLDIQMTQTTSSLSASLGDRVTISCRASQDISKYLNWYQQKPDGTVKLLIYHTSRLHSGVPSRFSGSGSGTDYSLTIS
NLEQEDIATYFCQQGNTLPYTFGGGTKLEITGSTSGSGKPGSGEGSTKGEVKLQESGPGLVAPSQSLSVTCTVSGVSLPD
YGVSWIRQPPRKGLEWLGVIWGSETTYYNSALKSRLTIIKDNSKSQVFLKMNSLQTDDTAIYYCAKHYYYGGSYAMDYWG
QGTSVTVSSGSNWSHPQFEKGGSGGYPYDVPDYAPTTTPAPRPPTPAPTIASQPLSLRPEASRPAAGGAVHTRGLTSFWV
LVVVGGVLACYSLLVTVAFIIFWVKRGRKKLLYIFKQPFMRPVQTTQEEDGCSCRFPEEEEGGCELHMGSGATNFSLLKQ
AGDVEENPGPMTEYKPTVRLATRDDVPRAVRTLAAAFADYPATRHTVDPDRHIERVTELQELFLTRVGLDIGKVWVADDG
AAVAVWTTPESVEAGAVFAEIGPRMAELSGSRLAAQQQMEGLLAPHRPKEPAWFLATVGVSPDHQGKGLGSAVVLPGVEA
AERAGVPAFLETSAPRNLPFYERLGFTVTADVEVPEGPRTWCMTRKPGA

aCD19:**41BBz**-aCD19:**41BBz**-Puro

Nucleotide sequence:

```
CTCGAGACCATGTTGTTGTTGGTTACTTCACTCCTCTTGTGTGAACTTCCTCATCCGGCATTCCTTTTGATTCCTGAACA
AAAGCTCATTAGTGAGGAAGATTTGGAGCAAAAGTTGATTAGTGAAGAGGACCTCGATATACAAATGACGCAAACAACGT
CTTCATTGTCCGCATCCTTGGGAGATAGGGTCACAATTTCATGTAGAGCGTCCCAAGATATTTCAAAATACCTCAATTGG
TACCAACAAAAGCCAGATGGAACAGTGAAATTGTTGATTTATCATACGAGTAGACTTCATTCTGGAGTACCATCCCGCTT
CTCCGGATCTGGTTCAGGGACAGATTATTCTCTCACTATATCAAATTTGGAGCAAGAGGACATTGCAACTTATTTCTGTC
AACAAGGGAATACCTTGCCTTATACTTTCGGAGGAGGGACGAAACTTGAGATTACAGGGTCAACATCAGGGTCTGGGAAA
CCCGGGTCAGGGGAAGGGTCCACTAAAGGAGAAGTAAAATTGCAAGAGAGTGGACCCGGTCTTGTCGCTCCTTCCCAATC
CTTGTCAGTCACTTGTACTGTCTCCGGAGTCTCTCTCCCGGATTATGGGGTTTCCTGGATTAGACAACCACCACGGAAAG
GACTGGAGTGGCTCGGAGTCATTTGGGGTTCTGAAACGACTTATTATAATTCCGCTCTCAAAAGTCGCTTGACTATAATT
AAAGATAATTCAAAGAGTCAAGTCTTCTTGAAAATGAACTCTCTCCAGACCGACGACACTGCTATTTATTATTGTGCTAA
ACATTATTATTATGGCGGGTCTTATGCAATGGACTATTGGGGACAAGGGACTTCTGTCACTGTATCCTCAGGGAGCAATT
GGAGTCATCCACAATTTGAGAAAGGCGGTAGTGGTGGGAAACCAATACCTAATCCACTCCTCGGTTTGGATAGTACTCCA
ACAACAACTCCTGCCCCTCGGCCCCCAACCCCTGCACCAACTATTGCAAGTCAACCTCTCTCTTTGCGTCCTGAAGCCTC
TCGCCCCGCCGCCGGCGGTGCCGTTCATACACGAGGTCTTGACGCGTTCTGGGTGCTGGTGGTGGTCGGAGGCGTGCTGG
CCTGCTACAGCCTGCTGGTCACCGTGGCCTTCATCATCTTTTGGGTGAAACGGGGCAGAAAGAAACTCCTGTATATATTC
AAACAACCATTTATGAGACCAGTACAAACTACTCAAGAGGAAGATGGCTGTAGCTGCCGATTTCCAGAAGAAGAAGAAGG
AGGATGTGAACTGCGGGTGAAGTTCAGCAGAAGCGCCGACGCCCCTGCCTACCAGCAGGGCCAGAATCAGCTGTACAACG
AGCTGAACCTGGGCAGAAGGGAAGAGTACGACGTCCTGGATAAGCGGAGAGGCCGGGACCCTGAGATGGGCGGCAAGCCT
CGGCGGAAGAACCCCCAGGAAGGCCTGTATAACGAACTGCAGAAAGACAAGATGGCCGAGGCCTACAGCGAGATCGGCAT
GAAGGGCGAGCGGAGGCGGGGCAAGGGCCACGACGGCCTGTATCAGGGCCTGTCCACCGCCACCAAGGATACCTACGACG
CCCTGCACATGCAGGCCCTGCCCCCAAGGGGATCCGGAGAAGGTCGGGGCTCCCTCTTGACATGTGGGGATGTAGAAGAA
AATCCTGGGCCTATGTTGTTGCTGGTCACTAGCTTGCTCCTTTGTGAGCTTCCCCATCCAGCGTTTCTGCTCATTCCAGA
GCAAAAGCTTATTTCCGAAGAAGATCTTGAACAAAAGCTCATTTCTGAAGAAGATCTTGATATCCAAATGACTCAAACCA
CTTCCAGCCTTAGTGCGTCACTCGGTGATCGAGTCACAATCTCTTGTCGTGCTTCTCAAGATATATCCAAATATTTGAAT
TGGTATCAACAGAAACCAGATGGAACTGTTAAACTCTTGATCTACCATACTTCTCGTCTTCATTCTGGCGTCCCGAGTCG
CTTTTCAGGAAGCGGGTCAGGGACTGATTATAGTCTCACCATATCTAATTTGGAACAAGAAGATATTGCAACTTATTTCT
GTCAACAAGGGAATACACTGCCCTATACTTTTGGAGGAGGTACGAAATTGGAAATTACTGGAAGTACAAGTGGGTCTGGA
AAGCCTGGTTCCGGTGAGGGGAGCACTAAAGGAGAGGTAAAACTCCAAGAGAGTGGACCAGGGCTCGTAGCTCCTTCACA
ATCTTTGTCCGTCACGTGTACCGTTAGCGGTGTTAGTTTGCCGGATTATGGGGTTTCTTGGATTCGCCAACCACCGAGGA
AAGGGTTGGAATGGTTGGGCGTTATTTGGGGCTCAGAAACAACGTACTACAATAGTGCTCTTAAAAGCAGGTTGACCATA
ATTAAAGACAATAGCAAAAGCCAAGTTTTCCTCAAGATGAATTCACTTCAAACAGACGACACTGCAATTTACTATTGTGC
TAAGCATTACTACTACGGTGGAAGTTATGCTATGGATTACTGGGGTCAAGGCACGTCAGTTACTGTAAGTAGTGGGAGCA
ATTGGAGTCATCCACAATTCGAAAAGGGTGGCAGTGGTGGTTATCCGTATGATGTCCCAGATTATGCTCCCACAACAACA
CCTGCTCCAAGACCCCCTACTCCAGCACCCACAATTGCTTCCCAACCACTTTCACTCAGGCCAGAAGCGTCACGCCCTGC
AGCAGGCGGGGCGGTCCATACACGTGGATTGACTAGTTTCTGGGTTCTGGTTGTTGTTGGTGGGGTCCTTGCATGTTACT
CCCTGCTGGTCACCGTAGCTTTTATCATATTTTGGGTTAAGCGCGGGAGGAAAAAGCTGCTCTACATTTTTAAGCAGCCT
TTCATGAGGCCTGTACAGACAACGCAGGAAGAGGACGGGTGCAGTTGTCGTTTCCCTGAGGAGGAGGAGGGTGGCTGCGA
GCTCAGGGTTAAATTTTCCCGATCTGCTGATGCGCCAGCGTATCAACAAGGGCAAAACCAACTTTATAATGAACTTAATT
TGGGACGGCGAGAGGAATATGATGTGTTGGACAAACGACGAGGACGAGATCCCGAAATGGGTGGAAAACCACGACGCAAG
AATCCTCAAGAGGGACTCTACAATGAGCTTCAAAAGGATAAAATGGCTGAAGCATATTCCGAAATAGGAATGAAAGGAGA
AAGACGGAGAGGTAAAGGGCATGATGGATTGTACCAAGGTTTGAGCACAGCTACAAAAGACACGTACGATGCACTCCACA
TGCAAGCACTTCCACCCCGTCATATGGGGTCTGGGGCGACAAACTTTTCCCTTTTGAAACAAGCTGGTGATGTAGAAGAA
AATCCTGGACCTATGACGGAATATAAACCAACCGTCAGGCTGGCTACTAGAGATGATGTTCCGCGCGCAGTTCGGACTTT
GGCTGCTGCATTTGCAGATTATCCTGCGACCAGACATACGGTAGACCCTGATCGGCATATTGAAAGGGTTACTGAACTTC
AGGAGCTGTTTCTGACTAGGGTGGGACTGGATATTGGAAAAGTTTGGGTAGCCGATGATGGGGCTGCAGTTGCCGTTTGG
ACAACCCCCGAATCTGTCGAGGCTGGCGCAGTATTTGCGGAAATTGGACCTCGAATGGCGGAACTCTCCGGCTCTAGGTT
GGCTGCCCAACAGCAAATGGAAGGATTGCTTGCACCACATAGGCCAAAAGAACCTGCTTGGTTTCTGGCAACAGTAGGGG
TGAGTCCGGATCATCAAGGGAAAGGCTTGGGTTCTGCGGTGGTTCTTCCTGGTGTCGAAGCCGCTGAACGAGCTGGCGTT
CCTGCTTTTCTCGAAACTTCAGCCCCGCGGAATTTGCCATTTTATGAACGACTGGGGTTTACTGTTACAGCTGATGTGGA
AGTACCAGAGGGTCCAAGAACATGGTGTATGACTAGGAAACCAGGGGCATAAGCGGCCGC
```

Features:

XhoI	: [1 : 6]
anti-CD19 scFv	: [10 : 870]
Peptide tag 1 (Strep)	: [871 : 903]
linker GGSG	: [904 : 915]
Peptide tag 2 (V5)	: [916 : 957]
CD8 Hinge	: [958 : 1080]
MluI	: [1082 : 1087]
CD28 TM (X15)	: [1088 : 1167]
signal motif 1 4-1BB	: [1168 : 1293]

signal motif 1 CD3z (X15)	: [1294 : 1629]
BamHI	: [1630 : 1635]
T2A	: [1636 : 1692]
anti-CD19 scFv	: [1693 : 2553]
Peptide tag 1 (Strep)	: [2554 : 2586]
linker GGSGG	: [2587 : 2601]
Peptide tag 3 (HA)	: [2602 : 2628]
CD8 Hinge	: [2629 : 2751]
SpeI	: [2752 : 2757]
CD28 TM	: [2758 : 2838]
signal motif 2 4-1BB	: [2839 : 2964]
signal motif 2 CD3z	: [2965 : 3300]
NdeI	: [3301 : 3306]
P2A	: [3307 : 3372]
Puromycin N-acetyltransferase	: [3373 : 3972]
NotI	: [3973 : 3980]

Protein sequence

LETMLLLVTSLLLCELPHPAFLLIPEQKLISEEDLEQKLISEEDLDIQMTQTTSSLSASLGDRVTISCRASQDISKYLNW
YQQKPDGTVKLLIYHTSRLHSGVPSRFSGSGSGTDYSLTISNLEQEDIATYFCQQGNTLPYTFGGGTKLEITGSTSGSGK
PGSGEGSTKGEVKLQESGPGLVAPSQSLSVTCTVSGVSLPDYGVSWIRQPPRKGLEWLGVIWGSETTYYNSALKSRLTII
KDNSKSQVFLKMNSLQTDDTAIYYCAKHYYYGGSYAMDYWGQGTSVTVSSGSNWSHPQFEKGGSGGKPIPNPLLGLDSTP
TTTPAPRPPTPAPTIASQPLSLRPEASRPAAGGAVHTRGLDAFWVLVVVGGVLACYSLLVTVAFIIFWVKRGRKKLLYIF
KQPFMRPVQTTQEEDGCSCRFPEEEEGGCELRVKFSRSADAPAYQQGQNQLYNELNLGRREEYDVLDKRRGRDPEMGGKP
RRKNPQEGLYNELQKDKMAEAYSEIGMKGERRRGKGHDGLYQGLSTATKDTYDALHMQALPPRGSGEGRGSLLTCGDVEE
NPGPMLLLVTSLLLCELPHPAFLLIPEQKLISEEDLEQKLISEEDLDIQMTQTTSSLSASLGDRVTISCRASQDISKYLN
WYQQKPDGTVKLLIYHTSRLHSGVPSRFSGSGSGTDYSLTISNLEQEDIATYFCQQGNTLPYTFGGGTKLEITGSTSGSG
KPGSGEGSTKGEVKLQESGPGLVAPSQSLSVTCTVSGVSLPDYGVSWIRQPPRKGLEWLGVIWGSETTYYNSALKSRLTI
IKDNSKSQVFLKMNSLQTDDTAIYYCAKHYYYGGSYAMDYWGQGTSVTVSSGSNWSHPQFEKGGSGGYPYDVPDYAPTTT
PAPRPPTPAPTIASQPLSLRPEASRPAAGGAVHTRGLTSFWVLVVVGGVLACYSLLVTVAFIIFWVKRGRKKLLYIFKQP
FMRPVQTTQEEDGCSCRFPEEEEGGCELRVKFSRSADAPAYQQGQNQLYNELNLGRREEYDVLDKRRGRDPEMGGKPRRK
NPQEGLYNELQKDKMAEAYSEIGMKGERRRGKGHDGLYQGLSTATKDTYDALHMQALPPRHMGSGATNFSLLKQAGDVEE
NPGPMTEYKPTVRLATRDDVPRAVRTLAAAFADYPATRHTVDPDRHIERVTELQELFLTRVGLDIGKVWVADDGAAVAVW
TTPESVEAGAVFAEIGPRMAELSGSRLAAQQQMEGLLAPHRPKEPAWFLATVGVSPDHQGKGLGSAVVLPGVEAAERAGV
PAFLETSAPRNLPFYERLGFTVTADVEVPEGPRTWCMTRKPGA

12.1.2 Single CARs

aCD19:**CD3z**-Puro

Nucleotide sequence:

```
CTCGAGACCATGTTGTTGTTGGTTACTTCACTCCTCTTGTGTGAACTTCCTCATCCGGCATTCCTTTTGATTCCTGAACA
AAAGCTCATTAGTGAGGAAGATTTGGAGCAAAAGTTGATTAGTGAAGAGGACCTCGATATACAAATGACGCAAACAACGT
CTTCATTGTCCGCATCCTTGGGAGATAGGGTCACAATTTCATGTAGAGCGTCCCAAGATATTTCAAAATACCTCAATTGG
TACCAACAAAAGCCAGATGGAACAGTGAAATTGTTGATTTATCATACGAGTAGACTTCATTCTGGAGTACCATCCCGCTT
CTCCGGATCTGGTTCAGGGACAGATTATTCTCTCACTATATCAAATTTGGAGCAAGAGGACATTGCAACTTATTTCTGTC
AACAAGGGAATACCTTGCCTTATACTTTCGGAGGAGGGACGAAACTTGAGATTACAGGGTCAACATCAGGGTCTGGGAAA
CCCGGGTCAGGGGAAGGGTCCACTAAAGGAGAAGTAAAATTGCAAGAGAGTGGACCCGGTCTTGTCGCTCCTTCCCAATC
CTTGTCAGTCACTTGTACTGTCTCCGGAGTCTCTCTCCCGGATTATGGGGTTTCCTGGATTAGACAACCACCACGGAAAG
GACTGGAGTGGCTCGGAGTCATTTGGGGTTCTGAAACGACTTATTATAATTCCGCTCTCAAAAGTCGCTTGACTATAATT
AAAGATAATTCAAAGAGTCAAGTCTTCTTGAAAATGAACTCTCTCCAGACCGACGACACTGCTATTTATTATTGTGCTAA
ACATTATTATTATGGCGGGTCTTATGCAATGGACTATTGGGGACAAGGGACTTCTGTCACTGTATCCTCAGGGAGCAATT
GGAGTCATCCACAATTTGAGAAAGGCGGTAGTGGTGGGAAACCAATACCTAATCCACTCCTCGGTTTGGATAGTACTCCC
ACAACAACACCTGCTCCAAGACCCCCTACTCCAGCACCCACAATTGCTTCCCAACCACTTTCACTCAGGCCAGAAGCGTC
ACGCCCTGCAGCAGGCGGGGCGGTCCATACACGTGGATTGGACGCGTTCTGGGTATTGGTAGTCGTAGGTGGAGTCCTCG
CATGTTATTCACTCTTGGTAACAGTTGCATTTATTATTTTCTGGGTCAGGGTTAAATTTTCCCGATCTGCTGATGCGCCA
GCGTATCAACAAGGGCAAAACCAACTTTATAATGAACTTAATTTGGGACGGCGAGAGGAATATGATGTGTTGGACAAACG
ACGAGGACGAGATCCCGAAATGGGTGGAAAACCACGACGCAAGAATCCTCAAGAGGGACTCTACAATGAGCTTCAAAAGG
ATAAAATGGCTGAAGCATATTCCGAAATAGGAATGAAAGGAGAAAGACGGAGAGGTAAAGGGCATGATGGATTGTACCAA
GGTTTGAGCACAGCTACAAAAGACACGTACGATGCACTCCACATGCAAGCACTTCCACCCCGTGGATCCGGAGCTACTAA
CTTCAGCCTGCTGAAGCAGGCTGGAGACGTCGAGGAGAACCCTGGACCTATGACCGAGTACAAGCCCACGGTGCGCCTCG
CCACCCGCGACGACGTCCCCAGGGCCGTACGCACCCTCGCCGCCGCGTTCGCCGACTACCCCGCCACGCGCCACACCGTC
GATCCGGACCGCCACATCGAGCGGGTCACCGAGCTGCAAGAACTCTTCCTCACGCGCGTCGGGCTCGACATCGGCAAGGT
GTGGGTCGCGGACGACGGCGCCGCGGTGGCGGTCTGGACCACGCCGGAGAGCGTCGAAGCGGGGGCGGTGTTCGCCGAGA
TCGGCCCGCGCATGGCCGAGTTGAGCGGTTCCCGGCTGGCCGCGCAGCAACAGATGGAAGGCCTCCTGGCGCCGCACCGG
CCCAAGGAGCCCGCGTGGTTCCTGGCCACCGTCGGCGTCTCGCCCGACCACCAGGGCAAGGGTCTGGGCAGCGCCGTCGT
GCTCCCCGGAGTGGAGGCGGCCGAGCGCGCCGGGGTGCCCGCCTTCCTGGAGACCTCCGCGCCCCGCAACCTCCCCTTCT
ACGAGCGGCTCGGCTTCACCGTCACCGCCGACGTCGAGGTGCCCGAAGGACCGCGCACCTGGTGCATGACCCGCAAGCCC
GGTGCCTGAGCGGCCGC
```

Features:

```
XhoI                    : [1 : 6]
anti-CD19 scFv          : [10 : 870]
Peptide tag 1 (Strep)   : [871 : 903]
linker GGSG             : [904 : 915]
Peptide tag 2 (V5)      : [916 : 957]
CD8 Hinge               : [958 : 1080]
MluI                    : [1082 : 1087]
CD28 TM                 : [1090 : 1167]
signal motif 1 CD3z     : [1168 : 1503]
BamHI                   : [1504 : 1509]
P2A                     : [1510 : 1569]
PuroR                   : [1570 : 2169]
NotI                    : [2170 : 2177]
```

Protein sequence:

```
LETMLLLVTSLLLCELPHPAFLLIPEQKLISEEDLEQKLISEEDLDIQMTQTTSSLSASLGDRVTISCRASQDISKYLNW
YQQKPDGTVKLLIYHTSRLHSGVPSRFSGSGSGTDYSLTISNLEQEDIATYFCQQGNTLPYTFGGGTKLEITGSTSGSGK
PGSGEGSTKGEVKLQESGPGLVAPSQSLSVTCTVSGVSLPDYGVSWIRQPPRKGLEWLGVIWGSETTYYNSALKSRLTII
KDNSKSQVFLKMNSLQTDDTAIYYCAKHYYYGGSYAMDYWGQGTSVTVSSGSNWSHPQFEKGGSGGKPIPNPLLGLDSTP
TTTPAPRPPTPAPTIASQPLSLRPEASRPAAGGAVHTRGLDAFWVLVVVGGVLACYSLLVTVAFIIFWVRVKFSRSADAP
AYQQGQNQLYNELNLGRREEYDVLDKRRGRDPEMGGKPRRKNPQEGLYNELQKDKMAEAYSEIGMKGERRRGKGHDGLYQ
GLSTATKDTYDALHMQALPPRGSGATNFSLLKQAGDVEENPGPMTEYKPTVRLATRDDVPRAVRTLAAAFADYPATRHTV
DPDRHIERVTELQELFLTRVGLDIGKVWVADDGAAVAVWTTPESVEAGAVFAEIGPRMAELSGSRLAAQQQMEGLLAPHR
PKEPAWFLATVGVSPDHQGKGLGSAVVLPGVEAAERAGVPAFLETSAPRNLPFYERLGFTVTADVEVPEGPRTWCMTRKP
GA
```

aCD19:**CD28**-bla

Nucleotide sequence:

```
CTCGAGATGTTGTTGCTGGTCACTAGCTTGCTCCTTTGTGAGCTTCCCCATCCAGCGTTTCTGCTCATTCCAGAGCAAAA
GCTTATTTCCGAAGAAGATCTTGAACAAAAGCTCATTTCTGAAGAAGATCTTGATATCCAAATGACTCAAACCACTTCCA
GCCTTAGTGCGTCACTCGGTGATCGAGTCACAATCTCTTGTCGTGCTTCTCAAGATATATCCAAATATTTGAATTGGTAT
CAACAGAAACCAGATGGAACTGTTAAACTCTTGATCTACCATACTTCTCGTCTTCATTCTGGCGTCCCGAGTCGCTTTTC
AGGAAGCGGGTCAGGGACTGATTATAGTCTCACCATATCTAATTTGGAACAAGAAGATATTGCAACTTATTTCTGTCAAC
AAGGGAATACACTGCCCTATACTTTTGGAGGAGGTACGAAATTGGAAATTACTGGAAGTACAAGTGGGTCTGGAAAGCCT
GGTTCCGGTGAGGGGAGCACTAAAGGAGAGGTAAAACTCCAAGAGAGTGGACCAGGGCTCGTAGCTCCTTCACAATCTTT
GTCCGTCACGTGTACCGTTAGCGGTGTTAGTTTGCCGGATTATGGGGTTTCTTGGATTCGCCAACCACCGAGGAAAGGGT
TGGAATGGTTGGGCGTTATTTGGGGCTCAGAAACAACGTACTACAATAGTGCTCTTAAAAGCAGGTTGACCATAATTAAA
GACAATAGCAAAAGCCAAGTTTTCCTCAAGATGAATTCACTTCAAACAGACGACACTGCAATTTACTATTGTGCTAAGCA
TTACTACTACGGTGGAAGTTATGCTATGGATTACTGGGGTCAAGGCACGTCAGTTACTGTAAGTAGTGGGAGCAATTGGA
GTCATCCACAATTCGAAAAGGGTGGCAGTGGTGGTTATCCGTATGATGTCCCAGATTATGCTCCCACAACAACACCTGCT
CCAAGACCCCCTACTCCAGCACCCACAATTGCTTCCCAACCACTTTCACTCAGGCCAGAAGCGTCACGCCCTGCAGCAGG
CGGGGCGGTCCATACACGTGGATTGACTAGTTTCTGGGTTCTGGTTGTTGTTGGTGGGGTCCTTGCATGTTACTCCCTGC
TGGTCACCGTAGCTTTTATCATATTTTGGGTTCGAAGTAAACGGTCTAGGCTTCTTCATAGTGATTATATGAATATGACA
CCACGGCGTCCAGGACCTACGCGCAAACATTATCAACCGTATGCACCACCGCGCGATTTTGCGGCATATCGATCTGGATC
CGGAGCTACTAACTTCAGCCTGCTGAAGCAGGCTGGAGACGTCGAGGAGAACCCTGGACCTATGGCCAAGCCTTTGTCTC
AAGAAGAATCCACCCTCATTGAAAGAGCAACGGCTACAATCAACAGCATCCCCATCTCTGAAGACTACAGCGTCGCCAGC
GCAGCTCTCTCTAGCGACGGCCGCATCTTCACTGGTGTCAATGTATATCATTTTACTGGGGGACCTTGTGCAGAACTCGT
GGTGCTGGGCACTGCTGCTGCTGCGGCAGCTGGCAACCTGACTTGTATCGTCGCGATCGGAAATGAGAACAGGGGCATCT
TGAGCCCCTGCGGACGGTGCCGACAGGTGCTTCTCGATCTGCATCCTGGGATCAAAGCCATAGTGAAGGACAGTGATGGA
CAGCCGACGGCAGTTGGGATTCGTGAATTGCTGCCCTCTGGTTATGTGTGGGAGGGCTAAGCGGCCGC
```

Features:

XhoI	:	[1 : 6]
anti-CD19 scFv	:	[7 : 867]
Peptide tag 1 (Strep)	:	[868 : 900]
linker GGSG	:	[901 : 915]
Peptide tag 3 (HA)	:	[916 : 942]
CD8 Hinge	:	[943 : 1065]
SpeI	:	[1066 : 1071]
CD28 TM	:	[1072 : 1152]
CD28cyto	:	[1153 : 1275]
BamHI	:	[1276 : 1281]
P2A	:	[1282 : 1341]
BlaR	:	[1342 : 1740]
NotI	:	[1741 : 1748]

Protein sequence:

```
LEMLLLVTSLLLCELPHPAFLLIPEQKLISEEDLEQKLISEEDLDIQMTQTTSSLSASLGDRVTISCRASQDISKYLNWY
QQKPDGTVKLLIYHTSRLHSGVPSRFSGSGSGTDYSLTISNLEQEDIATYFCQQGNTLPYTFGGGTKLEITGSTSGSGKP
GSGEGSTKGEVKLQESGPGLVAPSQSLSVTCTVSGVSLPDYGVSWIRQPPRKGLEWLGVIWGSETTYYNSALKSRLTIIK
DNSKSQVFLKMNSLQTDDTAIYYCAKHYYYGGSYAMDYWGQGTSVTVSSGSNWSHPQFEKGGSGGYPYDVPDYAPTTTPA
PRPPTPAPTIASQPLSLRPEASRPAAGGAVHTRGLTSFWVLVVVGGVLACYSLLVTVAFIIFWVRSKRSRLLHSDYMNMT
PRRPGPTRKHYQPYAPPRDFAAYRSGSGATNFSLLKQAGDVEENPGPMAKPLSQEESTLIERATATINSIPISEDYSVAS
AALSSDGRIFTGVNVYHFTGGPCAELVVLGTAAAAAAGNLTCIVAIGNENRGILSPCGRCRQVLLDLHPGIKAIVKDSDG
QPTAVGIRELLPSGYVWEG
```

aCD19:**CD28z**-Puro

Nucleotide sequence:

```
CTCGAGACCATGTTGTTGTTGGTTACTTCACTCCTCTTGTGTGAACTTCCTCATCCGGCATTCCTTTTGATTCCTGAACA
AAAGCTCATTAGTGAGGAAGATTTGGAGCAAAAGTTGATTAGTGAAGAGGACCTCGATATACAAATGACGCAAACAACGT
CTTCATTGTCCGCATCCTTGGGAGATAGGGTCACAATTTCATGTAGAGCGTCCCAAGATATTTCAAAATACCTCAATTGG
TACCAACAAAAGCCAGATGGAACAGTGAAATTGTTGATTTATCATACGAGTAGACTTCATTCTGGAGTACCATCCCGCTT
CTCCGGATCTGGTTCAGGGACAGATTATTCTCTCACTATATCAAATTTGGAGCAAGAGGACATTGCAACTTATTTCTGTC
AACAAGGGAATACCTTGCCTTATACTTTCGGAGGAGGGACGAAACTTGAGATTACAGGGTCAACATCAGGGTCTGGGAAA
CCCGGGTCAGGGGAAGGGTCCACTAAAGGAGAAGTAAAATTGCAAGAGAGTGGACCCGGTCTTGTCGCTCCTTCCCAATC
CTTGTCAGTCACTTGTACTGTCTCCGGAGTCTCTCTCCCGGATTATGGGGTTTCCTGGATTAGACAACCACCACGGAAAG
GACTGGAGTGGCTCGGAGTCATTTGGGGTTCTGAAACGACTTATTATAATTCCGCTCTCAAAAGTCGCTTGACTATAATT
AAAGATAATTCAAAGAGTCAAGTCTTCTTGAAAATGAACTCTCTCCAGACCGACGACACTGCTATTTATTATTGTGCTAA
ACATTATTATTATGGCGGGTCTTATGCAATGGACTATTGGGGACAAGGGACTTCTGTCACTGTATCCTCAGGGAGCAATT
GGAGTCATCCACAATTTGAGAAAGGCGGTAGTGGTGGGAAACCAATACCTAATCCACTCCTCGGTTTGGATAGTACTCCA
ACAACAACTCCTGCCCCTCGGCCCCCAACCCCTGCACCAACTATTGCAAGTCAACCTCTCTCTTTGCGTCCTGAAGCCTC
TCGCCCCGCCGCCGGCGGTGCCGTTCATACACGAGGTCTTGACGCGTTCTGGGTGCTGGTGGTGGTCGGAGGCGTGCTGG
CCTGCTACAGCCTGCTGGTCACCGTGGCCTTCATCATCTTTTGGGTGAGGAGTAAGAGGAGCAGGCTCCTGCACAGTGAC
TACATGAACATGACTCCCCGCCGCCCCGGGCCCACCCGCAAGCATTACCAGCCCTATGCCCCACCACGCGACTTCGCAGC
CTATCGCTCCCGGGTGAAGTTCAGCAGAAGCGCCGACGCCCCTGCCTACCAGCAGGGCCAGAATCAGCTGTACAACGAGC
TGAACCTGGGCAGAAGGGAAGAGTACGACGTCCTGGATAAGCGGAGAGGCCGGGACCCTGAGATGGGCGGCAAGCCTCGG
CGGAAGAACCCCCAGGAAGGCCTGTATAACGAACTGCAGAAAGACAAGATGGCCGAGGCCTACAGCGAGATCGGCATGAA
GGGCGAGCGGAGGCGGGGCAAGGGCCACGACGGCCTGTATCAGGGCCTGTCCACCGCCACCAAGGATACCTACGACGCCC
TGCACATGCAGGCCCTGCCCCCAAGGGGATCCGGAGCTACTAACTTCAGCCTGCTGAAGCAGGCTGGAGACGTCGAGGAG
AACCCTGGACCTATGACCGAGTACAAGCCCACGGTGCGCCTCGCCACCCGCGACGACGTCCCCAGGGCCGTACGCACCCT
CGCCGCCGCGTTCGCCGACTACCCCGCCACGCGCCACACCGTCGATCCGGACCGCCACATCGAGCGGGTCACCGAGCTGC
AAGAACTCTTCCTCACGCGCGTCGGGCTCGACATCGGCAAGGTGTGGGTCGCGGACGACGGCGCCGCGGTGGCGGTCTGG
ACCACGCCGGAGAGCGTCGAAGCGGGGGCGGTGTTCGCCGAGATCGGCCCGCGCATGGCCGAGTTGAGCGGTTCCCGGCT
GGCCGCGCAGCAACAGATGGAAGGCCTCCTGGCGCCGCACCGGCCCAAGGAGCCCGCGTGGTTCCTGGCCACCGTCGGCG
TCTCGCCCGACCACCAGGGCAAGGGTCTGGGCAGCGCCGTCGTGCTCCCCGGAGTGGAGGCGGCCGAGCGCGCCGGGGTG
CCCGCCTTCCTGGAGACCTCCGCGCCCCGCAACCTCCCCTTCTACGAGCGGCTCGGCTTCACCGTCACCGCCGACGTCGA
GGTGCCCGAAGGACCGCGCACCTGGTGCATGACCCGCAAGCCCGGTGCCTGAGCGGCCGC
```

Features:

XhoI	: [1 : 6]
anti-CD19 scFv	: [10 : 870]
Peptide tag 1 (Strep)	: [871 : 903]
linker GGSG	: [904 : 915]
Peptide tag 2 (V5)	: [916 : 957]
CD8 Hinge	: [958 : 1080]
MluI	: [1082 : 1087]
CD28 TM (X15)	: [1088 : 1167]
signal motif 1 CD28 (X15)	: [1168 : 1290]
signal motif 1 CD3z (X15)	: [1291 : 1626]
BamHI	: [1627 : 1632]
P2A	: [1633 : 1692]
PuroR	: [1693 : 2292]
NotI	: [2293 : 2300]

Protein sequence:

```
LETMLLLVTSLLLCELPHPAFLLIPEQKLISEEDLEQKLISEEDLDIQMTQTTSSLSASLGDRVTISCRASQDISKYLNW
YQQKPDGTVKLLIYHTSRLHSGVPSRFSGSGSGTDYSLTISNLEQEDIATYFCQQGNTLPYTFGGGTKLEITGSTSGSGK
PGSGEGSTKGEVKLQESGPGLVAPSQSLSVTCTVSGVSLPDYGVSWIRQPPRKGLEWLGVIWGSETTYYNSALKSRLTII
KDNSKSQVFLKMNSLQTDDTAIYYCAKHYYYGGSYAMDYWGQGTSVTVSSGSNWSHPQFEKGGSGGKPIPNPLLGLDSTP
TTTPAPRPPTPAPTIASQPLSLRPEASRPAAGGAVHTRGLDAFWVLVVVGGVLACYSLLVTVAFIIFWVRSKRSRLLHSD
YMNMTPRRPGPTRKHYQPYAPPRDFAAYRSRVKFSRSADAPAYQQGQNQLYNELNLGRREEYDVLDKRRGRDPEMGGKPR
RKNPQEGLYNELQKDKMAEAYSEIGMKGERRRGKGHDGLYQGLSTATKDTYDALHMQALPPRGSGATNFSLLKQAGDVEE
NPGPMTEYKPTVRLATRDDVPRAVRTLAAAFADYPATRHTVDPDRHIERVTELQELFLTRVGLDIGKVWVADDGAAVAVW
TTPESVEAGAVFAEIGPRMAELSGSRLAAQQQMEGLLAPHRPKEPAWFLATVGVSPDHQGKGLGSAVVLPGVEAAERAGV
PAFLETSAPRNLPFYERLGFTVTADVEVPEGPRTWCMTRKPGA
```

aCD19:**41BB**-bla

Nucleotide sequence:

```
CTCGAGATGTTGTTGCTGGTCACTAGCTTGCTCCTTTGTGAGCTTCCCCATCCAGCGTTTCTGCTCATTCCAGAGCAAAA
GCTTATTTCCGAAGAAGATCTTGAACAAAAGCTCATTTCTGAAGAAGATCTTGATATCCAAATGACTCAAACCACTTCCA
GCCTTAGTGCGTCACTCGGTGATCGAGTCACAATCTCTTGTCGTGCTTCTCAAGATATATCCAAATATTTGAATTGGTAT
CAACAGAAACCAGATGGAACTGTTAAACTCTTGATCTACCATACTTCTCGTCTTCATTCTGGCGTCCCGAGTCGCTTTTC
AGGAAGCGGGTCAGGGACTGATTATAGTCTCACCATATCTAATTTGGAACAAGAAGATATTGCAACTTATTTCTGTCAAC
AAGGGAATACACTGCCCTATACTTTTGGAGGAGGTACGAAATTGGAAATTACTGGAAGTACAAGTGGGTCTGGAAAGCCT
GGTTCCGGTGAGGGGAGCACTAAAGGAGAGGTAAAACTCCAAGAGAGTGGACCAGGGCTCGTAGCTCCTTCACAATCTTT
GTCCGTCACGTGTACCGTTAGCGGTGTTAGTTTGCCGGATTATGGGGTTTCTTGGATTCGCCAACCACCGAGGAAAGGGT
TGGAATGGTTGGGCGTTATTTGGGGCTCAGAAACAACGTACTACAATAGTGCTCTTAAAAGCAGGTTGACCATAATTAAA
GACAATAGCAAAAGCCAAGTTTTCCTCAAGATGAATTCACTTCAAACAGACGACACTGCAATTTACTATTGTGCTAAGCA
TTACTACTACGGTGGAAGTTATGCTATGGATTACTGGGGTCAAGGCACGTCAGTTACTGTAAGTAGTGGGAGCAATTGGA
GTCATCCACAATTCGAAAAGGGTGGCAGTGGTGGTTATCCGTATGATGTCCCAGATTATGCTCCCACAACAACACCTGCT
CCAAGACCCCCTACTCCAGCACCCACAATTGCTTCCCAACCACTTTCACTCAGGCCAGAAGCGTCACGCCCTGCAGCAGG
CGGGGCGGTCCATACACGTGGATTGACTAGTTTCTGGGTTCTGGTTGTTGTTGGTGGGGTCCTTGCATGTTACTCCCTGC
TGGTCACCGTAGCTTTTATCATATTTTGGGTTAAGCGCGGGAGGAAAAAGCTGCTCTACATTTTTAAGCAGCCTTTCATG
AGGCCTGTACAGACAACGCAGGAAGAGGACGGGTGCAGTTGTCGTTTCCCTGAGGAGGAGGAGGGTGGCTGCGAGCTCGG
ATCCGGAGCTACTAACTTCAGCCTGCTGAAGCAGGCTGGAGACGTCGAGGAGAACCCTGGACCTATGGCCAAGCCTTTGT
CTCAAGAAGAATCCACCCTCATTGAAAGAGCAACGGCTACAATCAACAGCATCCCCATCTCTGAAGACTACAGCGTCGCC
AGCGCAGCTCTCTCTAGCGACGGCCGCATCTTCACTGGTGTCAATGTATATCATTTTACTGGGGGACCTTGTGCAGAACT
CGTGGTGCTGGGCACTGCTGCTGCTGCGGCAGCTGGCAACCTGACTTGTATCGTCGCGATCGGAAATGAGAACAGGGGCA
TCTTGAGCCCCTGCGGACGGTGCCGACAGGTGCTTCTCGATCTGCATCCTGGGATCAAAGCCATAGTGAAGGACAGTGAT
GGACAGCCGACGGCAGTTGGGATTCGTGAATTGCTGCCCTCTGGTTATGTGTGGGAGGGCTAAGCGGCCGC
```

Features:

XhoI	:	[1 : 6]
anti-CD19 scFv	:	[7 : 867]
Peptide tag 1 (Strep)	:	[868 : 900]
linker GGSGG	:	[901 : 915]
Peptide tag 3 (HA)	:	[916 : 942]
CD8 Hinge	:	[943 : 1065]
SpeI	:	[1066 : 1071]
CD28 TM	:	[1072 : 1152]
signal motif 2 4-1BB	:	[1153 : 1278]
BamHI	:	[1279 : 1284]
P2A	:	[1285 : 1344]
BlaR	:	[1345 : 1743]
NotI	:	[1744 : 1751]

Protein sequence:

```
LEMLLLVTSLLLCELPHPAFLLIPEQKLISEEDLEQKLISEEDLDIQMTQTTSSLSASLGDRVTISCRASQDISKYLNWY
QQKPDGTVKLLIYHTSRLHSGVPSRFSGSGSGTDYSLTISNLEQEDIATYFCQQGNTLPYTFGGGTKLEITGSTSGSGKP
GSGEGSTKGEVKLQESGPGLVAPSQSLSVTCTVSGVSLPDYGVSWIRQPPRKGLEWLGVIWGSETTYYNSALKSRLTIIK
DNSKSQVFLKMNSLQTDDTAIYYCAKHYYYGGSYAMDYWGQGTSVTVSSGSNWSHPQFEKGGSGGYPYDVPDYAPTTTPA
PRPPTPAPTIASQPLSLRPEASRPAAGGAVHTRGLTSFWVLVVVGGVLACYSLLVTVAFIIFWVKRGRKKLLYIFKQPFM
RPVQTTQEEDGCSCRFPEEEEGGCELGSGATNFSLLKQAGDVEENPGPMAKPLSQEESTLIERATATINSIPISEDYSVA
SAALSSDGRIFTGVNVYHFTGGPCAELVVLGTAAAAAAGNLTCIVAIGNENRGILSPCGRCRQVLLDLHPGIKAIVKDSD
GQPTAVGIRELLPSGYVWEG
```

aCD19:**41BBz**-bla

Nucleotide sequence:

```
CTCGAGATGTTGTTGCTGGTCACTAGCTTGCTCCTTTGTGAGCTTCCCCATCCAGCGTTTCTGCTCATTCCAGAGCAAAA
GCTTATTTCCGAAGAAGATCTTGAACAAAAGCTCATTTCTGAAGAAGATCTTGATATCCAAATGACTCAAACCACTTCCA
GCCTTAGTGCGTCACTCGGTGATCGAGTCACAATCTCTTGTCGTGCTTCTCAAGATATATCCAAATATTTGAATTGGTAT
CAACAGAAACCAGATGGAACTGTTAAACTCTTGATCTACCATACTTCTCGTCTTCATTCTGGCGTCCCGAGTCGCTTTTC
AGGAAGCGGGTCAGGGACTGATTATAGTCTCACCATATCTAATTTGGAACAAGAAGATATTGCAACTTATTTCTGTCAAC
AAGGGAATACACTGCCCTATACTTTTGGAGGAGGTACGAAATTGGAAATTACTGGAAGTACAAGTGGGTCTGGAAAGCCT
GGTTCCGGTGAGGGGAGCACTAAAGGAGAGGTAAAACTCCAAGAGAGTGGACCAGGGCTCGTAGCTCCTTCACAATCTTT
GTCCGTCACGTGTACCGTTAGCGGTGTTAGTTTGCCGGATTATGGGGTTTCTTGGATTCGCCAACCACCGAGGAAAGGGT
TGGAATGGTTGGGCGTTATTTGGGGCTCAGAAACAACGTACTACAATAGTGCTCTTAAAAGCAGGTTGACCATAATTAAA
GACAATAGCAAAAGCCAAGTTTTCCTCAAGATGAATTCACTTCAAACAGACGACACTGCAATTTACTATTGTGCTAAGCA
TTACTACTACGGTGGAAGTTATGCTATGGATTACTGGGGTCAAGGCACGTCAGTTACTGTAAGTAGTGGGAGCAATTGGA
GTCATCCACAATTCGAAAAGGGTGGCAGTGGTGGTTATCCGTATGATGTCCCAGATTATGCTCCCACAACAACACCTGCT
CCAAGACCCCCTACTCCAGCACCCACAATTGCTTCCCAACCACTTTCACTCAGGCCAGAAGCGTCACGCCCTGCAGCAGG
CGGGGCGGTCCATACACGTGGATTGACTAGTTTCTGGGTTCTGGTTGTTGTTGGTGGGGTCCTTGCATGTTACTCCCTGC
TGGTCACCGTAGCTTTTATCATATTTTGGGTTAAGCGCGGGAGGAAAAAGCTGCTCTACATTTTTAAGCAGCCTTTCATG
AGGCCTGTACAGACAACGCAGGAAGAGGACGGGTGCAGTTGTCGTTTCCCTGAGGAGGAGGAGGGTGGCTGCGAGCTCAG
GGTTAAATTTTCCCGATCTGCTGATGCGCCAGCGTATCAACAAGGGCAAAACCAACTTTATAATGAACTTAATTTGGGAC
GGCGAGAGGAATATGATGTGTTGGACAAACGACGAGGACGAGATCCCGAAATGGGTGGAAAACCACGACGCAAGAATCCT
CAAGAGGGACTCTACAATGAGCTTCAAAAGGATAAAATGGCTGAAGCATATTCCGAAATAGGAATGAAAGGAGAAAGACG
GAGAGGTAAAGGGCATGATGGATTGTACCAAGGTTTGAGCACAGCTACAAAAGACACGTACGATGCACTCCACATGCAAG
CACTTCCACCCCGTGGATCCGGAGCTACTAACTTCAGCCTGCTGAAGCAGGCTGGAGACGTCGAGGAGAACCCTGGACCT
ATGGCCAAGCCTTTGTCTCAAGAAGAATCCACCCTCATTGAAAGAGCAACGGCTACAATCAACAGCATCCCCATCTCTGA
AGACTACAGCGTCGCCAGCGCAGCTCTCTCTAGCGACGGCCGCATCTTCACTGGTGTCAATGTATATCATTTTACTGGGG
GACCTTGTGCAGAACTCGTGGTGCTGGGCACTGCTGCTGCTGCGGCAGCTGGCAACCTGACTTGTATCGTCGCGATCGGA
AATGAGAACAGGGGCATCTTGAGCCCCTGCGGACGGTGCCGACAGGTGCTTCTCGATCTGCATCCTGGGATCAAAGCCAT
AGTGAAGGACAGTGATGGACAGCCGACGGCAGTTGGGATTCGTGAATTGCTGCCCTCTGGTTATGTGTGGGAGGGCTAAG
CGGCCGC
```

Features:

XhoI	: [1 : 6]
anti-CD19 scFv	: [7 : 867]
Peptide tag 1 (Strep)	: [868 : 900]
linker GGSGG	: [901 : 915]
Peptide tag 3 (HA)	: [916 : 942]
CD8 Hinge	: [943 : 1065]
SpeI	: [1066 : 1071]
CD28 TM	: [1072 : 1152]
signal motif 2 4-1BB	: [1153 : 1278]
signal motif 2 CD3z	: [1279 : 1614]
BamHI	: [1615 : 1620]
P2A	: [1621 : 1680]
BlaR	: [1681 : 2079]
NotI	: [2080 : 2087]

Protein sequence:

```
LEMLLLVTSLLLCELPHPAFLLIPEQKLISEEDLEQKLISEEDLDIQMTQTTSSLSASLGDRVTISCRASQDISKYLNWY
QQKPDGTVKLLIYHTSRLHSGVPSRFSGSGSGTDYSLTISNLEQEDIATYFCQQGNTLPYTFGGGTKLEITGSTSGSGKP
GSGEGSTKGEVKLQESGPGLVAPSQSLSVTCTVSGVSLPDYGVSWIRQPPRKGLEWLGVIWGSETTYYNSALKSRLTIIK
DNSKSQVFLKMNSLQTDDTAIYYCAKHYYYGGSYAMDYWGQGTSVTVSSGSNWSHPQFEKGGSGGYPYDVPDYAPTTTPA
PRPPTPAPTIASQPLSLRPEASRPAAGGAVHTRGLTSFWVLVVVGGVLACYSLLVTVAFIIFWVKRGRKKLLYIFKQPFM
RPVQTTQEEDGCSCRFPEEEEGGCELRVKFSRSADAPAYQQGQNQLYNELNLGRREEYDVLDKRRGRDPEMGGKPRRKNP
QEGLYNELQKDKMAEAYSEIGMKGERRRGKGHDGLYQGLSTATKDTYDALHMQALPPRGSGATNFSLLKQAGDVEENPGP
MAKPLSQEESTLIERATATINSIPISEDYSVASAALSSDGRIFTGVNVYHFTGGPCAELVVLGTAAAAAAGNLTCIVAIG
NENRGILSPCGRCRQVLLDLHPGIKAIVKDSDGQPTAVGIRELLPSGYVWEG
```

12.1.3 Single CARs X variant

aCD19:**CD3z**-Puro

Nucleotide sequence:

```
CTCGAGACCATGCTGCTGCTGGTGACCAGCCTGCTGCTGTGCGAGCTGCCCCACCCCGCCTTTCTGCTGATCCCCGAGCA
GAAGCTGATCTCCGAAGAGGACCTGGAACAGAAACTGATCAGCGAGGAAGATCTGGACATCCAGATGACCCAGACCACCT
CCAGCCTGAGCGCCAGCCTGGGCGACCGGGTGACCATCAGCTGCCGGGCCAGCCAGGACATCAGCAAGTACCTGAACTGG
TATCAGCAGAAGCCCGACGGCACCGTCAAGCTGCTGATCTACCACACCAGCCGGCTGCACAGCGGCGTGCCCAGCCGGTT
TAGCGGCAGCGGCTCCGGCACCGACTACAGCCTGACCATCTCCAACCTGGAACAGGAAGATATCGCCACCTACTTTTGCC
AGCAGGGCAACACACTGCCCTACACCTTTGGCGGCGGAACAAAGCTGGAAATCACCGGCAGCACCTCCGGCAGCGGCAAG
CCTGGCAGCGGCGAGGGCAGCACCAAGGGCGAGGTGAAGCTGCAGGAAAGCGGCCCTGGCCTGGTGGCCCCCAGCCAGAG
CCTGAGCGTGACCTGCACCGTGAGCGGCGTGAGCCTGCCCGACTACGGCGTGAGCTGGATCCGGCAGCCCCCCAGGAAGG
GCCTGGAATGGCTGGGCGTGATCTGGGGCAGCGAGACCACCTACTACAACAGCGCCCTGAAGAGCCGGCTGACCATCATC
AAGGACAACAGCAAGAGCCAGGTGTTCCTGAAGATGAACAGCCTGCAGACCGACGACACCGCCATCTACTACTGCGCCAA
GCACTACTACTACGGCGGCAGCTACGCCATGGACTACTGGGGCCAGGGCACCAGCGTGACCGTGAGCAGCGGCTCCAACT
GGAGCCACCCCCAGTTCGAGAAGGGTGGCAGTGGTGGTTATCCGTATGATGTCCCAGATTATGCTCCCACCACGACGCCA
GCGCCGCGACCACCAACACCGGCGCCCACCATCGCGTCGCAGCCCCTGTCCCTGCGCCCAGAGGCGTCCCGGCCAGCGGC
GGGGGGCGCAGTGCACACGAGGGGGCTGGACGCGTTCTGGGTGCTGGTGGTGGTCGGAGGCGTGCTGGCCTGCTACAGCC
TGCTGGTCACCGTGGCCTTCATCATCTTTTGGGTGCGGGTGAAGTTCAGCAGAAGCGCCGACGCCCCTGCCTACCAGCAG
GGCCAGAATCAGCTGTACAACGAGCTGAACCTGGGCAGAAGGGAAGAGTACGACGTCCTGGATAAGCGGAGAGGCCGGGA
CCCTGAGATGGGCGGCAAGCCTCGGCGGAAGAACCCCCAGGAAGGCCTGTATAACGAACTGCAGAAAGACAAGATGGCCG
AGGCCTACAGCGAGATCGGCATGAAGGGCGAGCGGAGGCGGGGCAAGGGCCACGACGGCCTGTATCAGGGCCTGTCCACC
GCCACCAAGGATACCTACGACGCCCTGCACATGCAGGCCCTGCCCCCAAGGGGATCCGGAGCTACTAACTTCAGCCTGCT
GAAGCAGGCTGGAGACGTCGAGGAGAACCCTGGACCTATGACCGAGTACAAGCCCACGGTGCGCCTCGCCACCCGCGACG
ACGTCCCCAGGGCCGTACGCACCCTCGCCGCCGCGTTCGCCGACTACCCCGCCACGCGCCACACCGTCGATCCGGACCGC
CACATCGAGCGGGTCACCGAGCTGCAAGAACTCTTCCTCACGCGCGTCGGGCTCGACATCGGCAAGGTGTGGGTCGCGGA
CGACGGCGCCGCGGTGGCGGTCTGGACCACGCCGGAGAGCGTCGAAGCGGGGGCGGTGTTCGCCGAGATCGGCCCGCGCA
TGGCCGAGTTGAGCGGTTCCCGGCTGGCCGCGCAGCAACAGATGGAAGGCCTCCTGGCGCCGCACCGGCCCAAGGAGCCC
GCGTGGTTCCTGGCCACCGTCGGCGTCTCGCCCGACCACCAGGGCAAGGGTCTGGGCAGCGCCGTCGTGCTCCCCGGAGT
GGAGGCGGCCGAGCGCGCCGGGGTGCCCGCCTTCCTGGAGACCTCCGCGCCCCGCAACCTCCCCTTCTACGAGCGGCTCG
GCTTCACCGTCACCGCCGACGTCGAGGTGCCCGAAGGACCGCGCACCTGGTGCATGACCCGCAAGCCCGGTGCCTGAGCG
GCCGC
```

Features:

```
XhoI                : [1 : 6]
GM-CSF_Leader       : [10 : 60]
aCD19               : [61 : 870]
Strep-tag           : [871 : 903]
linker GGSGG        : [904 : 918]
HA-tag              : [919 : 945]
CD8-Hinge           : [946 : 1069]
MluI                : [1070 : 1075]
CD28TM              : [1076 : 1155]
CD3z                : [1156 : 1491]
BamHI (not2use)     : [1492 : 1497]
P2A                 : [1498 : 1557]
PuroR               : [1558 : 2165]
```

Protein sequence:

```
LETMLLLVTSLLLCELPHPAFLLIPEQKLISEEDLEQKLISEEDLDIQMTQTTSSLSASLGDRVTISCRASQDISKYLNW
YQQKPDGTVKLLIYHTSRLHSGVPSRFSGSGSGTDYSLTISNLEQEDIATYFCQQGNTLPYTFGGGTKLEITGSTSGSGK
PGSGEGSTKGEVKLQESGPGLVAPSQSLSVTCTVSGVSLPDYGVSWIRQPPRKGLEWLGVIWGSETTYYNSALKSRLTII
KDNSKSQVFLKMNSLQTDDTAIYYCAKHYYYGGSYAMDYWGQGTSVTVSSGSNWSHPQFEKGGSGGYPYDVPDYAPTTTP
APRPPTPAPTIASQPLSLRPEASRPAAGGAVHTRGLDAFWVLVVVGGVLACYSLLVTVAFIIFWVRVKFSRSADAPAYQQ
GQNQLYNELNLGRREEYDVLDKRRGRDPEMGGKPRRKNPQEGLYNELQKDKMAEAYSEIGMKGERRRGKGHDGLYQGLST
ATKDTYDALHMQALPPRGSGATNFSLLKQAGDVEENPGPMTEYKPTVRLATRDDVPRAVRTLAAAFADYPATRHTVDPDR
HIERVTELQELFLTRVGLDIGKVWVADDGAAVAVWTTPESVEAGAVFAEIGPRMAELSGSRLAAQQQMEGLLAPHRPKEP
AWFLATVGVSPDHQGKGLGSAVVLPGVEAAERAGVPAFLETSAPRNLPFYERLGFTVTADVEVPEGPRTWCMTRKPGA
```

aCD19:**CD28**-Puro

Nucleotide sequence:

```
CTCGAGACCATGCTGCTGCTGGTGACCAGCCTGCTGCTGTGCGAGCTGCCCCACCCCGCCTTTCTGCTGATCCCCGAGCA
GAAGCTGATCTCCGAAGAGGACCTGGAACAGAAACTGATCAGCGAGGAAGATCTGGACATCCAGATGACCCAGACCACCT
CCAGCCTGAGCGCCAGCCTGGGCGACCGGGTGACCATCAGCTGCCGGGCCAGCCAGGACATCAGCAAGTACCTGAACTGG
TATCAGCAGAAGCCCGACGGCACCGTCAAGCTGCTGATCTACCACACCAGCCGGCTGCACAGCGGCGTGCCCAGCCGGTT
TAGCGGCAGCGGCTCCGGCACCGACTACAGCCTGACCATCTCCAACCTGGAACAGGAAGATATCGCCACCTACTTTTGCC
AGCAGGGCAACACACTGCCCTACACCTTTGGCGGCGGAACAAAGCTGGAAATCACCGGCAGCACCTCCGGCAGCGGCAAG
CCTGGCAGCGGCGAGGGCAGCACCAAGGGCGAGGTGAAGCTGCAGGAAAGCGGCCCTGGCCTGGTGGCCCCCAGCCAGAG
CCTGAGCGTGACCTGCACCGTGAGCGGCGTGAGCCTGCCCGACTACGGCGTGAGCTGGATCCGGCAGCCCCCCAGGAAGG
GCCTGGAATGGCTGGGCGTGATCTGGGGCAGCGAGACCACCTACTACAACAGCGCCCTGAAGAGCCGGCTGACCATCATC
AAGGACAACAGCAAGAGCCAGGTGTTCCTGAAGATGAACAGCCTGCAGACCGACGACACCGCCATCTACTACTGCGCCAA
GCACTACTACTACGGCGGCAGCTACGCCATGGACTACTGGGGCCAGGGCACCAGCGTGACCGTGAGCAGCGGCTCCAACT
GGAGCCACCCCCAGTTCGAGAAGGGCGGTAGTGGTGGGAAACCAATACCTAATCCACTCCTCGGTTTGGATAGTACTCCC
ACCACGACGCCAGCGCCGCGACCACCAACACCGGCGCCCACCATCGCGTCGCAGCCCCTGTCCCTGCGCCCAGAGGCGTC
CCGGCCAGCGGCGGGGGGCGCAGTGCACACGAGGGGGCTGGACGCGTTCTGGGTGCTGGTGGTGGTCGGAGGCGTGCTGG
CCTGCTACAGCCTGCTGGTCACCGTGGCCTTCATCATCTTTTGGGTGAGGAGTAAGAGGAGCAGGCTCCTGCACAGTGAC
TACATGAACATGACTCCCCGCCGCCCCGGGCCCACCCGCAAGCATTACCAGCCCTATGCCCCACCACGCGACTTCGCAGC
CTATCGCTCCGGATCCGGAGCTACTAACTTCAGCCTGCTGAAGCAGGCTGGAGACGTCGAGGAGAACCCTGGACCTATGA
CCGAGTACAAGCCCACGGTGCGCCTCGCCACCCGCGACGACGTCCCCAGGGCCGTACGCACCCTCGCCGCCGCGTTCGCC
GACTACCCCGCCACGCGCCACACCGTCGATCCGGACCGCCACATCGAGCGGGTCACCGAGCTGCAAGAACTCTTCCTCAC
GCGCGTCGGGCTCGACATCGGCAAGGTGTGGGTCGCGGACGACGGCGCCGCGGTGGCGGTCTGGACCACGCCGGAGAGCG
TCGAAGCGGGGGCGGTGTTCGCCGAGATCGGCCCGCGCATGGCCGAGTTGAGCGGTTCCCGGCTGGCCGCGCAGCAACAG
ATGGAAGGCCTCCTGGCGCCGCACCGGCCCAAGGAGCCCGCGTGGTTCCTGGCCACCGTCGGCGTCTCGCCCGACCACCA
GGGCAAGGGTCTGGGCAGCGCCGTCGTGCTCCCCGGAGTGGAGGCGGCCGAGCGCGCCGGGGTGCCCGCCTTCCTGGAGA
CCTCCGCGCCCCGCAACCTCCCCTTCTACGAGCGGCTCGGCTTCACCGTCACCGCCGACGTCGAGGTGCCCGAAGGACCG
CGCACCTGGTGCATGACCCGCAAGCCCGGTGCCTGAGCGGCCGC
```

Features:

XhoI	:	[1 : 6]
GM-CSF-Leader	:	[10 : 60]
aCD19	:	[61 : 870]
Strep-tag	:	[871 : 903]
linker GGSG	:	[904 : 915]
V5-tag	:	[916 : 957]
CD8-Hinge	:	[958 : 1081]
MluI	:	[1082 : 1087]
CD28TM	:	[1088 : 1167]
CD28	:	[1168 : 1290]
BamHI (not2use)	:	[1291 : 1296]
P2A	:	[1297 : 1356]
PuroR	:	[1357 : 1956]
NotI	:	[1957 : 1964]

Protein sequence:

```
LETMLLLVTSLLLCELPHPAFLLIPEQKLISEEDLEQKLISEEDLDIQMTQTTSSLSASLGDRVTISCRASQDISKYLNW
YQQKPDGTVKLLIYHTSRLHSGVPSRFSGSGSGTDYSLTISNLEQEDIATYFCQQGNTLPYTFGGGTKLEITGSTSGSGK
PGSGEGSTKGEVKLQESGPGLVAPSQSLSVTCTVSGVSLPDYGVSWIRQPPRKGLEWLGVIWGSETTYYNSALKSRLTII
KDNSKSQVFLKMNSLQTDDTAIYYCAKHYYYGGSYAMDYWGQGTSVTVSSGSNWSHPQFEKGGSGGKPIPNPLLGLDSTP
TTTPAPRPPTPAPTIASQPLSLRPEASRPAAGGAVHTRGLDAFWVLVVVGGVLACYSLLVTVAFIIFWVRSKRSRLLHSD
YMNMTPRRPGPTRKHYQPYAPPRDFAAYRSGSGATNFSLLKQAGDVEENPGPMTEYKPTVRLATRDDVPRAVRTLAAAFA
DYPATRHTVDPDRHIERVTELQELFLTRVGLDIGKVWVADDGAAVAVWTTPESVEAGAVFAEIGPRMAELSGSRLAAQQQ
MEGLLAPHRPKEPAWFLATVGVSPDHQGKGLGSAVVLPGVEAAERAGVPAFLETSAPRNLPFYERLGFTVTADVEVPEGP
RTWCMTRKPGA
```

aCD19:**CD28z**-Puro

Nucleotide sequence:

```
CTCGAGACCATGCTGCTGCTGGTGACCAGCCTGCTGCTGTGCGAGCTGCCCCACCCCGCCTTTCTGCTGATCCCCGAGCA
GAAGCTGATCTCCGAAGAGGACCTGGAACAGAAACTGATCAGCGAGGAAGATCTGGACATCCAGATGACCCAGACCACCT
CCAGCCTGAGCGCCAGCCTGGGCGACCGGGTGACCATCAGCTGCCGGGCCAGCCAGGACATCAGCAAGTACCTGAACTGG
TATCAGCAGAAGCCCGACGGCACCGTCAAGCTGCTGATCTACCACACCAGCCGGCTGCACAGCGGCGTGCCCAGCCGGTT
TAGCGGCAGCGGCTCCGGCACCGACTACAGCCTGACCATCTCCAACCTGGAACAGGAAGATATCGCCACCTACTTTTGCC
AGCAGGGCAACACACTGCCCTACACCTTTGGCGGCGGAACAAAGCTGGAAATCACCGGCAGCACCTCCGGCAGCGGCAAG
CCTGGCAGCGGCGAGGGCAGCACCAAGGGCGAGGTGAAGCTGCAGGAAAGCGGCCCTGGCCTGGTGGCCCCCAGCCAGAG
CCTGAGCGTGACCTGCACCGTGAGCGGCGTGAGCCTGCCCGACTACGGCGTGAGCTGGATCCGGCAGCCCCCCAGGAAGG
GCCTGGAATGGCTGGGCGTGATCTGGGGCAGCGAGACCACCTACTACAACAGCGCCCTGAAGAGCCGGCTGACCATCATC
AAGGACAACAGCAAGAGCCAGGTGTTCCTGAAGATGAACAGCCTGCAGACCGACGACACCGCCATCTACTACTGCGCCAA
GCACTACTACTACGGCGGCAGCTACGCCATGGACTACTGGGGCCAGGGCACCAGCGTGACCGTGAGCAGCGGCTCCAACT
GGAGCCACCCCCAGTTCGAGAAGGGTGGCAGTGGTGGTTATCCGTATGATGTCCCAGATTATGCTCCCACCACGACGCCA
GCGCCGCGACCACCAACACCGGCGCCCACCATCGCGTCGCAGCCCCTGTCCCTGCGCCCAGAGGCGTCCCGGCCAGCGGC
GGGGGGCGCAGTGCACACGAGGGGGCTGGACGCGTTCTGGGTGCTGGTGGTGGTCGGAGGCGTGCTGGCCTGCTACAGCC
TGCTGGTCACCGTGGCCTTCATCATCTTTTGGGTGAGGAGTAAGAGGAGCAGGCTCCTGCACAGTGACTACATGAACATG
ACTCCCCGCCGCCCCGGGCCCACCCGCAAGCATTACCAGCCCTATGCCCCACCACGCGACTTCGCAGCCTATCGCTCCCG
GGTGAAGTTCAGCAGAAGCGCCGACGCCCCTGCCTACCAGCAGGGCCAGAATCAGCTGTACAACGAGCTGAACCTGGGCA
GAAGGGAAGAGTACGACGTCCTGGATAAGCGGAGAGGCCGGGACCCTGAGATGGGCGGCAAGCCTCGGCGGAAGAACCCC
CAGGAAGGCCTGTATAACGAACTGCAGAAAGACAAGATGGCCGAGGCCTACAGCGAGATCGGCATGAAGGGCGAGCGGAG
GCGGGGCAAGGGCCACGACGGCCTGTATCAGGGCCTGTCCACCGCCACCAAGGATACCTACGACGCCCTGCACATGCAGG
CCCTGCCCCCAAGGGGATCCGGAGCTACTAACTTCAGCCTGCTGAAGCAGGCTGGAGACGTCGAGGAGAACCCTGGACCT
ATGACCGAGTACAAGCCCACGGTGCGCCTCGCCACCCGCGACGACGTCCCCAGGGCCGTACGCACCCTCGCCGCCGCGTT
CGCCGACTACCCCGCCACGCGCCACACCGTCGATCCGGACCGCCACATCGAGCGGGTCACCGAGCTGCAAGAACTCTTCC
TCACGCGCGTCGGGCTCGACATCGGCAAGGTGTGGGTCGCGGACGACGGCGCCGCGGTGGCGGTCTGGACCACGCCGGAG
AGCGTCGAAGCGGGGGCGGTGTTCGCCGAGATCGGCCCGCGCATGGCCGAGTTGAGCGGTTCCCGGCTGGCCGCGCAGCA
ACAGATGGAAGGCCTCCTGGCGCCGCACCGGCCCAAGGAGCCCGCGTGGTTCCTGGCCACCGTCGGCGTCTCGCCCGACC
ACCAGGGCAAGGGTCTGGGCAGCGCCGTCGTGCTCCCCGGAGTGGAGGCGGCCGAGCGCGCCGGGGTGCCCGCCTTCCTG
GAGACCTCCGCGCCCCGCAACCTCCCCTTCTACGAGCGGCTCGGCTTCACCGTCACCGCCGACGTCGAGGTGCCCGAAGG
ACCGCGCACCTGGTGCATGACCCGCAAGCCCGGTGCCTGAGCGGCCGC
```

Features:

XhoI	:	[1 : 6]
GM-CSF-Leader	:	[10 : 60]
aCD19	:	[61 : 870]
Strep-tag	:	[871 : 903]
linker GGSGG	:	[904 : 918]
HA-tag	:	[919 : 945]
CD8-Hinge	:	[946 : 1069]
MluI	:	[1070 : 1075]
CD28TM	:	[1076 : 1155]
CD28	:	[1156 : 1278]
CD3z	:	[1279 : 1614]
BamHI (not2use)	:	[1615 : 1620]
P2A	:	[1621 : 1680]
PuroR	:	[1681 : 2288]

Protein sequence:

```
LETMLLLVTSLLLCELPHPAFLLIPEQKLISEEDLEQKLISEEDLDIQMTQTTSSLSASLGDRVTISCRASQDISKYLNW
YQQKPDGTVKLLIYHTSRLHSGVPSRFSGSGSGTDYSLTISNLEQEDIATYFCQQGNTLPYTFGGGTKLEITGSTSGSGK
PGSGEGSTKGEVKLQESGPGLVAPSQSLSVTCTVSGVSLPDYGVSWIRQPPRKGLEWLGVIWGSETTYYNSALKSRLTII
KDNSKSQVFLKMNSLQTDDTAIYYCAKHYYYGGSYAMDYWGQGTSVTVSSGSNWSHPQFEKGGSGGYPYDVPDYAPTTTP
APRPPTPAPTIASQPLSLRPEASRPAAGGAVHTRGLDAFWVLVVVGGVLACYSLLVTVAFIIFWVRSKRSRLLHSDYMNM
TPRRPGPTRKHYQPYAPPRDFAAYRSRVKFSRSADAPAYQQGQNQLYNELNLGRREEYDVLDKRRGRDPEMGGKPRRKNP
QEGLYNELQKDKMAEAYSEIGMKGERRRGKGHDGLYQGLSTATKDTYDALHMQALPPRGSGATNFSLLKQAGDVEENPGP
MTEYKPTVRLATRDDVPRAVRTLAAAFADYPATRHTVDPDRHIERVTELQELFLTRVGLDIGKVWVADDGAAVAVWTTPE
SVEAGAVFAEIGPRMAELSGSRLAAQQQMEGLLAPHRPKEPAWFLATVGVSPDHQGKGLGSAVVLPGVEAAERAGVPAFL
ETSAPRNLPFYERLGFTVTADVEVPEGPRTWCMTRKPGA
```

aCD19:**41BB**-Puro

Nucleotide sequence:

```
CTCGAGACCATGCTGCTGCTGGTGACCAGCCTGCTGCTGTGCGAGCTGCCCCACCCCGCCTTTCTGCTGATCCCCGAGCA
GAAGCTGATCTCCGAAGAGGACCTGGAACAGAAACTGATCAGCGAGGAAGATCTGGACATCCAGATGACCCAGACCACCT
CCAGCCTGAGCGCCAGCCTGGGCGACCGGGTGACCATCAGCTGCCGGGCCAGCCAGGACATCAGCAAGTACCTGAACTGG
TATCAGCAGAAGCCCGACGGCACCGTCAAGCTGCTGATCTACCACACCAGCCGGCTGCACAGCGGCGTGCCCAGCCGGTT
TAGCGGCAGCGGCTCCGGCACCGACTACAGCCTGACCATCTCCAACCTGGAACAGGAAGATATCGCCACCTACTTTTGCC
AGCAGGGCAACACACTGCCCTACACCTTTGGCGGCGGAACAAAGCTGGAAATCACCGGCAGCACCTCCGGCAGCGGCAAG
CCTGGCAGCGGCGAGGGCAGCACCAAGGGCGAGGTGAAGCTGCAGGAAAGCGGCCCTGGCCTGGTGGCCCCCAGCCAGAG
CCTGAGCGTGACCTGCACCGTGAGCGGCGTGAGCCTGCCCGACTACGGCGTGAGCTGGATCCGGCAGCCCCCCAGGAAGG
GCCTGGAATGGCTGGGCGTGATCTGGGGCAGCGAGACCACCTACTACAACAGCGCCCTGAAGAGCCGGCTGACCATCATC
AAGGACAACAGCAAGAGCCAGGTGTTCCTGAAGATGAACAGCCTGCAGACCGACGACACCGCCATCTACTACTGCGCCAA
GCACTACTACTACGGCGGCAGCTACGCCATGGACTACTGGGGCCAGGGCACCAGCGTGACCGTGAGCAGCGGCTCCAACT
GGAGCCACCCCCAGTTCGAGAAGGGCGGTAGTGGTGGGAAACCAATACCTAATCCACTCCTCGGTTTGGATAGTACTCCC
ACCACGACGCCAGCGCCGCGACCACCAACACCGGCGCCCACCATCGCGTCGCAGCCCCTGTCCCTGCGCCCAGAGGCGTC
CCGGCCAGCGGCGGGGGGCGCAGTGCACACGAGGGGGCTGGACGCGTTCTGGGTGCTGGTGGTGGTCGGAGGCGTGCTGG
CCTGCTACAGCCTGCTGGTCACCGTGGCCTTCATCATCTTTTGGGTGAAACGGGGCAGAAAGAAACTCCTGTATATATTC
AAACAACCATTTATGAGACCAGTACAAACTACTCAAGAGGAAGATGGCTGTAGCTGCCGATTTCCAGAAGAAGAAGAAGG
AGGATGTGAACTGGGATCCGGAGCTACTAACTTCAGCCTGCTGAAGCAGGCTGGAGACGTCGAGGAGAACCCTGGACCTA
TGACCGAGTACAAGCCCACGGTGCGCCTCGCCACCCGCGACGACGTCCCCAGGGCCGTACGCACCCTCGCCGCCGCGTTC
GCCGACTACCCCGCCACGCGCCACACCGTCGATCCGGACCGCCACATCGAGCGGGTCACCGAGCTGCAAGAACTCTTCCT
CACGCGCGTCGGGCTCGACATCGGCAAGGTGTGGGTCGCGGACGACGGCGCCGCGGTGGCGGTCTGGACCACGCCGGAGA
GCGTCGAAGCGGGGGCGGTGTTCGCCGAGATCGGCCCGCGCATGGCCGAGTTGAGCGGTTCCCGGCTGGCCGCGCAGCAA
CAGATGGAAGGCCTCCTGGCGCCGCACCGGCCCAAGGAGCCCGCGTGGTTCCTGGCCACCGTCGGCGTCTCGCCCGACCA
CCAGGGCAAGGGTCTGGGCAGCGCCGTCGTGCTCCCCGGAGTGGAGGCGGCCGAGCGCGCCGGGGTGCCCGCCTTCCTGG
AGACCTCCGCGCCCCGCAACCTCCCCTTCTACGAGCGGCTCGGCTTCACCGTCACCGCCGACGTCGAGGTGCCCGAAGGA
CCGCGCACCTGGTGCATGACCCGCAAGCCCGGTGCCTGAGCGGCCGC
```

Features:

XhoI	:	[1 : 6]
GM-CSF-Leader	:	[10 : 60]
aCD19	:	[61 : 870]
Strep-tag	:	[871 : 903]
linker GGSG	:	[904 : 915]
V5-tag	:	[916 : 957]
CD8-Hinge	:	[958 : 1081]
MluI	:	[1082 : 1087]
CD28TM	:	[1088 : 1167]
4-1BB	:	[1168 : 1293]
BamHI	:	[1294 : 1299]
P2A	:	[1300 : 1359]
PuroR	:	[1360 : 1959]
NotI	:	[1960 : 1967]

Protein sequence:

```
LETMLLLVTSLLLCELPHPAFLLIPEQKLISEEDLEQKLISEEDLDIQMTQTTSSLSASLGDRVTISCRASQDISKYLNW
YQQKPDGTVKLLIYHTSRLHSGVPSRFSGSGSGTDYSLTISNLEQEDIATYFCQQGNTLPYTFGGGTKLEITGSTSGSGK
PGSGEGSTKGEVKLQESGPGLVAPSQSLSVTCTVSGVSLPDYGVSWIRQPPRKGLEWLGVIWGSETTYYNSALKSRLTII
KDNSKSQVFLKMNSLQTDDTAIYYCAKHYYYGGSYAMDYWGQGTSVTVSSGSNWSHPQFEKGGSGGKPIPNPLLGLDSTP
TTTPAPRPPTPAPTIASQPLSLRPEASRPAAGGAVHTRGLDAFWVLVVVGGVLACYSLLVTVAFIIFWVKRGRKKLLYIF
KQPFMRPVQTTQEEDGCSCRFPEEEEGGCELGSGATNFSLLKQAGDVEENPGPMTEYKPTVRLATRDDVPRAVRTLAAAF
ADYPATRHTVDPDRHIERVTELQELFLTRVGLDIGKVWVADDGAAVAVWTTPESVEAGAVFAEIGPRMAELSGSRLAAQQ
QMEGLLAPHRPKEPAWFLATVGVSPDHQGKGLGSAVVLPGVEAAERAGVPAFLETSAPRNLPFYERLGFTVTADVEVPEG
PRTWCMTRKPGA
```

aCD19:**41BBz**-Puro

Nucleotide sequence:

```
CTCGAGACCATGCTGCTGCTGGTGACCAGCCTGCTGCTGTGCGAGCTGCCCCACCCCGCCTTTCTGCTGATCCCCGAGCA
GAAGCTGATCTCCGAAGAGGACCTGGAACAGAAACTGATCAGCGAGGAAGATCTGGACATCCAGATGACCCAGACCACCT
CCAGCCTGAGCGCCAGCCTGGGCGACCGGGTGACCATCAGCTGCCGGGCCAGCCAGGACATCAGCAAGTACCTGAACTGG
TATCAGCAGAAGCCCGACGGCACCGTCAAGCTGCTGATCTACCACACCAGCCGGCTGCACAGCGGCGTGCCCAGCCGGTT
TAGCGGCAGCGGCTCCGGCACCGACTACAGCCTGACCATCTCCAACCTGGAACAGGAAGATATCGCCACCTACTTTTGCC
AGCAGGGCAACACACTGCCCTACACCTTTGGCGGCGGAACAAAGCTGGAAATCACCGGCAGCACCTCCGGCAGCGGCAAG
CCTGGCAGCGGCGAGGGCAGCACCAAGGGCGAGGTGAAGCTGCAGGAAAGCGGCCCTGGCCTGGTGGCCCCCAGCCAGAG
CCTGAGCGTGACCTGCACCGTGAGCGGCGTGAGCCTGCCCGACTACGGCGTGAGCTGGATCCGGCAGCCCCCCAGGAAGG
GCCTGGAATGGCTGGGCGTGATCTGGGGCAGCGAGACCACCTACTACAACAGCGCCCTGAAGAGCCGGCTGACCATCATC
AAGGACAACAGCAAGAGCCAGGTGTTCCTGAAGATGAACAGCCTGCAGACCGACGACACCGCCATCTACTACTGCGCCAA
GCACTACTACTACGGCGGCAGCTACGCCATGGACTACTGGGGCCAGGGCACCAGCGTGACCGTGAGCAGCGGCTCCAACT
GGAGCCACCCCCAGTTCGAGAAGGGTGGCAGTGGTGGTTATCCGTATGATGTCCCAGATTATGCTCCCACCACGACGCCA
GCGCCGCGACCACCAACACCGGCGCCCACCATCGCGTCGCAGCCCCTGTCCCTGCGCCCAGAGGCGTCCCGGCCAGCGGC
GGGGGGCGCAGTGCACACGAGGGGGCTGGACGCGTTCTGGGTGCTGGTGGTGGTCGGAGGCGTGCTGGCCTGCTACAGCC
TGCTGGTCACCGTGGCCTTCATCATCTTTTGGGTGAAACGGGGCAGAAAGAAACTCCTGTATATATTCAAACAACCATTT
ATGAGACCAGTACAAACTACTCAAGAGGAAGATGGCTGTAGCTGCCGATTTCCAGAAGAAGAAGAAGGAGGATGTGAACT
GCGGGTGAAGTTCAGCAGAAGCGCCGACGCCCCTGCCTACCAGCAGGGCCAGAATCAGCTGTACAACGAGCTGAACCTGG
GCAGAAGGGAAGAGTACGACGTCCTGGATAAGCGGAGAGGCCGGGACCCTGAGATGGGCGGCAAGCCTCGGCGGAAGAAC
CCCCAGGAAGGCCTGTATAACGAACTGCAGAAAGACAAGATGGCCGAGGCCTACAGCGAGATCGGCATGAAGGGCGAGCG
GAGGCGGGGCAAGGGCCACGACGGCCTGTATCAGGGCCTGTCCACCGCCACCAAGGATACCTACGACGCCCTGCACATGC
AGGCCCTGCCCCCAAGGGGATCCGGAGCTACTAACTTCAGCCTGCTGAAGCAGGCTGGAGACGTCGAGGAGAACCCTGGA
CCTATGACCGAGTACAAGCCCACGGTGCGCCTCGCCACCCGCGACGACGTCCCCAGGGCCGTACGCACCCTCGCCGCCGC
GTTCGCCGACTACCCCGCCACGCGCCACACCGTCGATCCGGACCGCCACATCGAGCGGGTCACCGAGCTGCAAGAACTCT
TCCTCACGCGCGTCGGGCTCGACATCGGCAAGGTGTGGGTCGCGGACGACGGCGCCGCGGTGGCGGTCTGGACCACGCCG
GAGAGCGTCGAAGCGGGGGCGGTGTTCGCCGAGATCGGCCCGCGCATGGCCGAGTTGAGCGGTTCCCGGCTGGCCGCGCA
GCAACAGATGGAAGGCCTCCTGGCGCCGCACCGGCCCAAGGAGCCCGCGTGGTTCCTGGCCACCGTCGGCGTCTCGCCCG
ACCACCAGGGCAAGGGTCTGGGCAGCGCCGTCGTGCTCCCCGGAGTGGAGGCGGCCGAGCGCGCCGGGGTGCCCGCCTTC
CTGGAGACCTCCGCGCCCCGCAACCTCCCCTTCTACGAGCGGCTCGGCTTCACCGTCACCGCCGACGTCGAGGTGCCCGA
AGGACCGCGCACCTGGTGCATGACCCGCAAGCCCGGTGCCTGAGCGGCCGC
```

Features:

XhoI	:	[1 : 6]
GM-CSF-Leader	:	[10 : 60]
aCD19	:	[61 : 870]
Strep-tag	:	[871 : 903]
linker GGSGG	:	[904 : 918]
HA-tag	:	[919 : 945]
CD8-Hinge	:	[946 : 1069]
MluI	:	[1070 : 1075]
CD28TM	:	[1076 : 1155]
4-1BB	:	[1156 : 1281]
CD3z	:	[1282 : 1617]
BamHI (not2use)	:	[1618 : 1623]
P2A	:	[1624 : 1683]
PuroR	:	[1684 : 2291]

Protein sequence:

```
LETMLLLVTSLLLCELPHPAFLLIPEQKLISEEDLEQKLISEEDLDIQMTQTTSSLSASLGDRVTISCRASQDISKYLNW
YQQKPDGTVKLLIYHTSRLHSGVPSRFSGSGSGTDYSLTISNLEQEDIATYFCQQGNTLPYTFGGGTKLEITGSTSGSGK
PGSGEGSTKGEVKLQESGPGLVAPSQSLSVTCTVSGVSLPDYGVSWIRQPPRKGLEWLGVIWGSETTYYNSALKSRLTII
KDNSKSQVFLKMNSLQTDDTAIYYCAKHYYYGGSYAMDYWGQGTSVTVSSGSNWSHPQFEKGGSGGYPYDVPDYAPTTTP
APRPPTPAPTIASQPLSLRPEASRPAAGGAVHTRGLDAFWVLVVVGGVLACYSLLVTVAFIIFWVKRGRKKLLYIFKQPF
MRPVQTTQEEDGCSCRFPEEEEGGCELRVKFSRSADAPAYQQGQNQLYNELNLGRREEYDVLDKRRGRDPEMGGKPRRKN
PQEGLYNELQKDKMAEAYSEIGMKGERRRGKGHDGLYQGLSTATKDTYDALHMQALPPRGSGATNFSLLKQAGDVEENPG
PMTEYKPTVRLATRDDVPRAVRTLAAAFADYPATRHTVDPDRHIERVTELQELFLTRVGLDIGKVWVADDGAAVAVWTTP
ESVEAGAVFAEIGPRMAELSGSRLAAQQQMEGLLAPHRPKEPAWFLATVGVSPDHQGKGLGSAVVLPGVEAAERAGVPAF
LETSAPRNLPFYERLGFTVTADVEVPEGPRTWCMTRKPGA
```

12.1.4 Single CARs X variant (PYAP)

aCD19:**CD3z_PYAP1**-Puro

Nucleotide sequence:

```
CTCGAGACCATGCTGCTGCTGGTGACCAGCCTGCTGCTGTGCGAGCTGCCCCACCCCGCCTTTCTGCTGATCCCCGAGCA
GAAGCTGATCTCCGAAGAGGACCTGGAACAGAAACTGATCAGCGAGGAAGATCTGGACATCCAGATGACCCAGACCACCT
CCAGCCTGAGCGCCAGCCTGGGCGACCGGGTGACCATCAGCTGCCGGGCCAGCCAGGACATCAGCAAGTACCTGAACTGG
TATCAGCAGAAGCCCGACGGCACCGTCAAGCTGCTGATCTACCACACCAGCCGGCTGCACAGCGGCGTGCCCAGCCGGTT
TAGCGGCAGCGGCTCCGGCACCGACTACAGCCTGACCATCTCCAACCTGGAACAGGAAGATATCGCCACCTACTTTTGCC
AGCAGGGCAACACACTGCCCTACACCTTTGGCGGCGGAACAAAGCTGGAAATCACCGGCAGCACCTCCGGCAGCGGCAAG
CCTGGCAGCGGCGAGGGCAGCACCAAGGGCGAGGTGAAGCTGCAGGAAAGCGGCCCTGGCCTGGTGGCCCCCAGCCAGAG
CCTGAGCGTGACCTGCACCGTGAGCGGCGTGAGCCTGCCCGACTACGGCGTGAGCTGGATCCGGCAGCCCCCCAGGAAGG
GCCTGGAATGGCTGGGCGTGATCTGGGGCAGCGAGACCACCTACTACAACAGCGCCCTGAAGAGCCGGCTGACCATCATC
AAGGACAACAGCAAGAGCCAGGTGTTCCTGAAGATGAACAGCCTGCAGACCGACGACACCGCCATCTACTACTGCGCCAA
GCACTACTACTACGGCGGCAGCTACGCCATGGACTACTGGGGCCAGGGCACCAGCGTGACCGTGAGCAGCGGCTCCAACT
GGAGCCACCCCCAGTTCGAGAAGCCCACCACGACGCCAGCGCCGCGACCACCAACACCGGCGCCCACCATCGCGTCGCAG
CCCCTGTCCCTGCGCCCAGAGGCGTCCCGGCCAGCGGCGGGGGGCGCAGTGCACACGAGGGGGCTGGACGCGTTCTGGGT
GCTGGTGGTGGTCGGAGGCGTGCTGGCCTGCTACAGCCTGCTGGTCACCGTGGCCTTCATCATCTTTTGGGTGGGGCCCA
CCCGCAAGCATTACCAGCCCTATGCCCCACCACGCGACTTCGCAGCCTATCGCTCCCGGGTGAAGTTCAGCAGAAGCGCC
GACGCCCCTGCCTACCAGCAGGGCCAGAATCAGCTGTACAACGAGCTGAACCTGGGCAGAAGGGAAGAGTACGACGTCCT
GGATAAGCGGAGAGGCCGGGACCCTGAGATGGGCGGCAAGCCTCGGCGGAAGAACCCCCAGGAAGGCCTGTATAACGAAC
TGCAGAAAGACAAGATGGCCGAGGCCTACAGCGAGATCGGCATGAAGGGCGAGCGGAGGCGGGGCAAGGGCCACGACGGC
CTGTATCAGGGCCTGTCCACCGCCACCAAGGATACCTACGACGCCCTGCACATGCAGGCCCTGCCCCCAAGGGGATCCGG
AGCTACTAACTTCAGCCTGCTGAAGCAGGCTGGAGACGTCGAGGAGAACCCTGGACCTATGACCGAGTACAAGCCCACGG
TGCGCCTCGCCACCCGCGACGACGTCCCCAGGGCCGTACGCACCCTCGCCGCCGCGTTCGCCGACTACCCCGCCACGCGC
CACACCGTCGATCCGGACCGCCACATCGAGCGGGTCACCGAGCTGCAAGAACTCTTCCTCACGCGCGTCGGGCTCGACAT
CGGCAAGGTGTGGGTCGCGGACGACGGCGCCGCGGTGGCGGTCTGGACCACGCCGGAGAGCGTCGAAGCGGGGGCGGTGT
TCGCCGAGATCGGCCCGCGCATGGCCGAGTTGAGCGGTTCCCGGCTGGCCGCGCAGCAACAGATGGAAGGCCTCCTGGCG
CCGCACCGGCCCAAGGAGCCCGCGTGGTTCCTGGCCACCGTCGGCGTCTCGCCCGACCACCAGGGCAAGGGTCTGGGCAG
CGCCGTCGTGCTCCCCGGAGTGGAGGCGGCCGAGCGCGCCGGGGTGCCCGCCTTCCTGGAGACCTCCGCGCCCCGCAACC
TCCCCTTCTACGAGCGGCTCGGCTTCACCGTCACCGCCGACGTCGAGGTGCCCGAAGGACCGCGCACCTGGTGCATGACC
CGCAAGCCCGGTGCCTGAGCGGCCGC
```

Features:

```
XhoI                : [1 : 6]
GM-CSF-Leader       : [10 : 60]
aCD19               : [61 : 870]
Strep-tag           : [871 : 903]
CD8-Hinge           : [904 : 1027]
MluI                : [1028 : 1033]
CD28TM              : [1034 : 1113]
PYAP 1              : [1114 : 1176]
CD3z                : [1177 : 1512]
BamHi (not2use)     : [1513 : 1518]
P2A                 : [1519 : 1578]
PuroR               : [1579 : 2186]
```

Protein sequence:

```
LETMLLLVTSLLLCELPHPAFLLIPEQKLISEEDLEQKLISEEDLDIQMTQTTSSLSASLGDRVTISCRASQDISKYLNW
YQQKPDGTVKLLIYHTSRLHSGVPSRFSGSGSGTDYSLTISNLEQEDIATYFCQQGNTLPYTFGGGTKLEITGSTSGSGK
PGSGEGSTKGEVKLQESGPGLVAPSQSLSVTCTVSGVSLPDYGVSWIRQPPRKGLEWLGVIWGSETTYYNSALKSRLTII
KDNSKSQVFLKMNSLQTDDTAIYYCAKHYYYGGSYAMDYWGQGTSVTVSSGSNWSHPQFEKPTTTPAPRPPTPAPTIASQ
PLSLRPEASRPAAGGAVHTRGLDAFWVLVVVGGVLACYSLLVTVAFIIFWVGPTRKHYQPYAPPRDFAAYRSRVKFSRSA
DAPAYQQGQNQLYNELNLGRREEYDVLDKRRGRDPEMGGKPRRKNPQEGLYNELQKDKMAEAYSEIGMKGERRRGKGHDG
LYQGLSTATKDTYDALHMQALPPRGSGATNFSLLKQAGDVEENPGPMTEYKPTVRLATRDDVPRAVRTLAAAFADYPATR
HTVDPDRHIERVTELQELFLTRVGLDIGKVWVADDGAAVAVWTTPESVEAGAVFAEIGPRMAELSGSRLAAQQQMEGLLA
PHRPKEPAWFLATVGVSPDHQGKGLGSAVVLPGVEAAERAGVPAFLETSAPRNLPFYERLGFTVTADVEVPEGPRTWCMT
RKPGA
```

aCD19:**CD3z_PYAP2**-Puro

Nucleotide sequence:

```
CTCGAGACCATGCTGCTGCTGGTGACCAGCCTGCTGCTGTGCGAGCTGCCCCACCCCGCCTTTCTGCTGATCCCCGAGCA
GAAGCTGATCTCCGAAGAGGACCTGGAACAGAAACTGATCAGCGAGGAAGATCTGGACATCCAGATGACCCAGACCACCT
CCAGCCTGAGCGCCAGCCTGGGCGACCGGGTGACCATCAGCTGCCGGGCCAGCCAGGACATCAGCAAGTACCTGAACTGG
TATCAGCAGAAGCCCGACGGCACCGTCAAGCTGCTGATCTACCACACCAGCCGGCTGCACAGCGGCGTGCCCAGCCGGTT
TAGCGGCAGCGGCTCCGGCACCGACTACAGCCTGACCATCTCCAACCTGGAACAGGAAGATATCGCCACCTACTTTTGCC
AGCAGGGCAACACACTGCCCTACACCTTTGGCGGCGGAACAAAGCTGGAAATCACCGGCAGCACCTCCGGCAGCGGCAAG
CCTGGCAGCGGCGAGGGCAGCACCAAGGGCGAGGTGAAGCTGCAGGAAAGCGGCCCTGGCCTGGTGGCCCCCAGCCAGAG
CCTGAGCGTGACCTGCACCGTGAGCGGCGTGAGCCTGCCCGACTACGGCGTGAGCTGGATCCGGCAGCCCCCCAGGAAGG
GCCTGGAATGGCTGGGCGTGATCTGGGGCAGCGAGACCACCTACTACAACAGCGCCCTGAAGAGCCGGCTGACCATCATC
AAGGACAACAGCAAGAGCCAGGTGTTCCTGAAGATGAACAGCCTGCAGACCGACGACACCGCCATCTACTACTGCGCCAA
GCACTACTACTACGGCGGCAGCTACGCCATGGACTACTGGGGCCAGGGCACCAGCGTGACCGTGAGCAGCGGCTCCAACT
GGAGCCACCCCCAGTTCGAGAAGCCCACCACGACGCCAGCGCCGCGACCACCAACACCGGCGCCCACCATCGCGTCGCAG
CCCCTGTCCCTGCGCCCAGAGGCGTCCCGGCCAGCGGCGGGGGGCGCAGTGCACACGAGGGGGCTGGACGCGTTCTGGGT
GCTGGTGGTGGTCGGAGGCGTGCTGGCCTGCTACAGCCTGCTGGTCACCGTGGCCTTCATCATCTTTTGGGTGCGGGTGA
AGTTCAGCAGAAGCGCCGACGCCCCTGCCTACCAGCAGGGCCAGAATCAGCTGTACAACGAGCTGAACCTGGGCAGAAGG
GAAGAGTACGACGTCCTGGATAAGCGGAGAAAGCATTACCAGCCCTATGCCCCACCACGCGACTTCCGGCGGAAGAACCC
CCAGGAAGGCCTGTATAACGAACTGCAGAAAGACAAGATGGCCGAGGCCTACAGCGAGATCGGCATGAAGGGCGAGCGGA
GGCGGGGCAAGGGCCACGACGGCCTGTATCAGGGCCTGTCCACCGCCACCAAGGATACCTACGACGCCCTGCACATGCAG
GCCCTGCCCCCAAGGGGATCCGGATCCGGAGCTACTAACTTCAGCCTGCTGAAGCAGGCTGGAGACGTCGAGGAGAACCC
TGGACCTATGACCGAGTACAAGCCCACGGTGCGCCTCGCCACCCGCGACGACGTCCCCAGGGCCGTACGCACCCTCGCCG
CCGCGTTCGCCGACTACCCCGCCACGCGCCACACCGTCGATCCGGACCGCCACATCGAGCGGGTCACCGAGCTGCAAGAA
CTCTTCCTCACGCGCGTCGGGCTCGACATCGGCAAGGTGTGGGTCGCGGACGACGGCGCCGCGGTGGCGGTCTGGACCAC
GCCGGAGAGCGTCGAAGCGGGGGCGGTGTTCGCCGAGATCGGCCCGCGCATGGCCGAGTTGAGCGGTTCCCGGCTGGCCG
CGCAGCAACAGATGGAAGGCCTCCTGGCGCCGCACCGGCCCAAGGAGCCCGCGTGGTTCCTGGCCACCGTCGGCGTCTCG
CCCGACCACCAGGGCAAGGGTCTGGGCAGCGCCGTCGTGCTCCCCGGAGTGGAGGCGGCCGAGCGCGCCGGGGTGCCCGC
CTTCCTGGAGACCTCCGCGCCCCGCAACCTCCCCTTCTACGAGCGGCTCGGCTTCACCGTCACCGCCGACGTCGAGGTGC
CCGAAGGACCGCGCACCTGGTGCATGACCCGCAAGCCCGGTGCCTGAGCGGCCGC
```

Features:

```
XhoI                : [1 : 6]
GM-CSF-Leader       : [10 : 60]
aCD19               : [61 : 870]
Strep-tag           : [871 : 903]
CD8-Hinge           : [904 : 1027]
MluI                : [1028 : 1033]
CD28TM              : [1034 : 1113]
CD3z                : [1114 : 1461]
PYAP 2              : [1231 : 1266]
BamHI (not2use)     : [1462 : 1467]
P2A                 : [1468 : 1527]
PuroR               : [1528 : 2135]
```

Protein sequence:

```
LETMLLLVTSLLLCELPHPAFLLIPEQKLISEEDLEQKLISEEDLDIQMTQTTSSLSASLGDRVTISCRASQDISKYLNW
YQQKPDGTVKLLIYHTSRLHSGVPSRFSGSGSGTDYSLTISNLEQEDIATYFCQQGNTLPYTFGGGTKLEITGSTSGSGK
PGSGEGSTKGEVKLQESGPGLVAPSQSLSVTCTVSGVSLPDYGVSWIRQPPRKGLEWLGVIWGSETTYYNSALKSRLTII
KDNSKSQVFLKMNSLQTDDTAIYYCAKHYYYGGSYAMDYWGQGTSVTVSSGSNWSHPQFEKPTTTPAPRPPTPAPTIASQ
PLSLRPEASRPAAGGAVHTRGLDAFWVLVVVGGVLACYSLLVTVAFIIFWVRVKFSRSADAPAYQQGQNQLYNELNLGRR
EEYDVLDKRRKHYQPYAPPRDFRRKNPQEGLYNELQKDKMAEAYSEIGMKGERRRGKGHDGLYQGLSTATKDTYDALHMQ
ALPPRGSGSGATNFSLLKQAGDVEENPGPMTEYKPTVRLATRDDVPRAVRTLAAAFADYPATRHTVDPDRHIERVTELQE
LFLTRVGLDIGKVWVADDGAAVAVWTTPESVEAGAVFAEIGPRMAELSGSRLAAQQQMEGLLAPHRPKEPAWFLATVGVS
PDHQGKGLGSAVVLPGVEAAERAGVPAFLETSAPRNLPFYERLGFTVTADVEVPEGPRTWCMTRKPGA
```

aCD19:**CD3z_PYAP3**-Puro

Nucleotide sequence:

CTCGAGACCATGCTGCTGCTGGTGACCAGCCTGCTGCTGTGCGAGCTGCCCCACCCCGCCTTTCTGCTGATCCCCGAGCA
GAAGCTGATCTCCGAAGAGGACCTGGAACAGAAACTGATCAGCGAGGAAGATCTGGACATCCAGATGACCCAGACCACCT
CCAGCCTGAGCGCCAGCCTGGGCGACCGGGTGACCATCAGCTGCCGGGCCAGCCAGGACATCAGCAAGTACCTGAACTGG
TATCAGCAGAAGCCCGACGGCACCGTCAAGCTGCTGATCTACCACACCAGCCGGCTGCACAGCGGCGTGCCCAGCCGGTT
TAGCGGCAGCGGCTCCGGCACCGACTACAGCCTGACCATCTCCAACCTGGAACAGGAAGATATCGCCACCTACTTTTGCC
AGCAGGGCAACACACTGCCCTACACCTTTGGCGGCGGAACAAAGCTGGAAATCACCGGCAGCACCTCCGGCAGCGGCAAG
CCTGGCAGCGGCGAGGGCAGCACCAAGGGCGAGGTGAAGCTGCAGGAAAGCGGCCCTGGCCTGGTGGCCCCCAGCCAGAG
CCTGAGCGTGACCTGCACCGTGAGCGGCGTGAGCCTGCCCGACTACGGCGTGAGCTGGATCCGGCAGCCCCCCAGGAAGG
GCCTGGAATGGCTGGGCGTGATCTGGGGCAGCGAGACCACCTACTACAACAGCGCCCTGAAGAGCCGGCTGACCATCATC
AAGGACAACAGCAAGAGCCAGGTGTTCCTGAAGATGAACAGCCTGCAGACCGACGACACCGCCATCTACTACTGCGCCAA
GCACTACTACTACGGCGGCAGCTACGCCATGGACTACTGGGGCCAGGGCACCAGCGTGACCGTGAGCAGCGGCTCCAACT
GGAGCCACCCCCAGTTCGAGAAGCCCACCACGACGCCAGCGCCGCGACCACCAACACCGGCGCCCACCATCGCGTCGCAG
CCCCTGTCCCTGCGCCCAGAGGCGTCCCGGCCAGCGGCGGGGGGCGCAGTGCACACGAGGGGGCTGGACGCGTTCTGGGT
GCTGGTGGTGGTCGGAGGCGTGCTGGCCTGCTACAGCCTGCTGGTCACCGTGGCCTTCATCATCTTTTGGGTGCGGGTGA
AGTTCAGCAGAAGCGCCGACGCCCCTGCCTACCAGCAGGGCCAGAATCAGCTGTACAACGAGCTGAACCTGGGCAGAAGG
GAAGAGTACGACGTCCTGGATAAGCGGAGAGGCCGGGACCCTGAGATGGGCGGCAAGCCTCGGCGGAAGAACCCCCAGGA
AGGCCTGTATAACGAACTGCAGAAAGACAAGATGGCCGAGGCCTACAGCGAGATCGGCATGAAGGGCGAGCGGAGGCGGG
GCAAGGGCCACGACGGCCTGTATCAGGGCCTGTCCACCGCCACCAAGGATACCTACGACGCCCTGCACATGCAGGCCCTG
CCCCCAAGGAAGCATTACCAGCCCTATGCCCCACCACGCGACTTCGCAGCCTATCGCTCCGGATCCGGATCCGGAGCTAC
TAACTTCAGCCTGCTGAAGCAGGCTGGAGACGTCGAGGAGAACCCTGGACCTATGACCGAGTACAAGCCCACGGTGCGCC
TCGCCACCCGCGACGACGTCCCCAGGGCCGTACGCACCCTCGCCGCCGCGTTCGCCGACTACCCCGCCACGCGCCACACC
GTCGATCCGGACCGCCACATCGAGCGGGTCACCGAGCTGCAAGAACTCTTCCTCACGCGCGTCGGGCTCGACATCGGCAA
GGTGTGGGTCGCGGACGACGGCGCCGCGGTGGCGGTCTGGACCACGCCGGAGAGCGTCGAAGCGGGGGCGGTGTTCGCCG
AGATCGGCCCGCGCATGGCCGAGTTGAGCGGTTCCCGGCTGGCCGCGCAGCAACAGATGGAAGGCCTCCTGGCGCCGCAC
CGGCCCAAGGAGCCCGCGTGGTTCCTGGCCACCGTCGGCGTCTCGCCCGACCACCAGGGCAAGGGTCTGGGCAGCGCCGT
CGTGCTCCCCGGAGTGGAGGCGGCCGAGCGCGCCGGGGTGCCCGCCTTCCTGGAGACCTCCGCGCCCCGCAACCTCCCCT
TCTACGAGCGGCTCGGCTTCACCGTCACCGCCGACGTCGAGGTGCCCGAAGGACCGCGCACCTGGTGCATGACCCGCAAG
CCCGGTGCCTGAGCGGCCGC

Features:

XhoI	:	[1 : 6]
GM-CSF-Leader	:	[10 : 60]
aCD19	:	[61 : 870]
Strep-tag	:	[871 : 903]
CD8-Hinge	:	[904 : 1027]
MluI	:	[1028 : 1033]
CD28TM	:	[1034 : 1113]
CD3z	:	[1114 : 1506]
PYAP 3	:	[1450 : 1500]
BamHI (not2use)	:	[1507 : 1512]
P2A	:	[1513 : 1572]
PuroR	:	[1573 : 2180]

Protein sequence:

LETMLLLVTSLLLCELPHPAFLLIPEQKLISEEDLEQKLISEEDLDIQMTQTTSSLSASLGDRVTISCRASQDISKYLNW
YQQKPDGTVKLLIYHTSRLHSGVPSRFSGSGSGTDYSLTISNLEQEDIATYFCQQGNTLPYTFGGGTKLEITGSTSGSGK
PGSGEGSTKGEVKLQESGPGLVAPSQSLSVTCTVSGVSLPDYGVSWIRQPPRKGLEWLGVIWGSETTYYNSALKSRLTII
KDNSKSQVFLKMNSLQTDDTAIYYCAKHYYYGGSYAMDYWGQGTSVTVSSGSNWSHPQFEKPTTTPAPRPPTPAPTIASQ
PLSLRPEASRPAAGGAVHTRGLDAFWVLVVVGGVLACYSLLVTVAFIIFWVRVKFSRSADAPAYQQGQNQLYNELNLGRR
EEYDVLDKRRGRDPEMGGKPRRKNPQEGLYNELQKDKMAEAYSEIGMKGERRRGKGHDGLYQGLSTATKDTYDALHMQAL
PPRKHYQPYAPPRDFAAYRSGSGSGATNFSLLKQAGDVEENPGPMTEYKPTVRLATRDDVPRAVRTLAAAFADYPATRHT
VDPDRHIERVTELQELFLTRVGLDIGKVWVADDGAAVAVWTTPESVEAGAVFAEIGPRMAELSGSRLAAQQQMEGLLAPH
RPKEPAWFLATVGVSPDHQGKGLGSAVVLPGVEAAERAGVPAFLETSAPRNLPFYERLGFTVTADVEVPEGPRTWCMTRK
PGA

13 Supplementary data

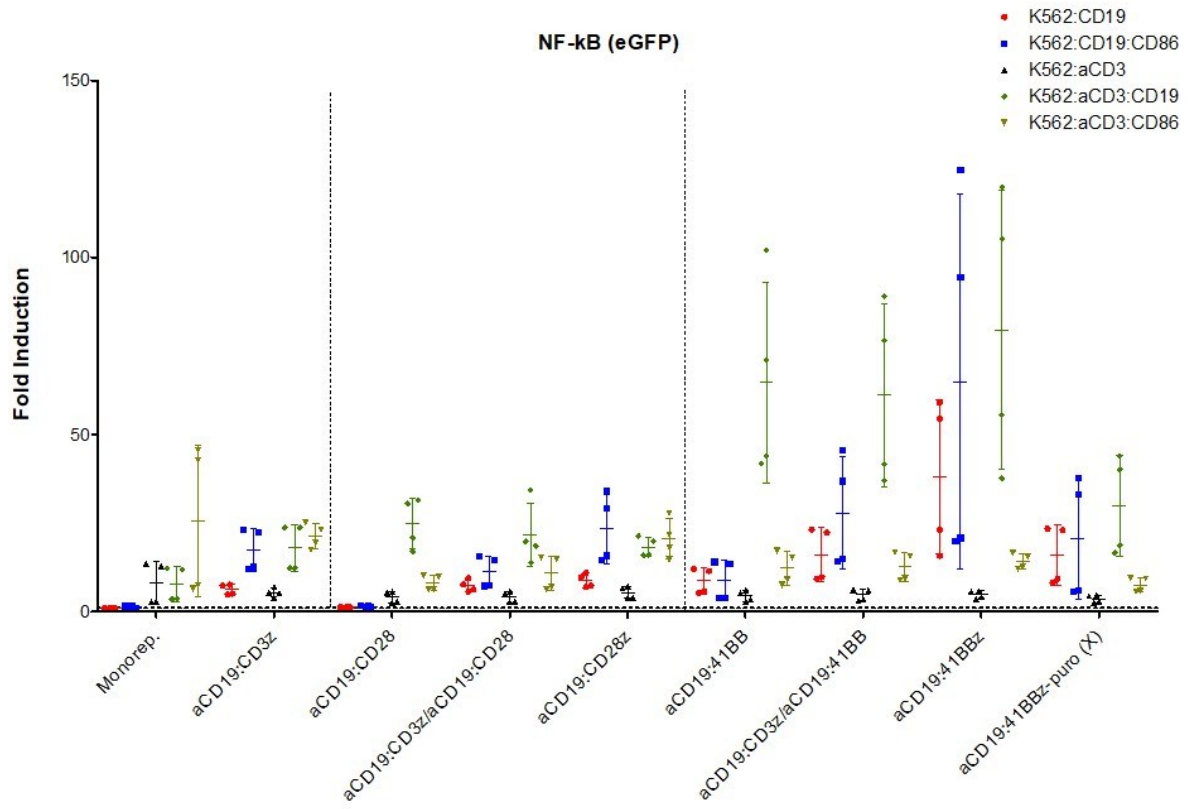

Supplementary Figure 1: Functional comparison of different aCD19 CARs harboring various signaling domains and no puromycin or blasticidin resistance marker in an NF-κB-reporter cell system. NF-κB-reporter cells served as controls. Reporter control cells and reporter cells expressing aCD19 CAR variants were left unstimulated or co-cultured with K562, K562:CD19, K562:CD19:CD86, K562:aCD3, K562:aCD3:CD19 and K562:aCD3:CD86. Reporter activation is shown as fold induction (gMFI of K562-ligand stimulated reporter cells/K562 control stimulated reporter cells). Left panel shows control reporter cells and 1st generation CAR. Middle panel shows stimulation of CARs containing CD28 signaling domains. Right panel shows stimulation of CARs containing 4-1BB signaling domains. aCD19:41BBz (X) harbors a puromycin resistance marker. Activation of CAR constructs was measured via FACS analysis. Results of 2 independent experiments performed in duplicates are depicted. Mean (SD) values are depicted.

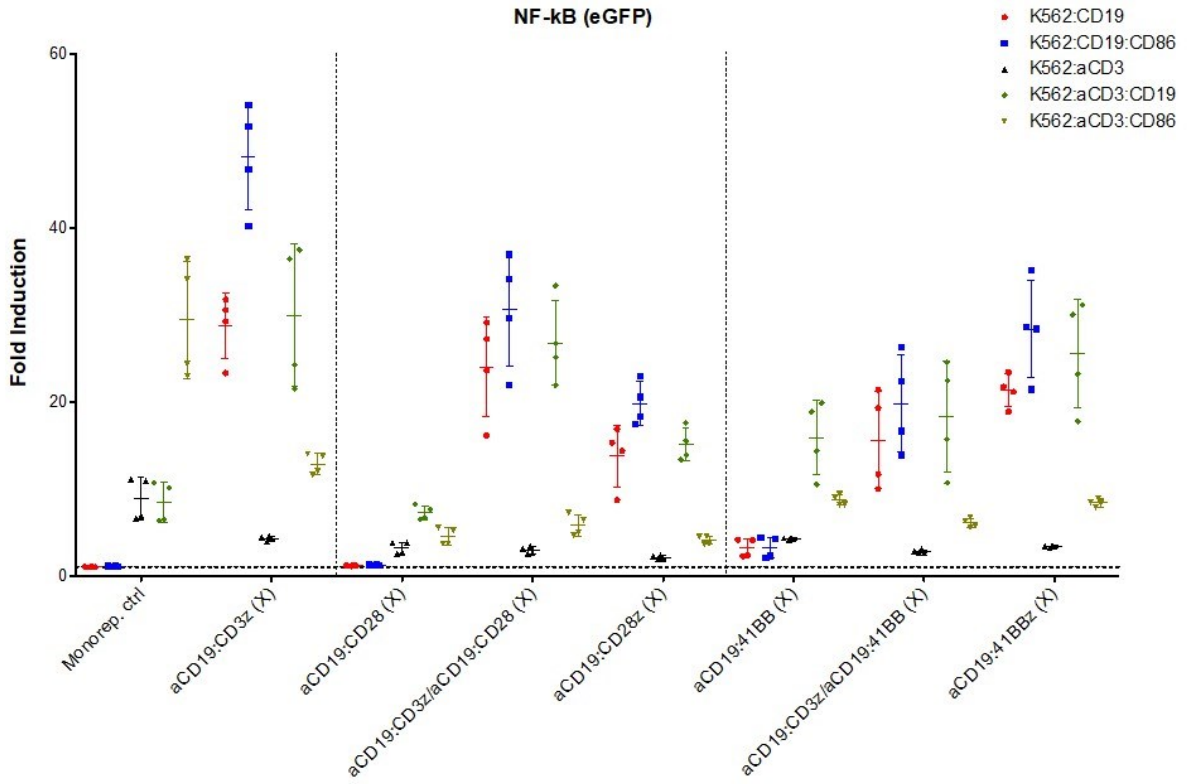

Supplementary Figure 2: Functional comparison of different aCD19 CARs (X) harboring various signaling domains in an NF-κB-reporter cell system. NF-κB-reporter cells served as controls. Reporter control cells and reporter cells expressing aCD19 CAR X variants were left unstimulated or co-cultured with K562, K562:CD19, K562:CD19:CD86, K562:aCD3, K562:aCD3:CD19 and K562:aCD3:CD86. Reporter activation is shown as fold induction (gMFI of K562-ligand stimulated reporter cells/K562 control stimulated reporter cells). Left panel shows control reporter cells and 1st generation CAR. Middle panel shows stimulation of CARs containing CD28 signaling domains. Right panel shows stimulation of CARs containing 4-1BB signaling domains. All CAR constructs harbor a puromycin or blasticidin resistance marker. Activation of CAR constructs was measured via FACS analysis. Results of 2 independent experiments performed in duplicates are depicted. Mean (SD) values are depicted.

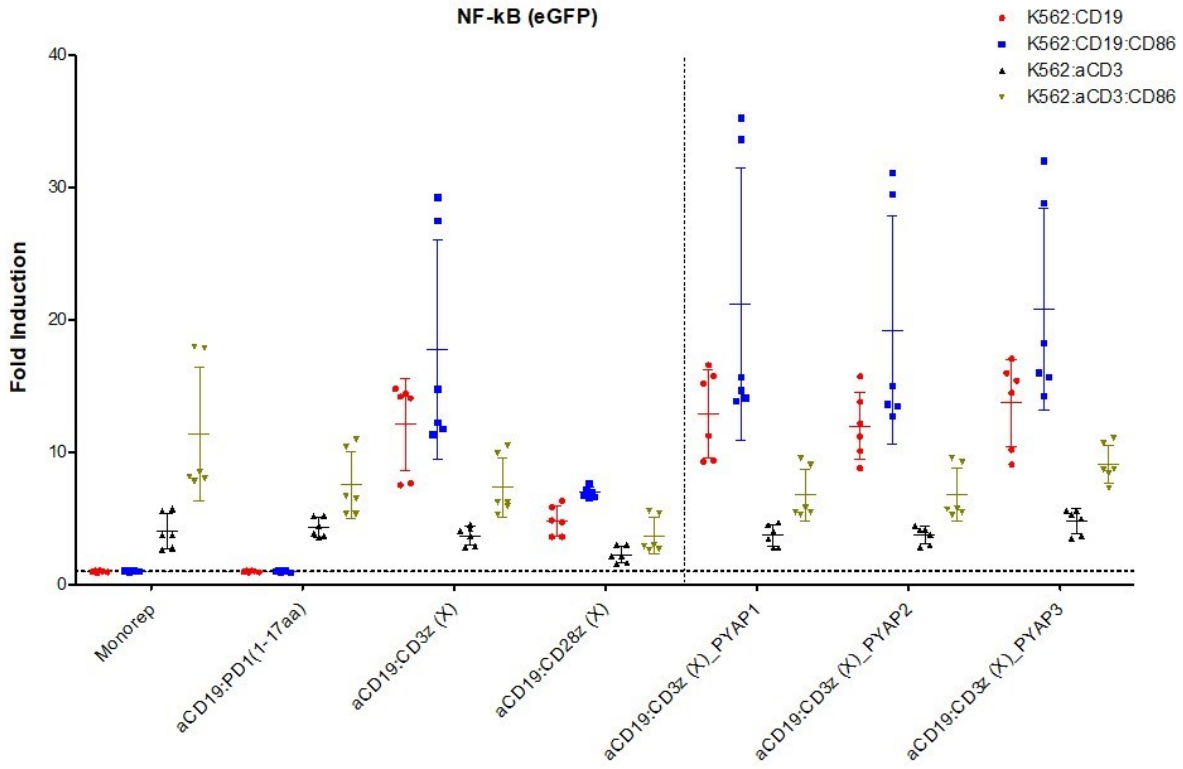

*Supplementary Figure 3: Functional comparison of different aCD19 CAR (X) constructs on NF-κB-reporter cells harboring various signaling domains. Constructs comprise of a CD3z domain with a PYAP motif appended. As controls, aCD19:PD1$_{1\text{-}17aa}$, aCD19:CD3z, aCD19:CD28z and non-transduced TPR cells were used. TPR control and TPR expressing aCD19 CAR X variants were left unstimulated or co-cultured with K562, K562:CD19, K562:CD19:CD86, K562:aCD3 or K562:aCD3:CD86. Reporter activation is shown as fold induction (gMFI of K562-ligand stimulated reporter cells/K562 control stimulated reporter cells). **A)** indicates NF-κB-eCFP activation **B)** indicates NFAT-eGFP and **C)** indicates AP-1-mCherry activation.). Left panel shows control reporter cells. Right panel shows stimulation of CARs containing a PYAP motif. All CAR constructs harbor a puromycin resistance marker. Activation of CAR constructs was measured via FACS analysis. Results of 3 independent experiments performed in duplicates are depicted. Mean (SD) values are depicted.*

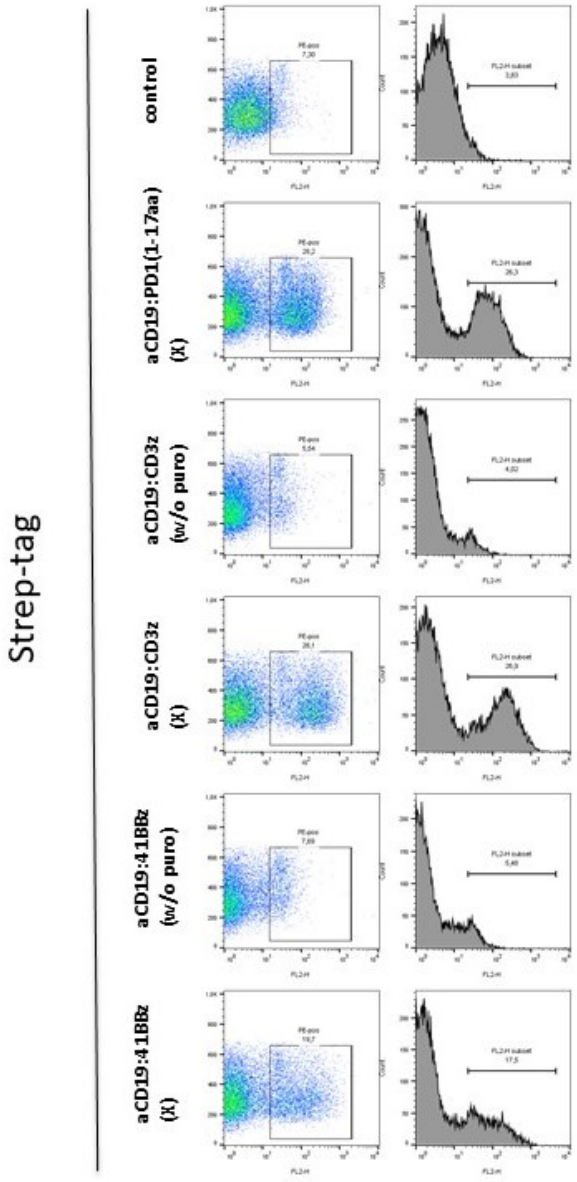

Supplementary Figure 4: Cell surface expression of aCD19 CAR constructs transduced in CD14 negative-selected peripheral blood mononuclear cells (PBMCs) from different a donor than in main thesis. Non-transduced PBMCs and aCD19:PD1$_{1\text{-}17aa}$ (X) construct are used as controls. Detection was performed via a NWSHPQFEK Tag-bio (Strep-tag) antibody followed by streptavidine-PE antibody Numbers and lines in histograms indicate percentage of transduced cells. Dot plot and histograms are shown

A

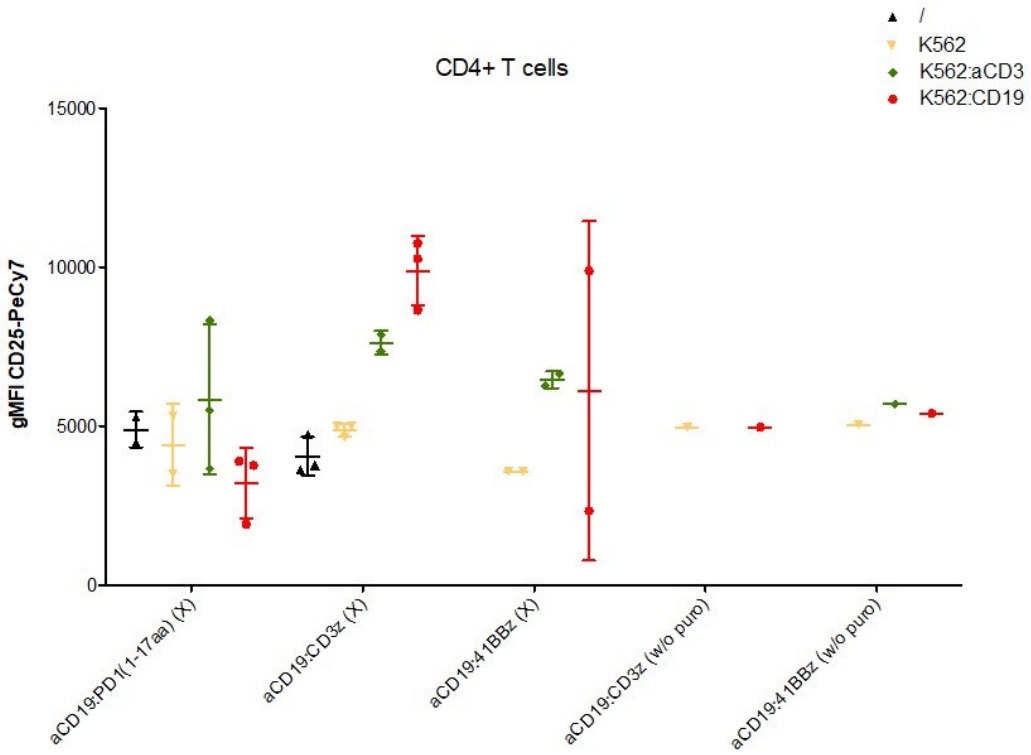
CD4+ T cells
/
K562
K562:aCD3
K562:CD19
gMFI CD25-PeCy7
15000
10000
5000
0
aCD19:PD1(1-17aa) (X)
aCD19:CD3z (X)
aCD19:41BBz (X)
aCD19:CD3z (w/o puro)
aCD19:41BBz (w/o puro)

B

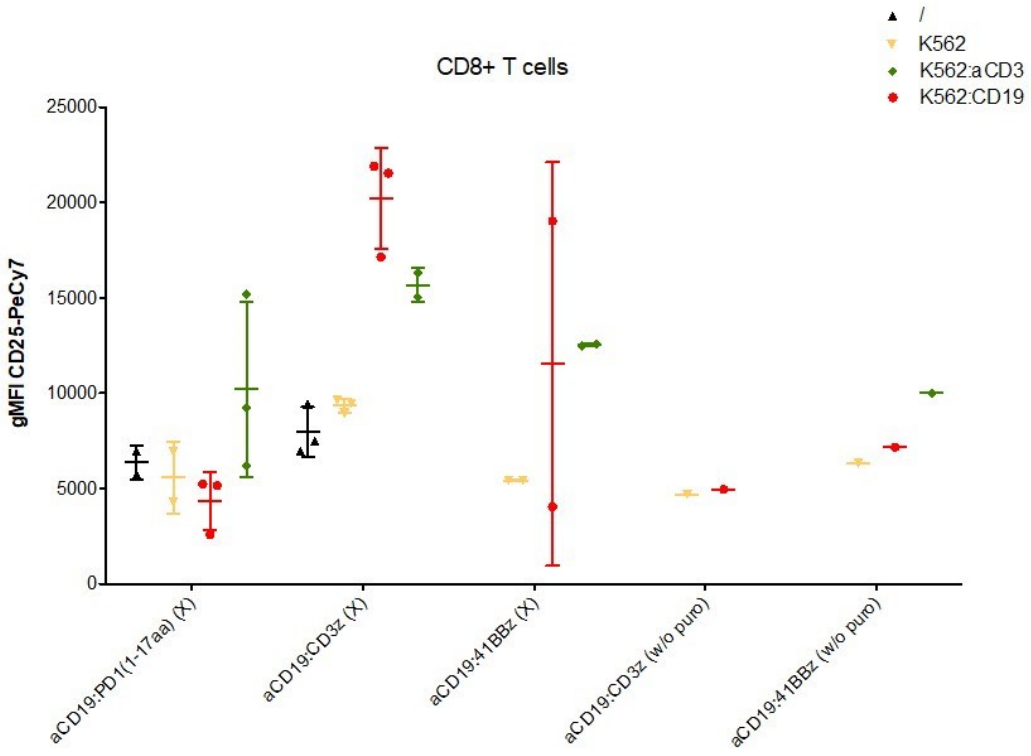
CD8+ T cells
/
K562
K562:aCD3
K562:CD19
gMFI CD25-PeCy7
25000
20000
15000
10000
5000
0
aCD19:PD1(1-17aa) (X)
aCD19:CD3z (X)
aCD19:41BBz (X)
aCD19:CD3z (w/o puro)
aCD19:41BBz (w/o puro)

Supplementary Figure 5: Functional comparison of different aCD19 CARs (X) harboring various signaling domains in primary CD4+ and CD8+ T cells from a different donor than in main thesis. Prior to stimulation of cells, cells expressing aCD19 CARs were sorted. Cells expressing aCD19 CAR were left unstimulated or co-cultured with K562, K562:CD19 or K562:aCD3. T cell activation in the CD4+ and CD8+ T cell subsets is shown as geometric mean upon staining with the T cell activation marker CD25 with a CD25-PeCy7 antibody. ***A)*** *shows activation of CD4+ T cells and* ***B)*** *shows activation of CD8+ T cells. For some CARs triplicates are depicted, otherwise duplicates or single wells. Activation of CAR constructs in primary cells was measured via FACS analysis. Mean (SD) values are depicted.*

A

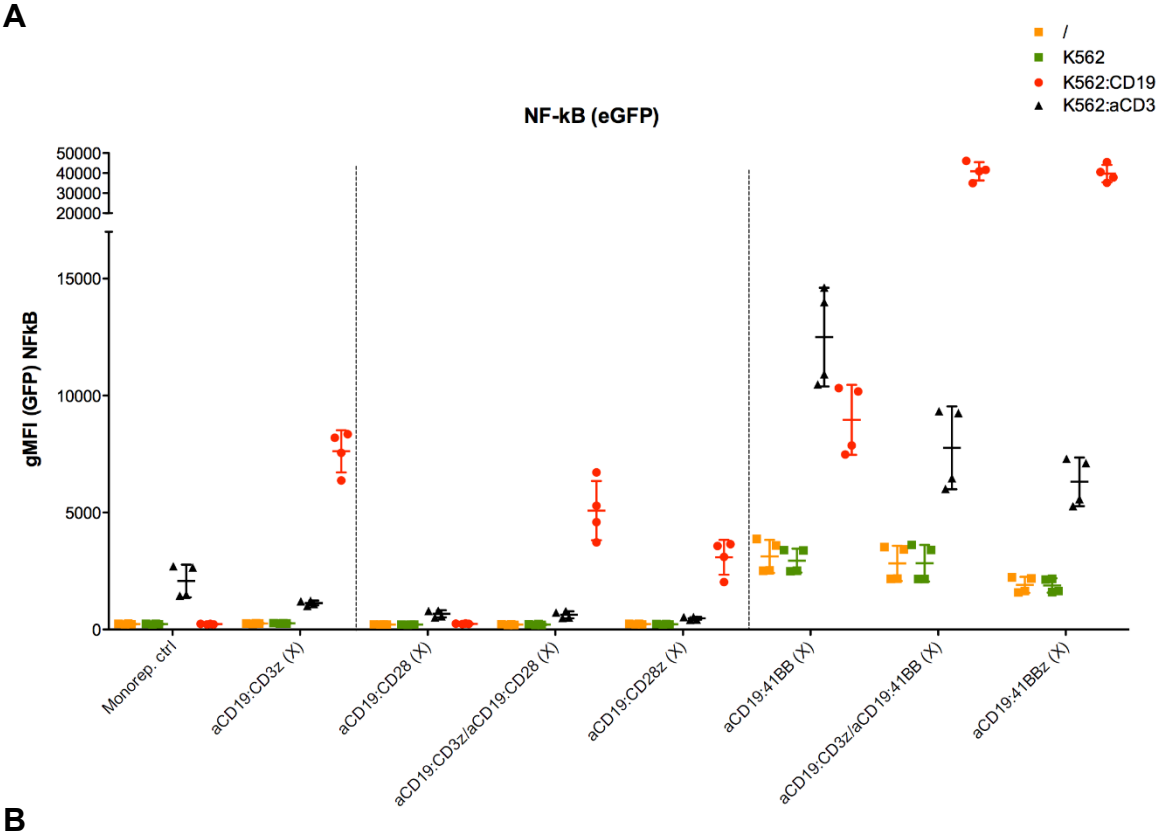
NF-kB (eGFP)
/
K562
K562:CD19
K562:aCD3
gMFI (GFP) NFkB
50000
40000
30000
20000
15000
10000
5000
0
Monorep. ctrl
aCD19:CD3z (X)
aCD19:CD28 (X)
aCD19:CD3z/aCD19:CD28 (X)
aCD19:CD28z (X)
aCD19:41BB (X)
aCD19:CD3z/aCD19:41BB (X)
aCD19:41BBz (X)

B

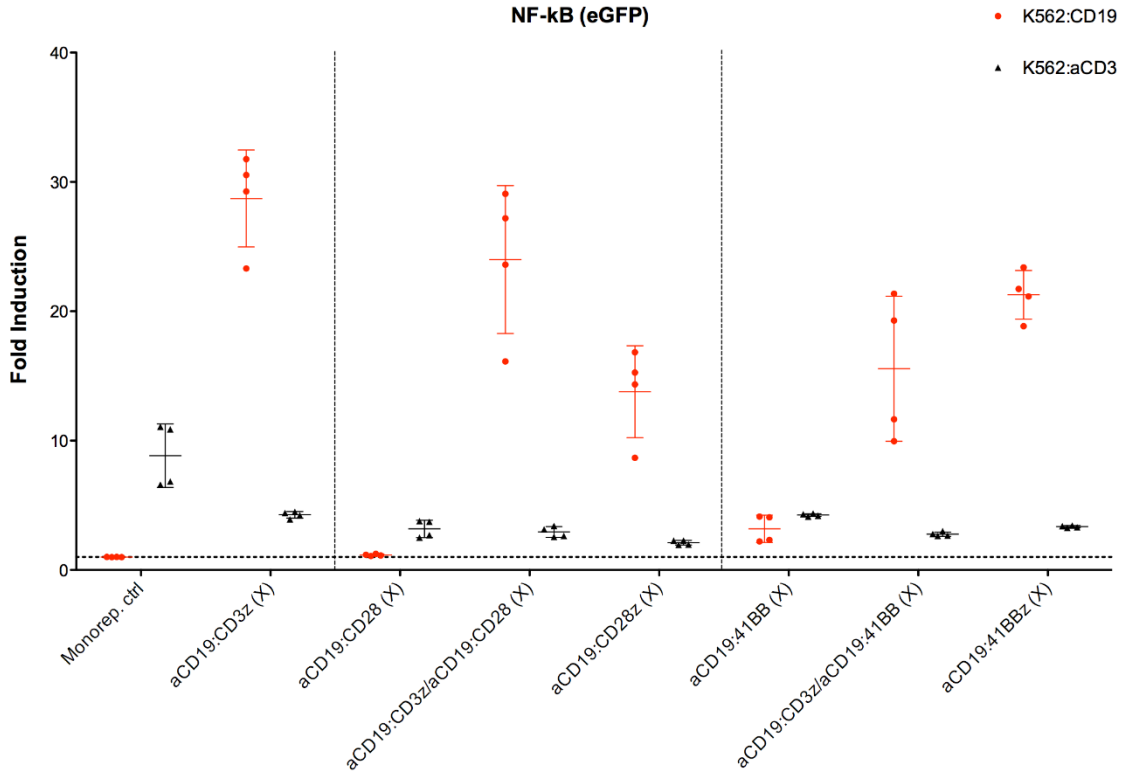
NF-kB (eGFP)
K562:CD19
K562:aCD3
Fold Induction
40
30
20
10
0
Monorep. ctrl
aCD19:CD3z (X)
aCD19:CD28 (X)
aCD19:CD3z/aCD19:CD28 (X)
aCD19:CD28z (X)
aCD19:41BB (X)
aCD19:CD3z/aCD19:41BB (X)
aCD19:41BBz (X)

*Supplementary Figure 7: Tonic signaling via 4-1BB signaling motif in a CD19 CAR. Stimulation of different aCD19 CARs (X variant) harboring various signaling domains in an NF-κB-reporter system are shown. NF-κB-reporter control and NF-κB-reporter expressing aCD19 CAR variants were left unstimulated or co-cultured with K562, K562:aCD3 and K562:CD19. Reporter activation (NF-κB-eGFP) is shown as **A)** gMFI and **B)** fold induction (gMFI of K562-ligand stimulated reporter cells/K562 control stimulated reporter cells). Left panel shows control reporter cells and a 1st generation CAR. Middle panel shows stimulation of CARs containing CD28 signaling domains. Right panel shows stimulation of CARs containing 4-1BB signaling domains. Activation of CAR constructs was measured via FACS analysis. Results of 2 independent experiments performed in duplicates are depicted. Mean (SD) values are depicted.*